Walther Meißner Institut

BAdW | BAYERISCHE AKADEMIE DER WISSENSCHAFTEN

Technische Universität München

Superconductivity and Low Temperature Physics I

Lecture Notes
Winter Semester 2021/2022

R. Gross

Chapter 7

High Temperature Superconductivity

Walther Meißner Institut

BAdW | BAYERISCHE AKADEMIE DER WISSENSCHAFTEN

Technische Universität München

Superconductivity and Low Temperature Physics I

Lecture No. 13
27 January 2022

R. Gross

7 High Temperature Superconductivity

Possible High T_c Superconductivity in the Ba – La – Cu – O System

J.G. Bednorz and K.A. Müller
IBM Zürich Research Laboratory, Rüschlikon, Switzerland

Received April 17, 1986

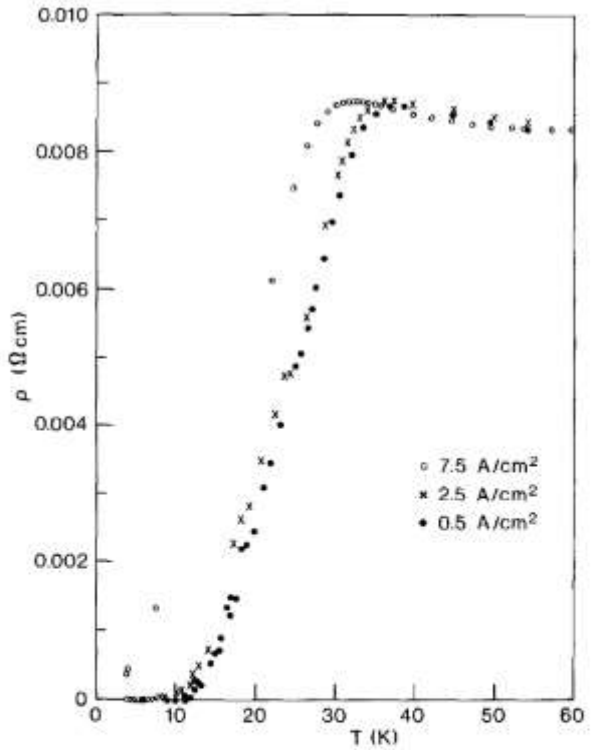

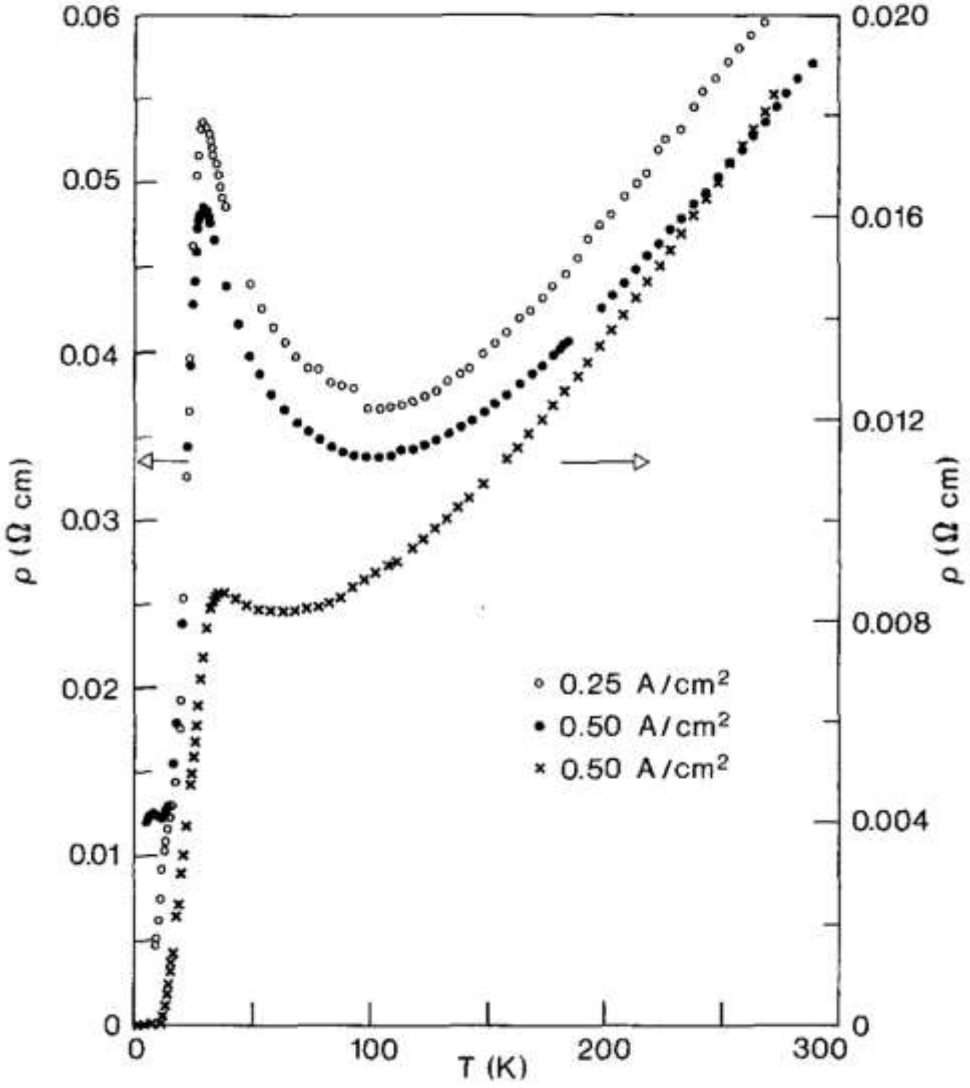

→ **no Meißner effect demonstrated !!**

7.1 Discovery of the High Tc Superconductivity

Karl Alexander Müller
* 20. April 1927 in Basel

Johannes Georg Bednorz
* 16. Mai 1950 in Neuenkirchen im Kreis Steinfurt

7.1 Discovery of the High Tc Superconductivity

VOLUME 58, NUMBER 9 PHYSICAL REVIEW LETTERS 2 MARCH 1987

Superconductivity at 93 K in a New Mixed-Phase Y-Ba-Cu-O Compound System at Ambient Pressure

M. K. Wu, J. R. Ashburn, and C. J. Torng
Department of Physics, University of Alabama, Huntsville, Alabama 35899

and

P. H. Hor, R. L. Meng, L. Gao, Z. J. Huang, Y. Q. Wang, and C. W. Chu[a]
Department of Physics and Space Vacuum Epitaxy Center, University of Houston, Houston, Texas 77004

(Received 6 February 1987; Revised manuscript received 18 February 1987)

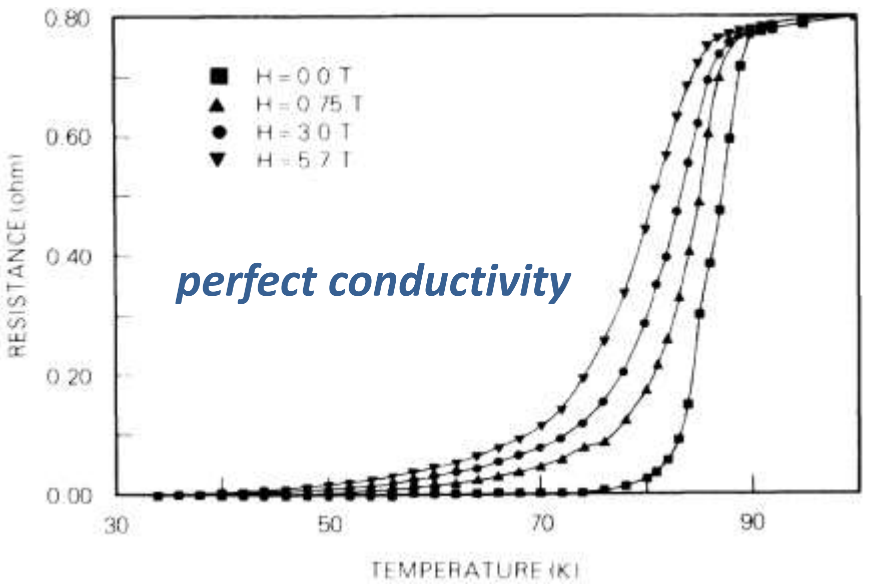

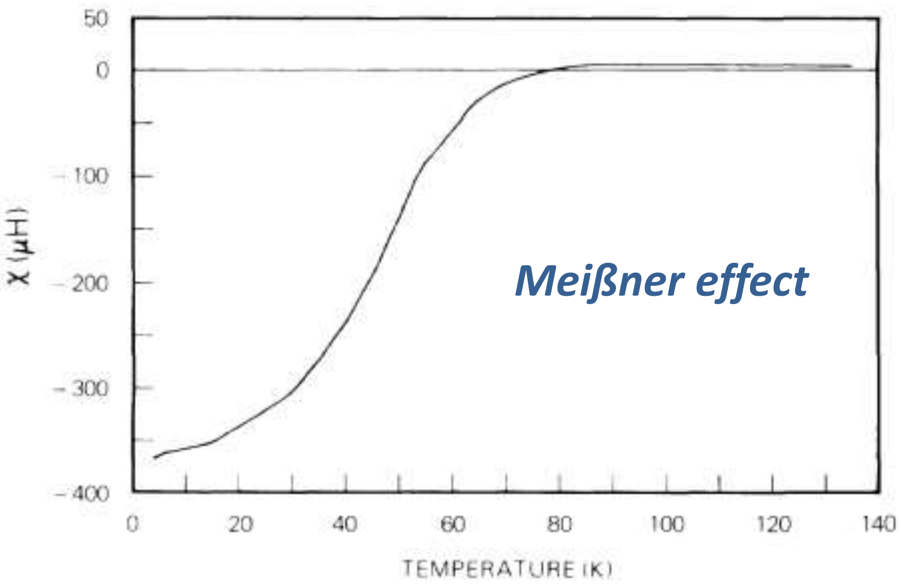

➔ „Woodstock of Physics“ at APS March Meeting 1987

J. Georg Bednorz (b. 1950) **K. Alexander Müller (b. 1927)**

Nobel Prize in Physics 1987

"for their important break-through in the discovery of superconductivity in ceramic materials"

original idea: search for materials with strong electron-phonon coupling → ***ferroelectrics***

7.1 Discovery of the High Tc Superconductivity

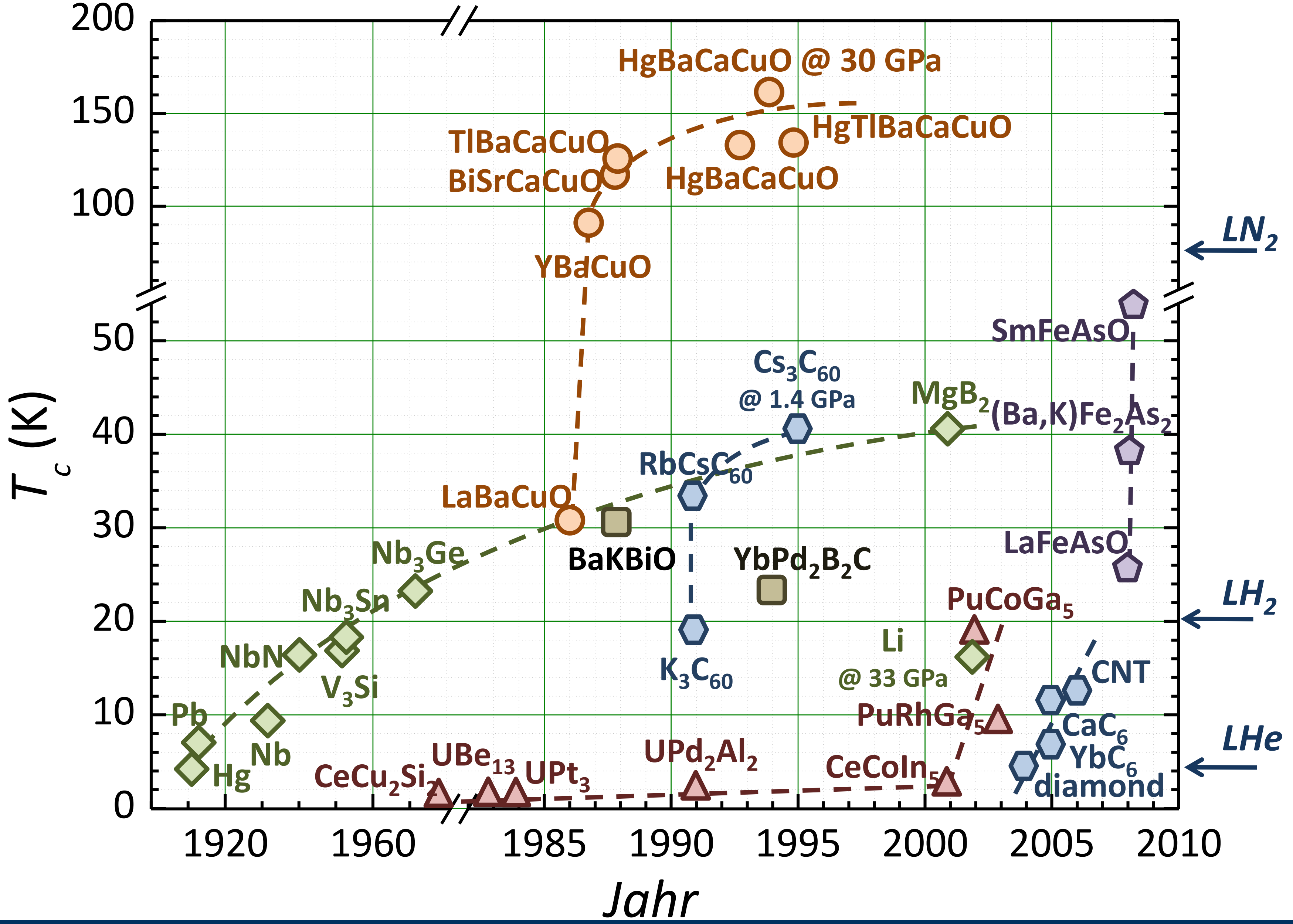

7.1 Discovery of the High Tc Superconductivity

- **evidence for Cooper pairing in cuprate superconductors**

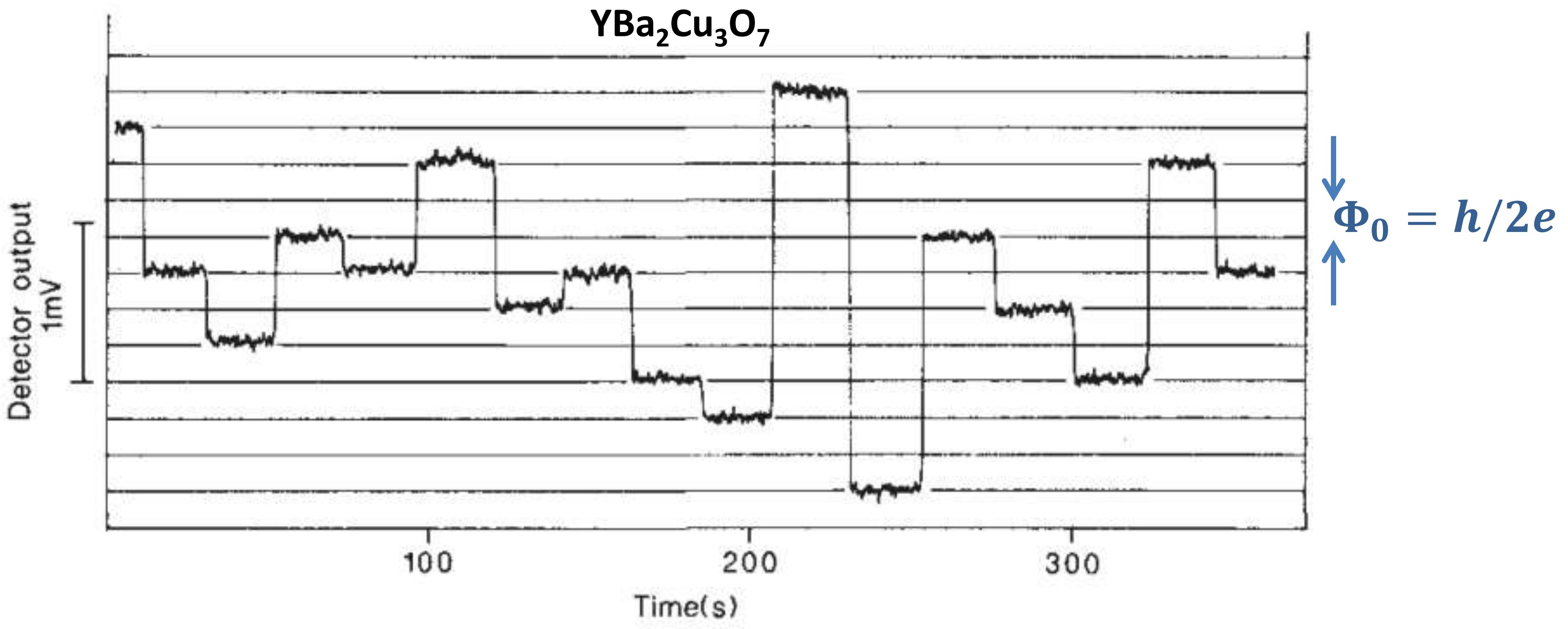

detection of flux jumps with height $n \cdot \Phi_0 = n \cdot \frac{h}{2e}$

C.E. Gough *et al.*,
Nature **326**, 855 (30 April 1987); doi:10.1038/326855a0

Knight shift: spin-singlet Cooper pairs

S. E. Barret *et al.*,
Phys. Rev. B **41** 6283 (1990); doi:10.1103/PhysRevB.41.6283

7.1 Discovery of the High Tc Superconductivity

LTS

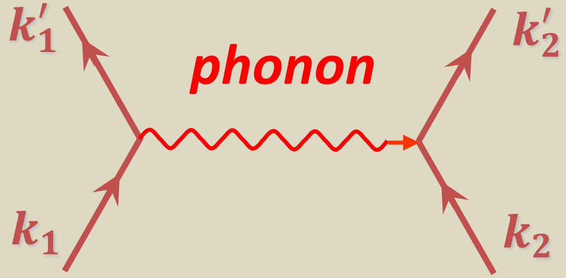

- *spin singlet Cooper pairs ($S=0$)*
- *orbital symmetry: s-wave*
- $\xi^3 \gg 1/n_s$ → *rigid phase*
- *isotropic*

normal state:

→ *metals (Fermi liquid)*

HTS

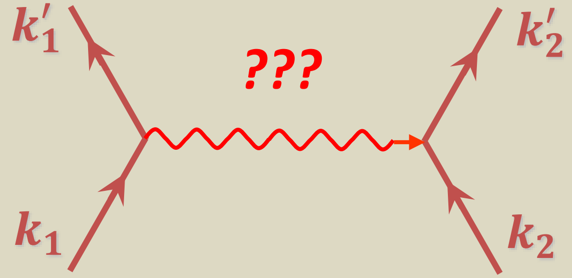

- *spin singlet Cooper pairs ($S=0$)*
- *orbital symmetry: d-wave, mixed*
- $\xi^3 \simeq 1/n_s$ → *phase fluctuations*
- *anisotropic*

normal state:

→ *doped afm insulators*

→ *competing / coexisting ordering phenomena*

- ***crystal structure of cuprate superconductors***

  - discovered by ***Bednorz*** and ***Müller*** in 1986 in $La_{2-x}Ba_xCuO_4$ (Zurich oxide)

  - until today several compounds found with T_c up to 135 K (165 K under pressure)

  - layered crystal structure formed by CuO_2 planes and charge reservoir layers

hole doping by replacing trivalent La by divalent Sr

$La_{2-x}Sr_xCuO_4$

$T_c = 40$ K

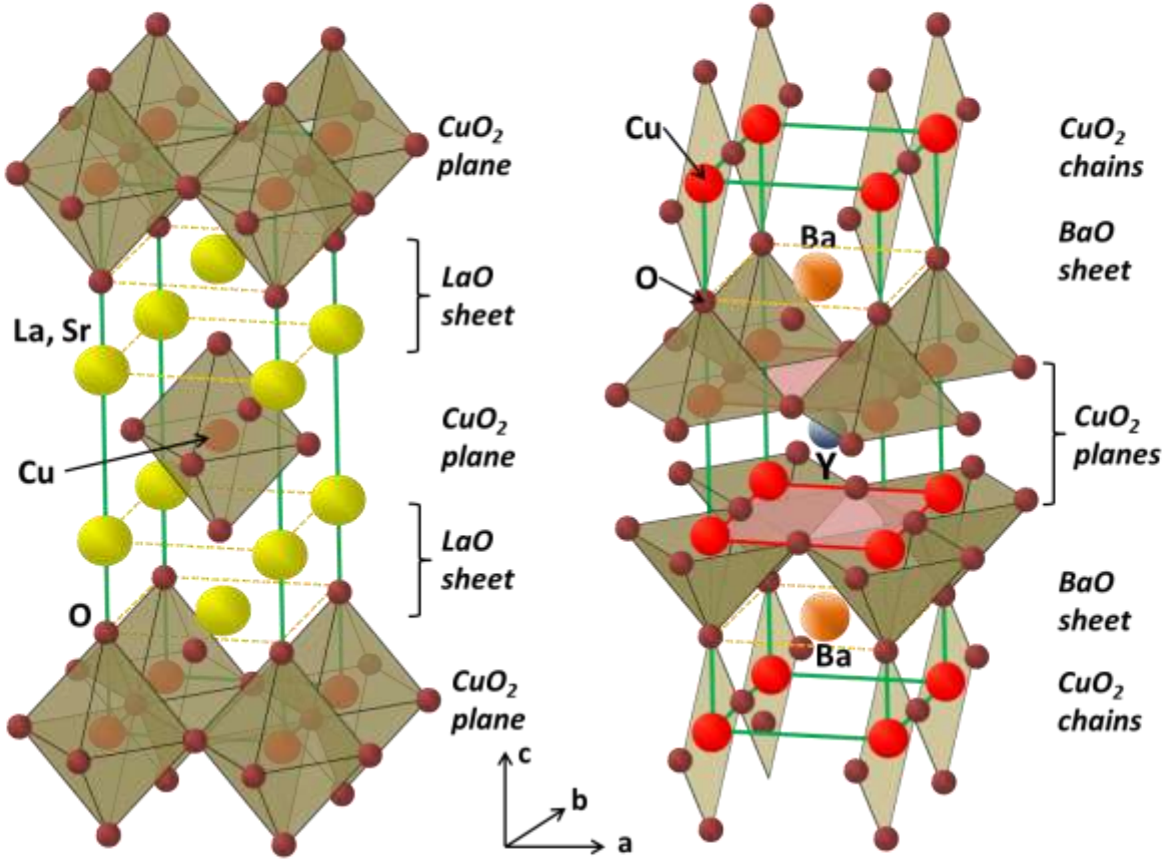

hole doping by changing oxygen content

$YBa_2Cu_3O_{7-\delta}$

$T_c = 93$ K

7.2.1 Crystal Structure

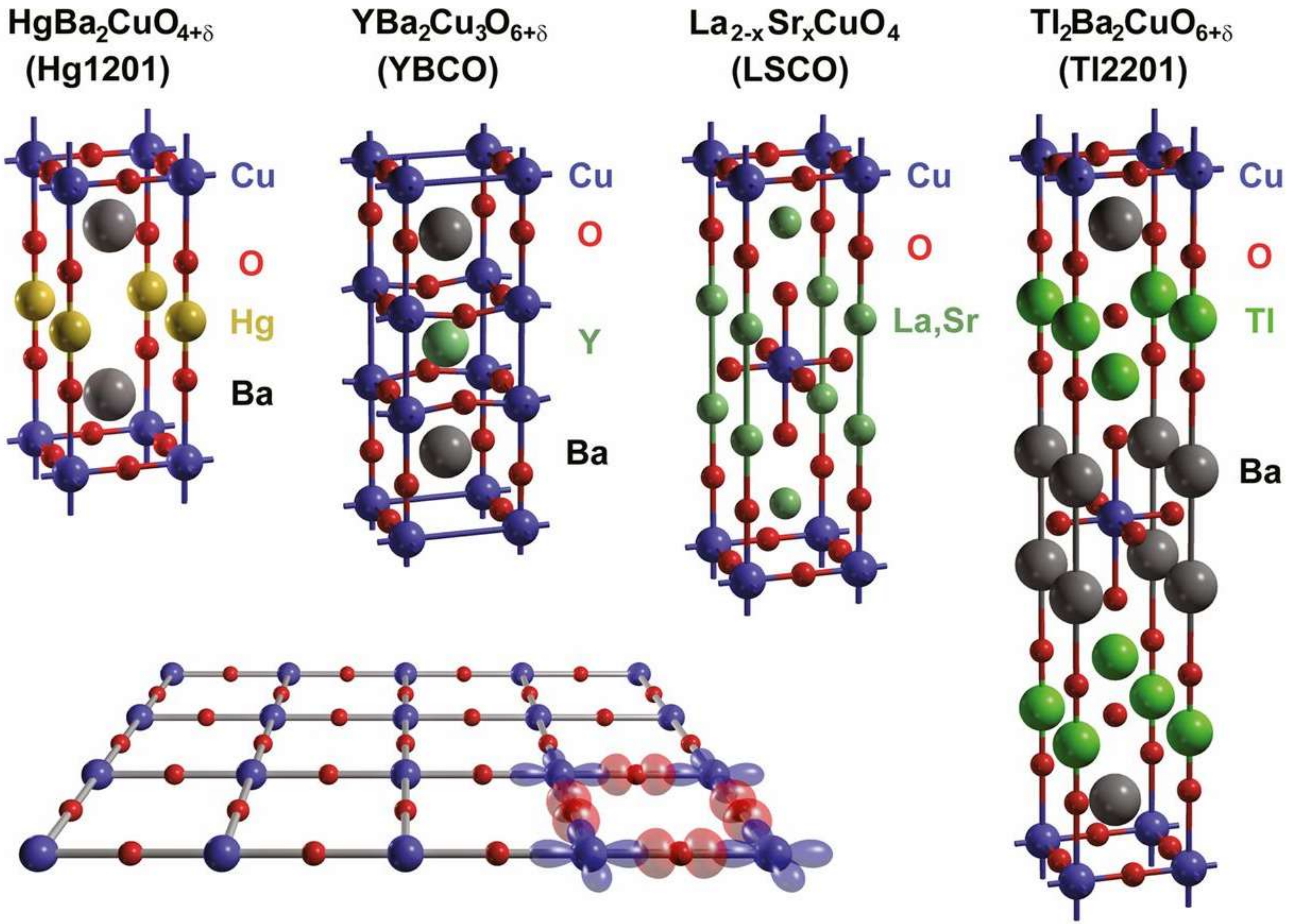

7.2.1 Crystal Structure

- HTS materials usually have complicated crystal structures
- almost all of the compounds consist of at least three different chemical elements
- most of the materials are layered cuprates, i.e., they consist of CuO planes separated by other planes of insulating rare-earth elements or other oxides
- the crystal lattice is composed of three different building blocks:

(i) perovskite (ii) the rock-salt (iii) fluorite blocks

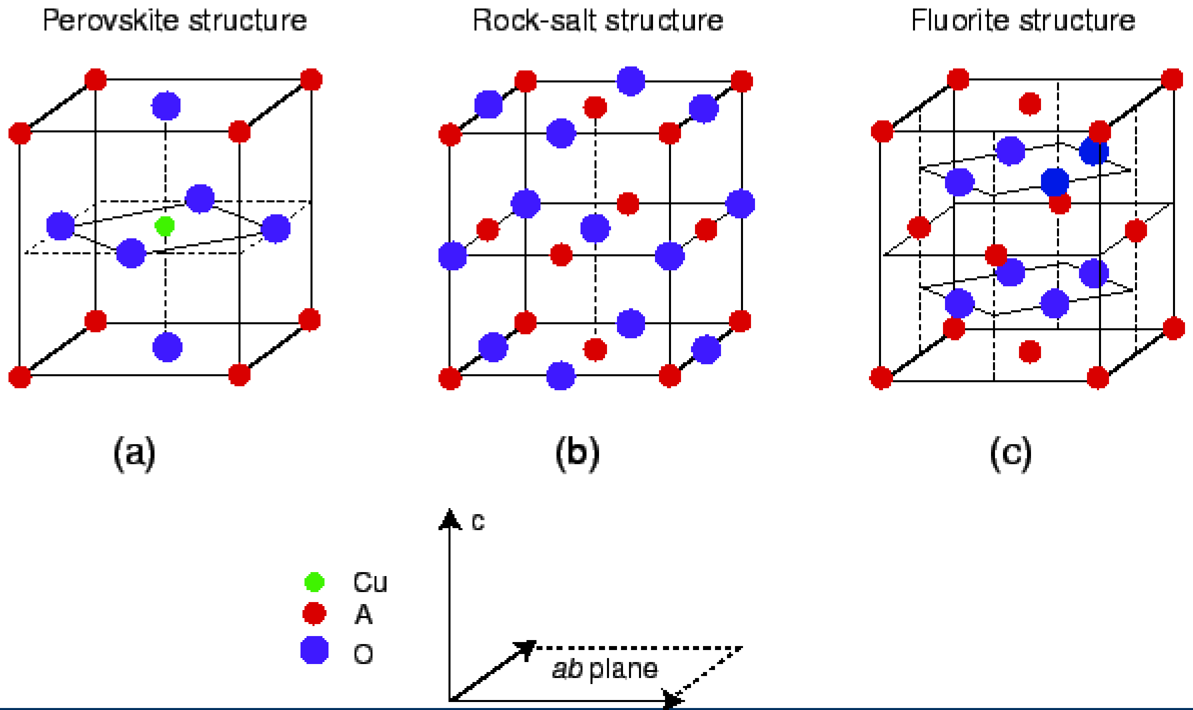

7.2.1 Crystal Structure

$Bi_2Sr_2Ca_1Cu_2O_8$
= Bi-2212 (≈ 90 K)

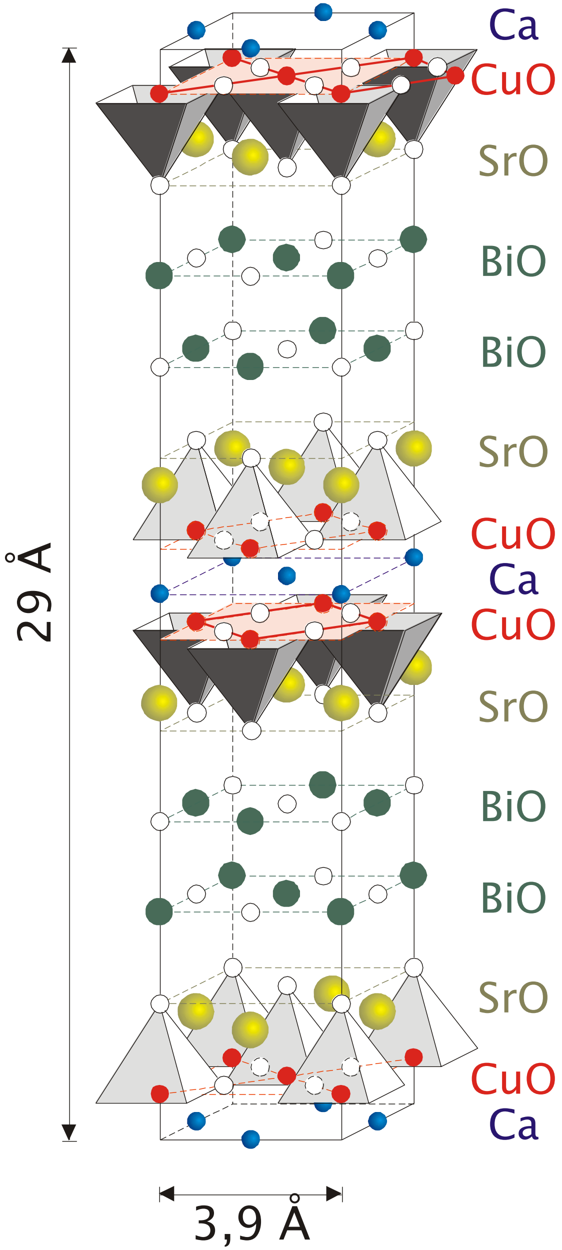

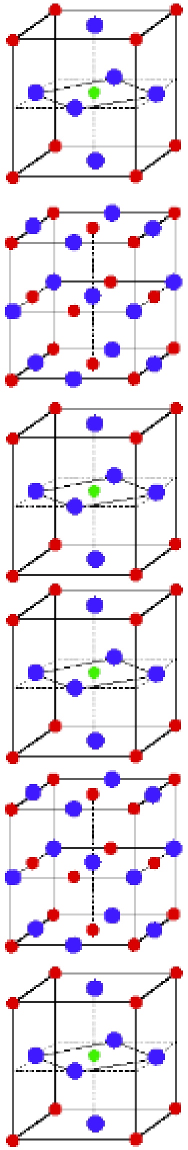

4 component systems

$$A_m B_2 Ca_{n-1} Cu_n O_{2+m+2n}$$

Bi, Tl, Hg → A

Ba, Sr = alcaline earth metals → B

examples

$Bi_2Sr_2Ca_2Cu_3O_{10}$ = Bi-2223 (110 K)
$Tl_2Ba_2Ca_2Cu_3O_{10}$ = Tl-2223 (127 K)
$HgBa_2Ca_2Cu_3O_9$ = Hg-1223 (135 K)

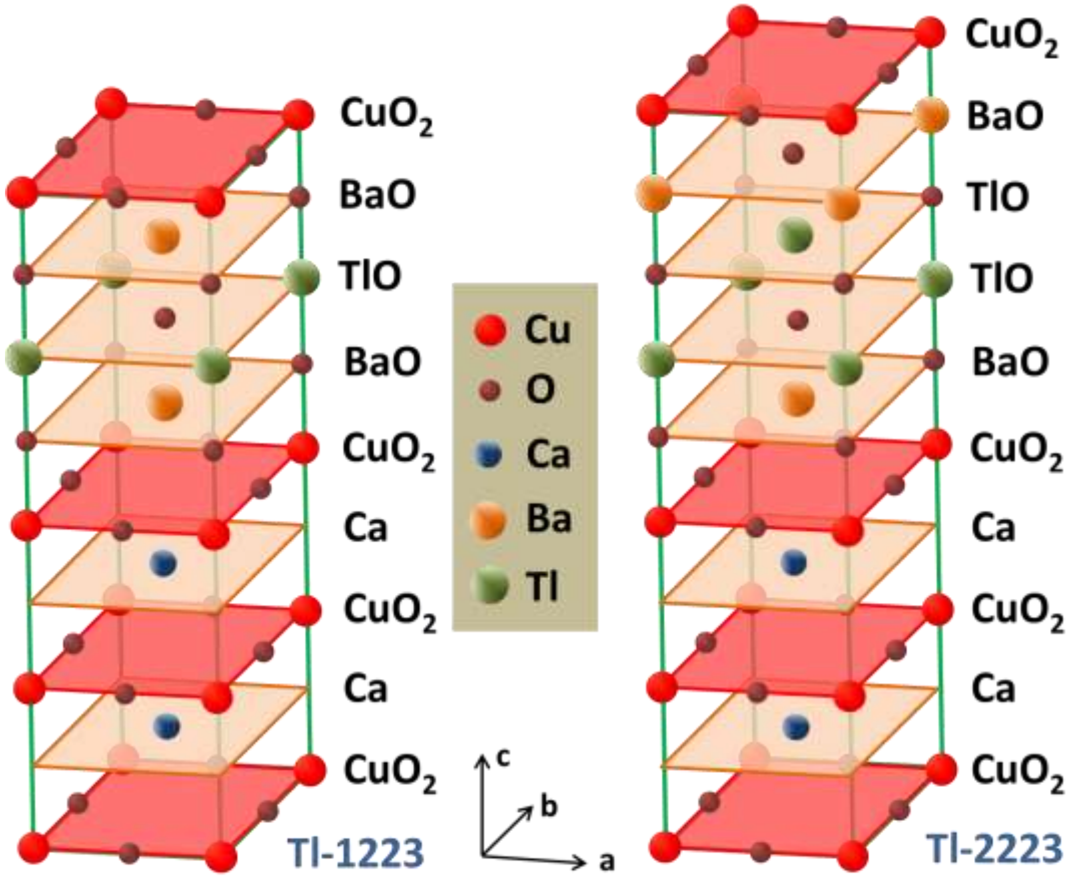

7.2.2 Phase Diagram

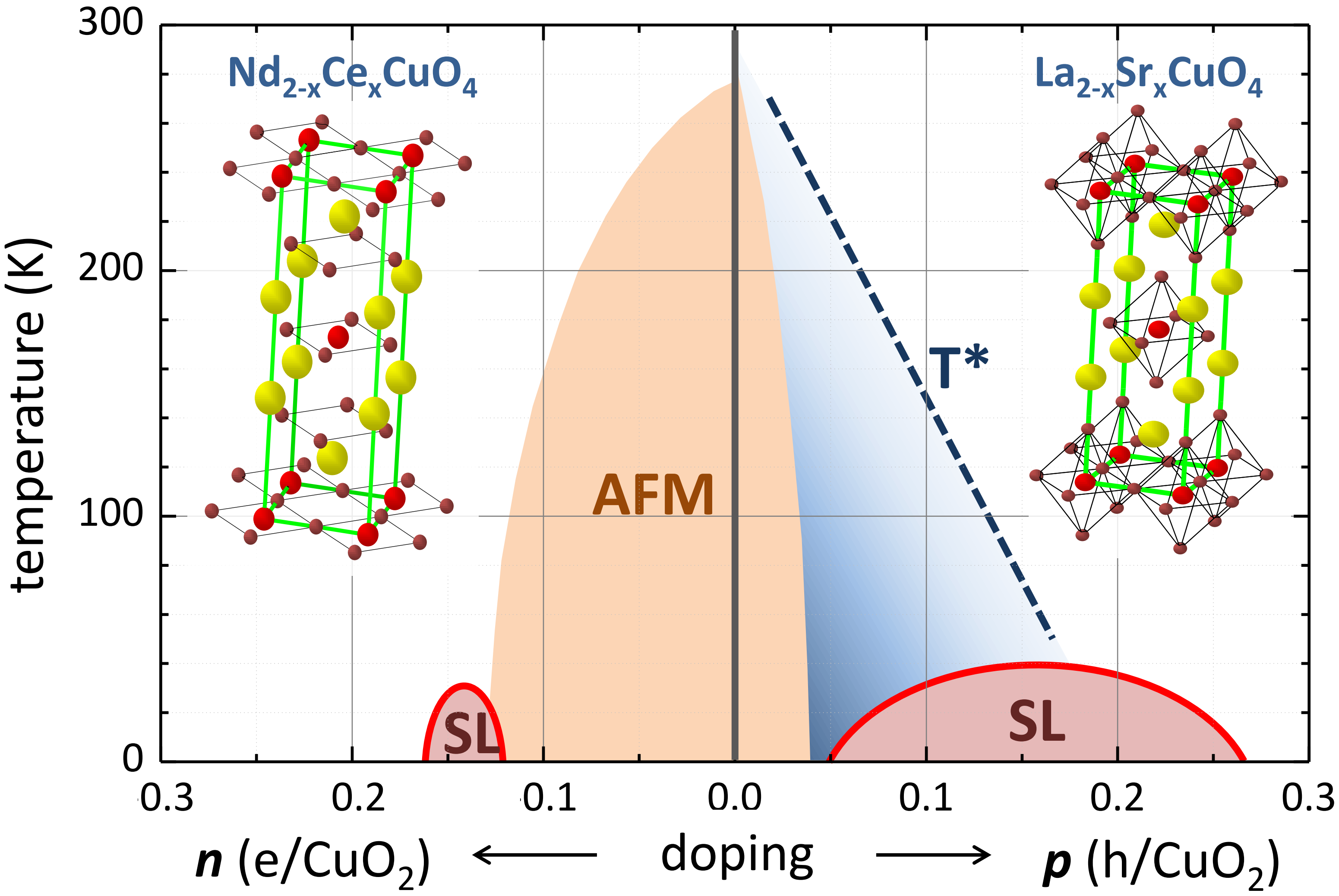

- without doping: ***cuprate superconductors are antiferromagnetic insulators***

7.2.2 Phase Diagram

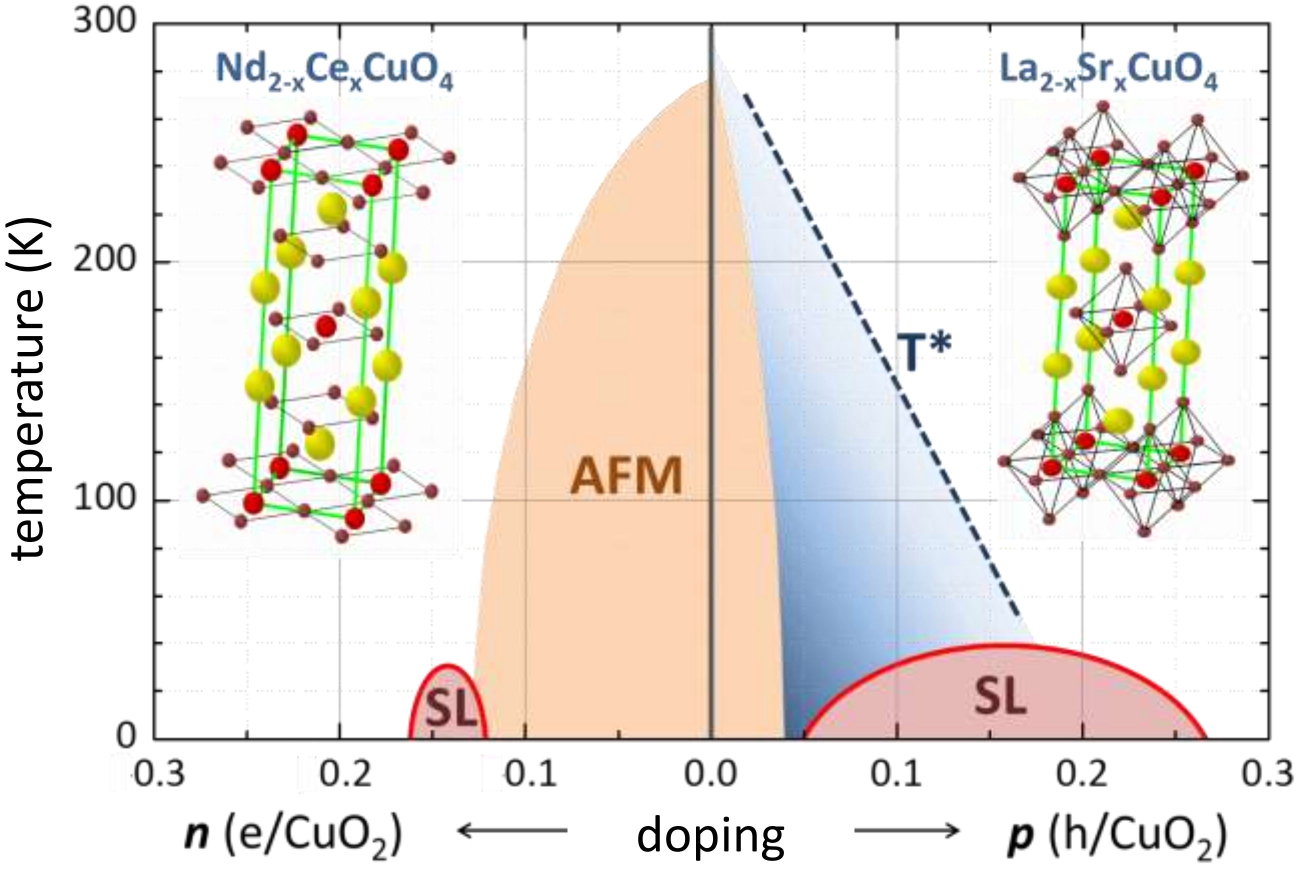

$$\frac{T_c(n)}{T_c^{max}} \simeq 1 - 1320(n - 0.1466)^2$$

$$\frac{T_c(p)}{T_c^{max}} \simeq 1 - 82.6(p - 0.16)^2$$

M. Lambacher, Ph.D. Thesis, Walther-Meißner-Institut (2008)

7.2.2 Phase Diagram

example: parent compound of Zurich oxide:

La_2CuO_4 (ionic bonding)

La^{3+} O^{2-}

Cu^{2+}

- electronic configuration of Cu: **$[Ar]3d^{10}4s^1$**

- electronic configuration of Cu^{2+}: **$[Ar]3d^9$**

→ naïve view: one hole per unit cell → half-filled band → should be a ***metal*** !!!???

→ contradicts all experimental observations

7.2.2 Phase Diagram

- why are parent compounds of cuprate superconductors afm insulators ??
  → band splits up into lower and upper Hubbard band due to strong electronic correlations (Mott insulator)

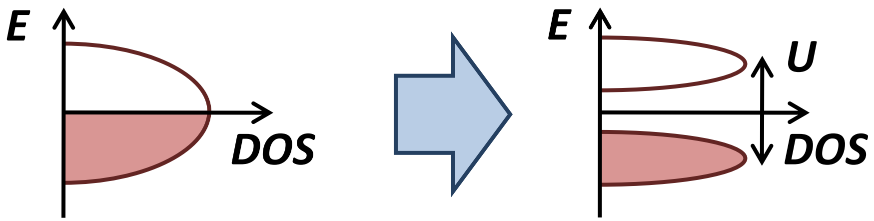

U: on-site Coulomb repulsion

(second electron at Cu-site has to pay a high on-site Coulomb repulsion $U > 1$ eV)

Hubbard - Modell

creates electron with spin σ at site i

destroys electron with spin σ at site j

particle number operator $n_{i,\sigma} = c^\dagger_{i,\sigma} c_{i,\sigma}$

$$\mathcal{H}_{\text{Hubbard}} = -t \sum_{\langle i.j \rangle,\, \sigma} \underbrace{\left(c^\dagger_{i,\sigma}\, c_{j,\sigma} + c^\dagger_{j,\sigma}\, c_{i,\sigma} \right)} + \underbrace{\sum_i U\, n_{i,\uparrow} n_{i,\downarrow}}$$

summation over nearest neighbors

spin: $\sigma = \uparrow, \downarrow$

hopping between neighboring sites, hopping amplitude t

Coulomb energy for multiple occupancy of single site

7.2.2 Phase Diagram

- why are parent compounds of cuprate superconductors afm insulators ??
  → band splits up into lower and upper Hubbard band due to strong electronic correlations (Mott insulator)

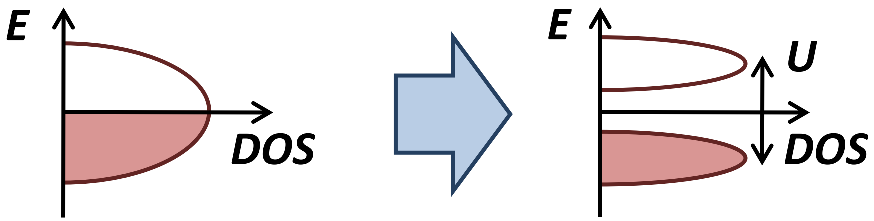

U: on-site Coulomb repulsion

(second electron at Cu-site has to pay a high on-site Coulomb repulsion $U > 1$ eV)

- detailed analysis of undoped CuO_2 plane → ***charge transfer insulator ($\Delta < U$)***

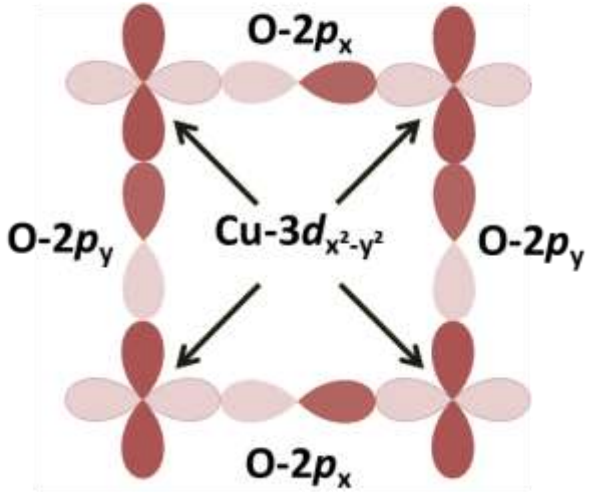

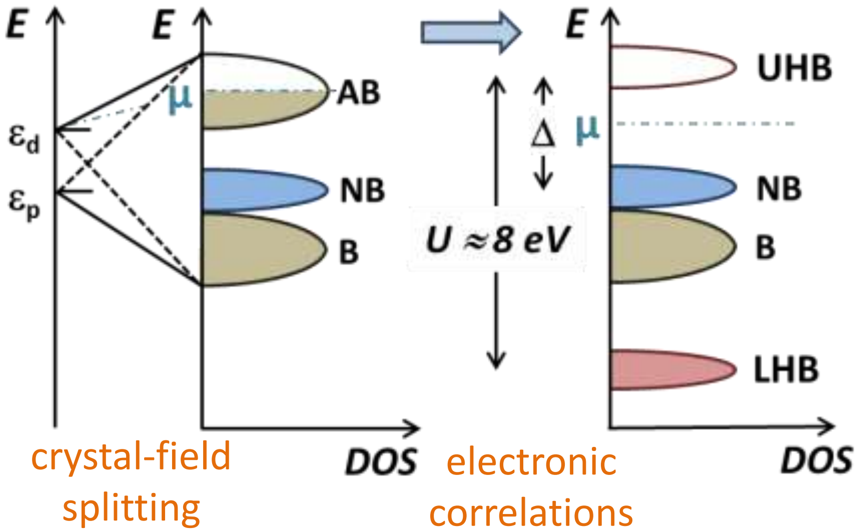

7.2.2 Phase Diagram

- antiferromagnetic interaction in CuO_2 plane (undoped parent compound)

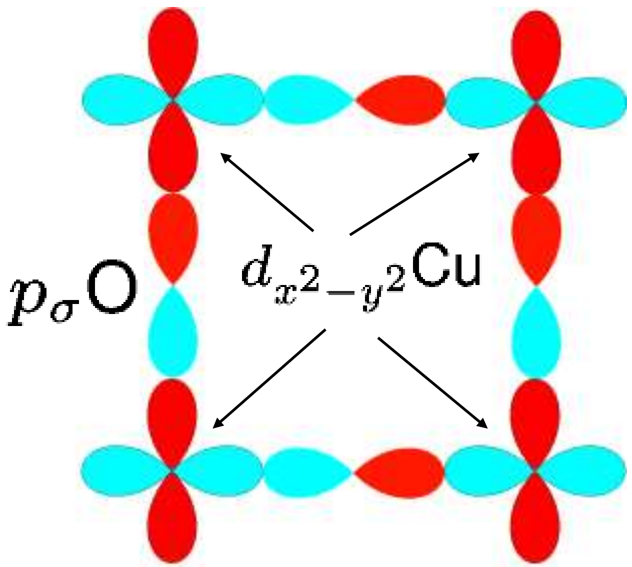

180° superexchange

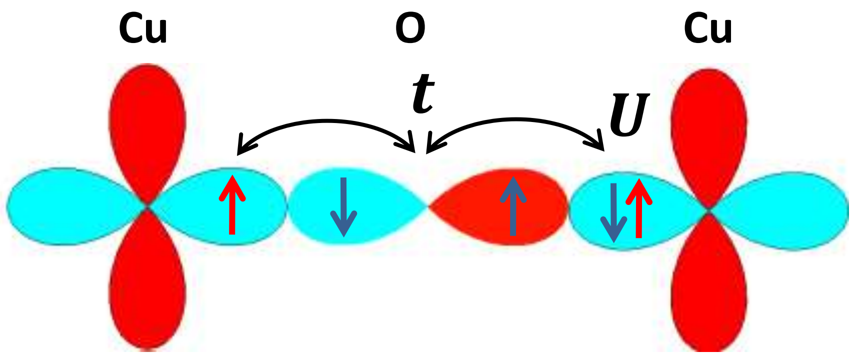

How to dope cuprates to to get superconductivity ?

delocalization of electrons via virtual hopping:
- hopping amplitude t
- virtual hopping only possible for anti-parallel spins on Cu-site (Pauli)
- real hopping prevented by on-site Coulomb repulsion $U \gg t$

- energy gain by virtual hopping $\propto t^2/U$

7.2.2 Phase Diagram

- **analogy to modulation doping in semiconductors (e.g. GaAs/AlGaAs)**

  → generation of high mobility electron gas (dopant atoms in neighboring layer)

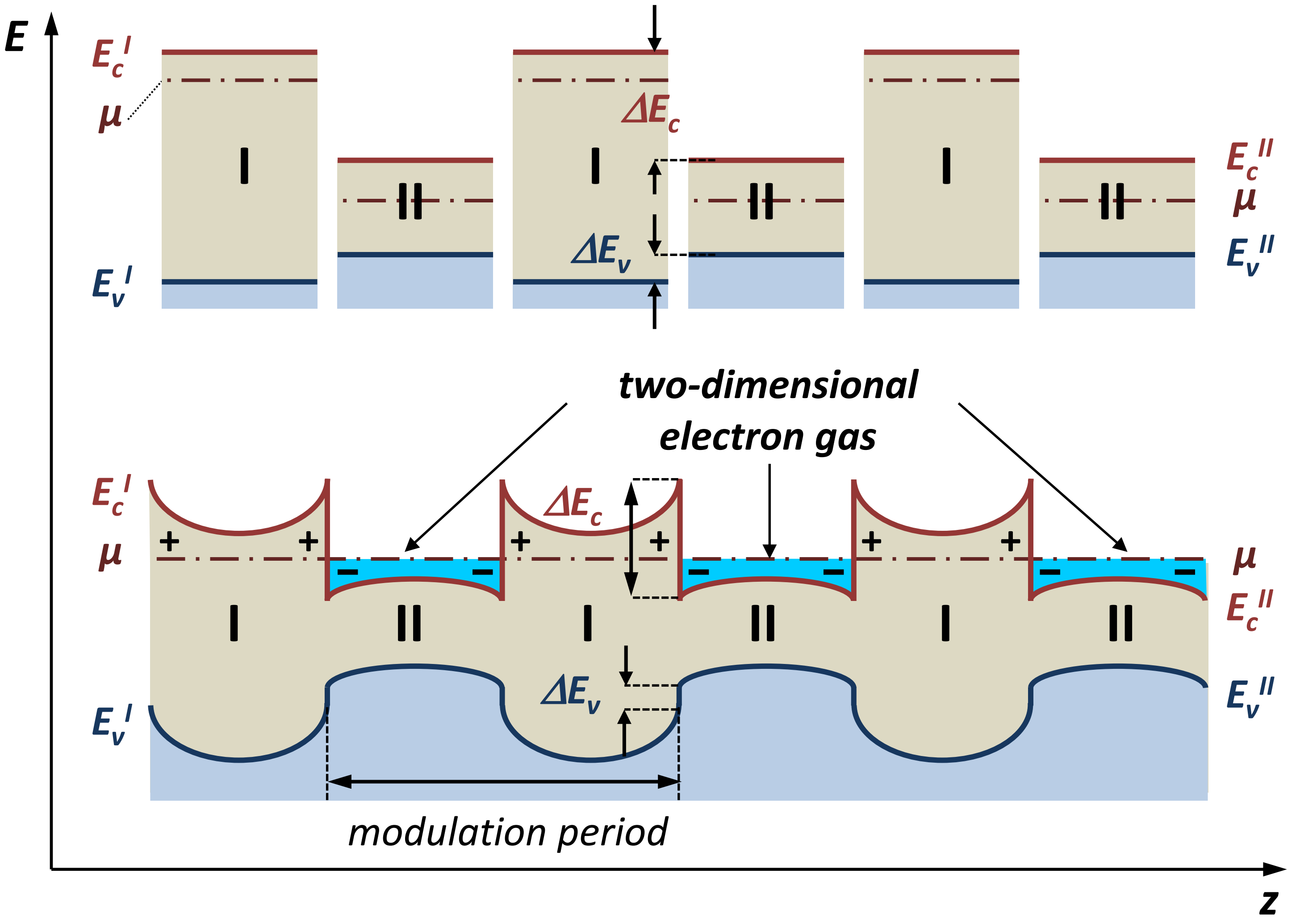

semiconductor composition superlattice

7.2.2 Phase Diagram

- cuprate superconductors = *intrinsically modulation doped materials*

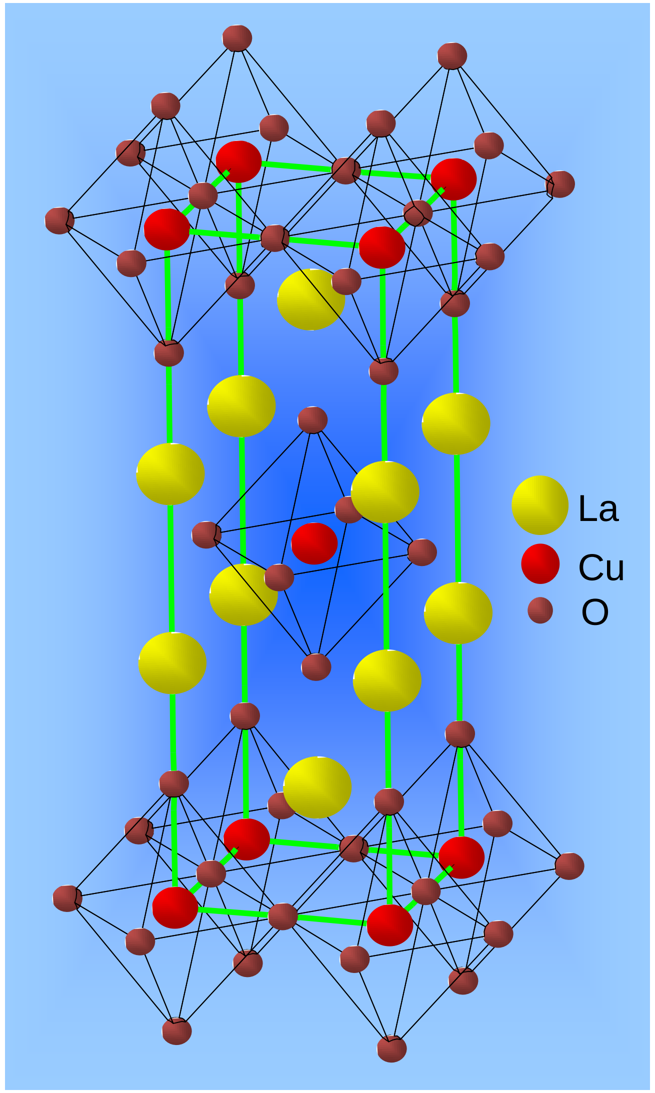

CuO_2 plane

charge reservoir layer:
partially replace La^{3+} by Sr^{2+} → hole doping

CuO_2 plane

charge reservoir layer:
partially replace La^{3+} by Sr^{2+} → hole doping

CuO_2 plane

7.2.2 Phase Diagram

- **How is the afm ordering in the undoped parent compound affected by doping?**

→ destruction of afm ordering in CuO_2 planes by hole and electron doping

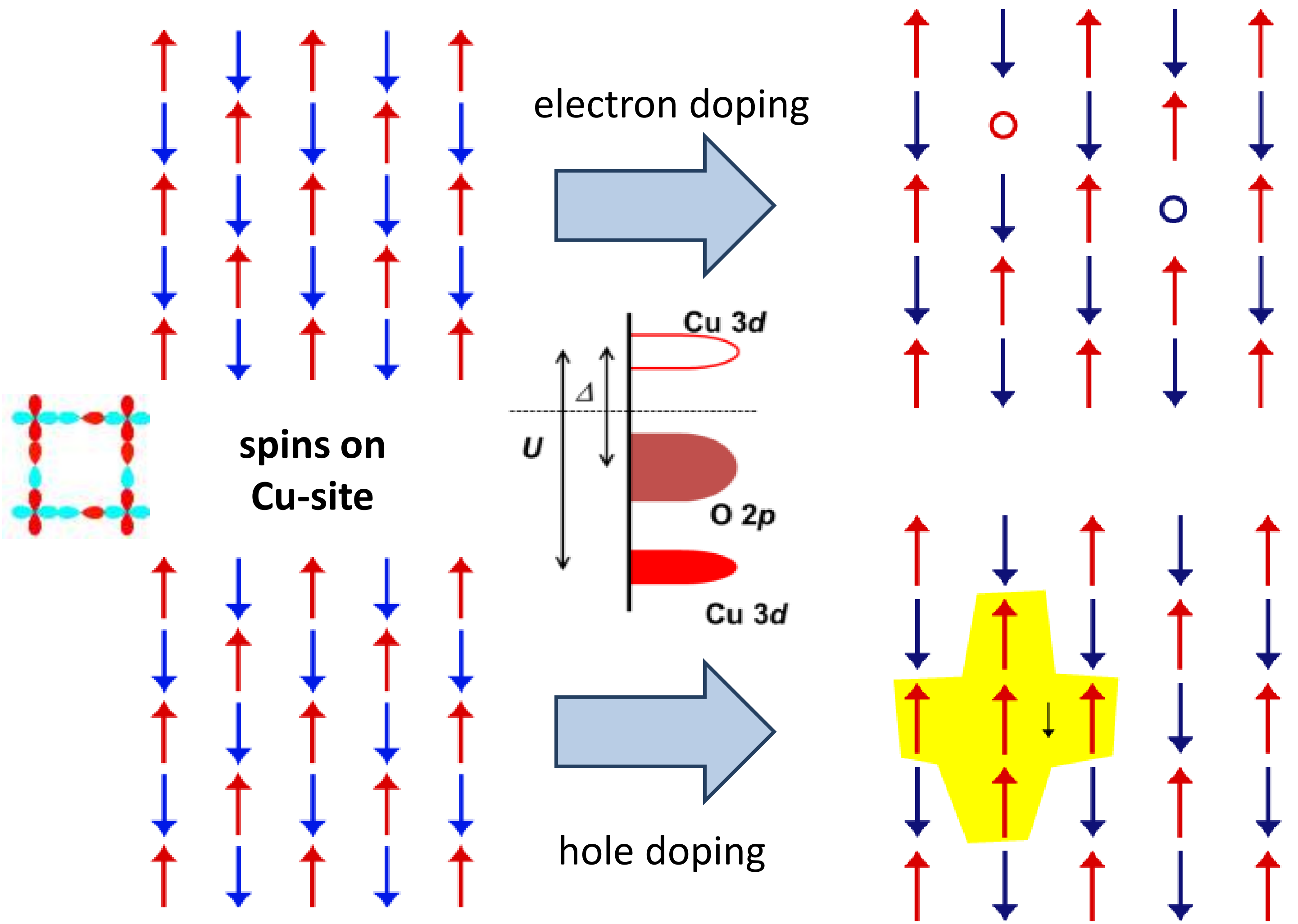

electron doping:
removes hole spin
→ **spin dilution**

hole doping:
adds hole spin
→ **spin frustration**

7.2.2 Phase Diagram

- **asymmetry of phase diagram regarding electron and hole doping**

- doping into different bands:
  → electrons into Cu 3d band
  → holes into O 2p band
- different effect on afm ordering:
  → spin dilution for electron doping
  → spin frustration for hole doping

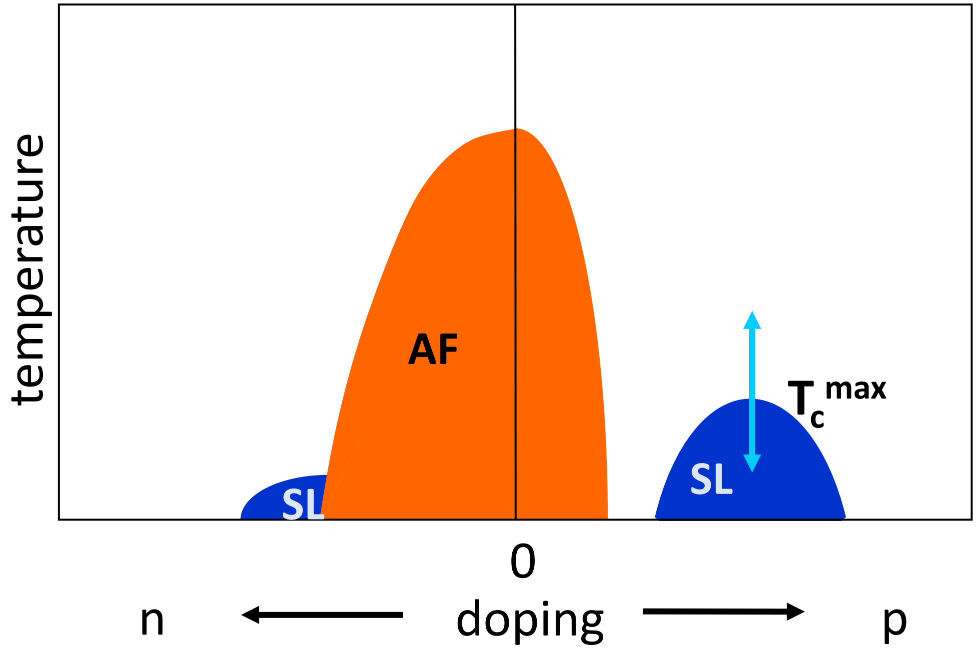

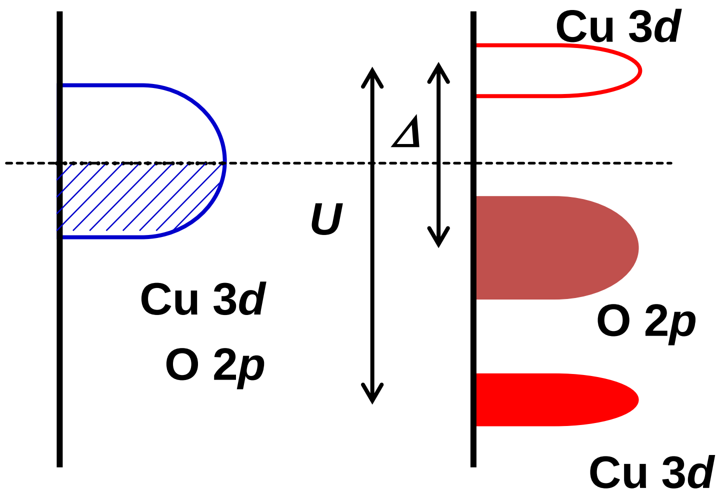

7.3 Electronic Structure

- simple approach: *tight binding model*

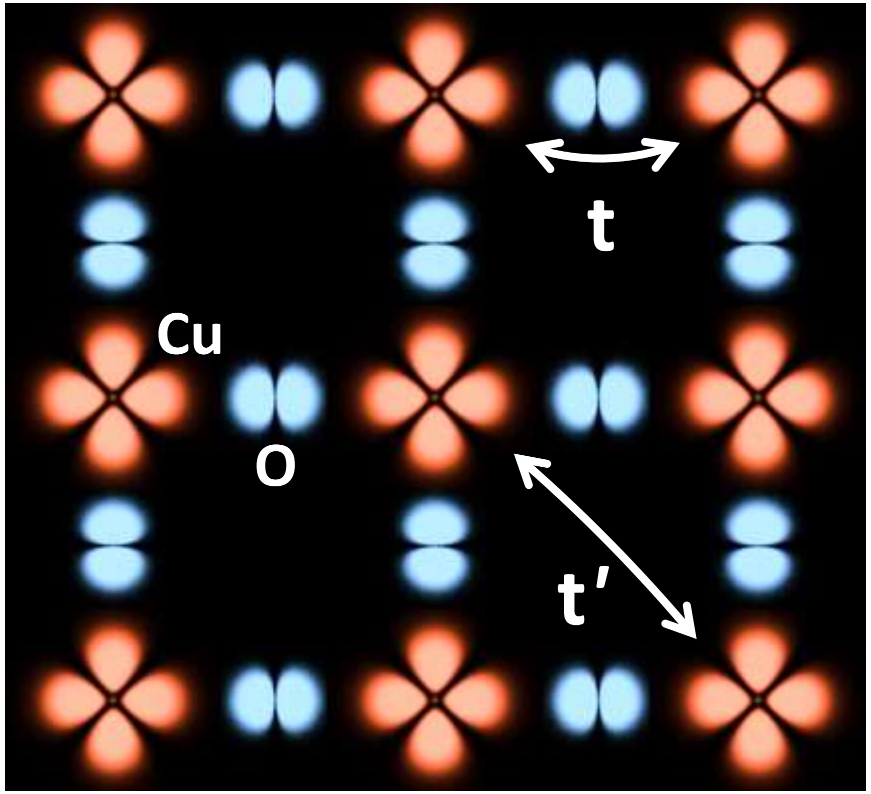

nearest neighbor hopping **t**

next-nearest neighbor hopping **t'**

O $2p_x, 2p_y$

Cu $3d_{x^2-y^2}$

$t' = 0$

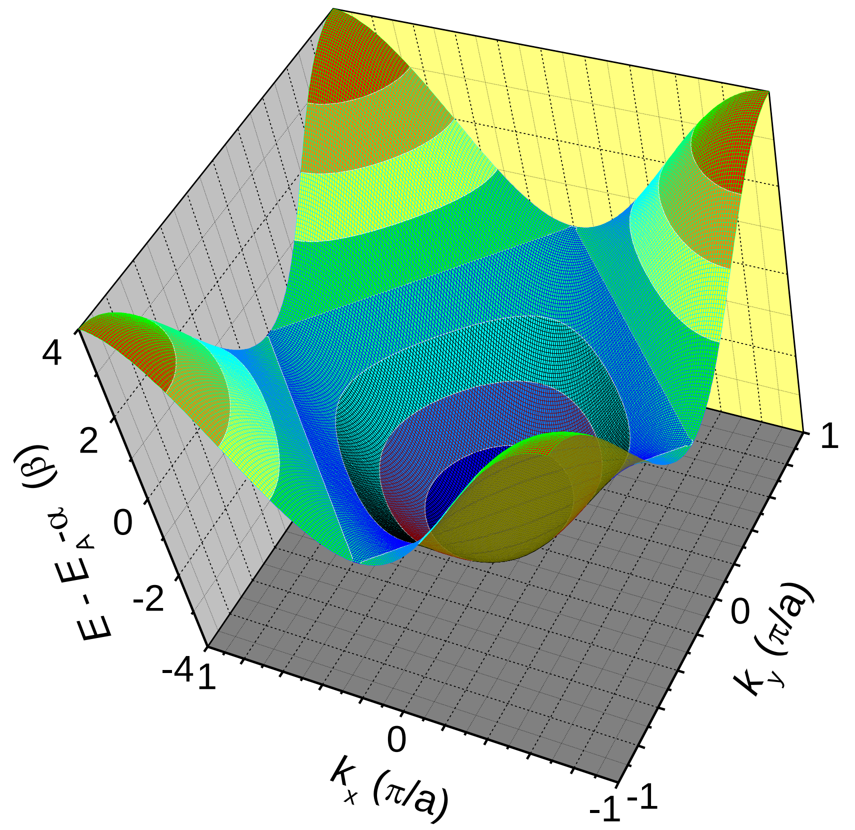

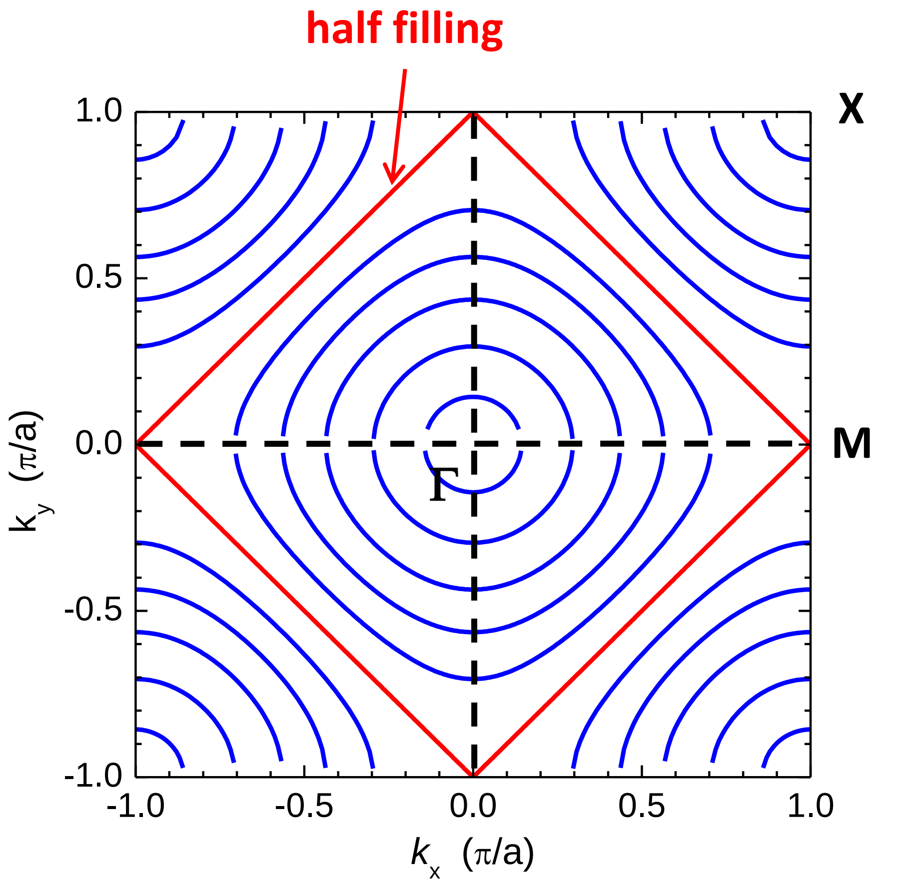

$$E(\mathbf{k}) = E_\mathrm{A} - \alpha - 2\beta\left[\cos(k_x a) + \cos\left(k_y a\right)\right]$$

$t' \neq 0$

nearest neighbor hopping t

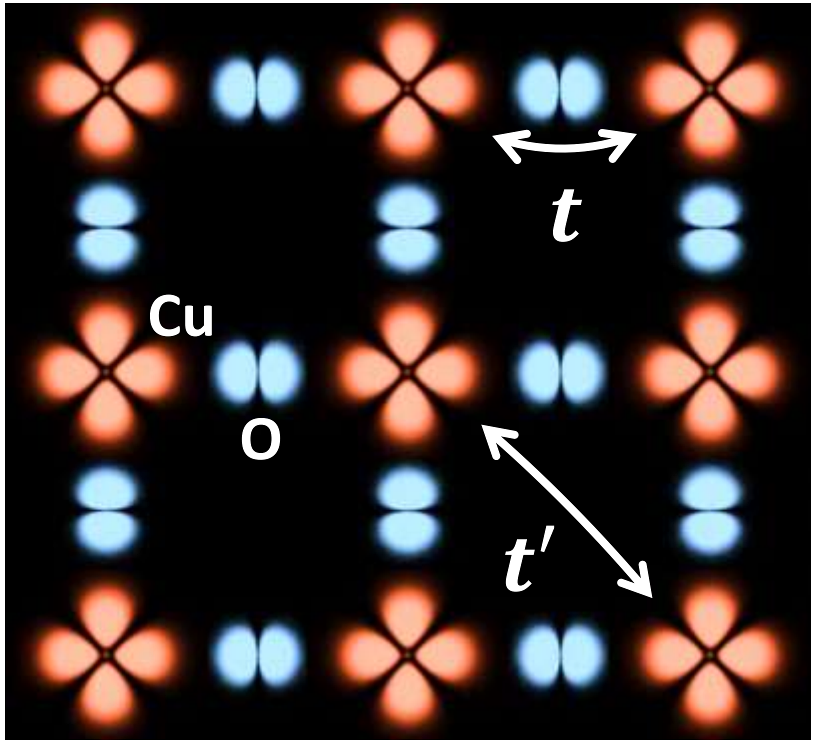

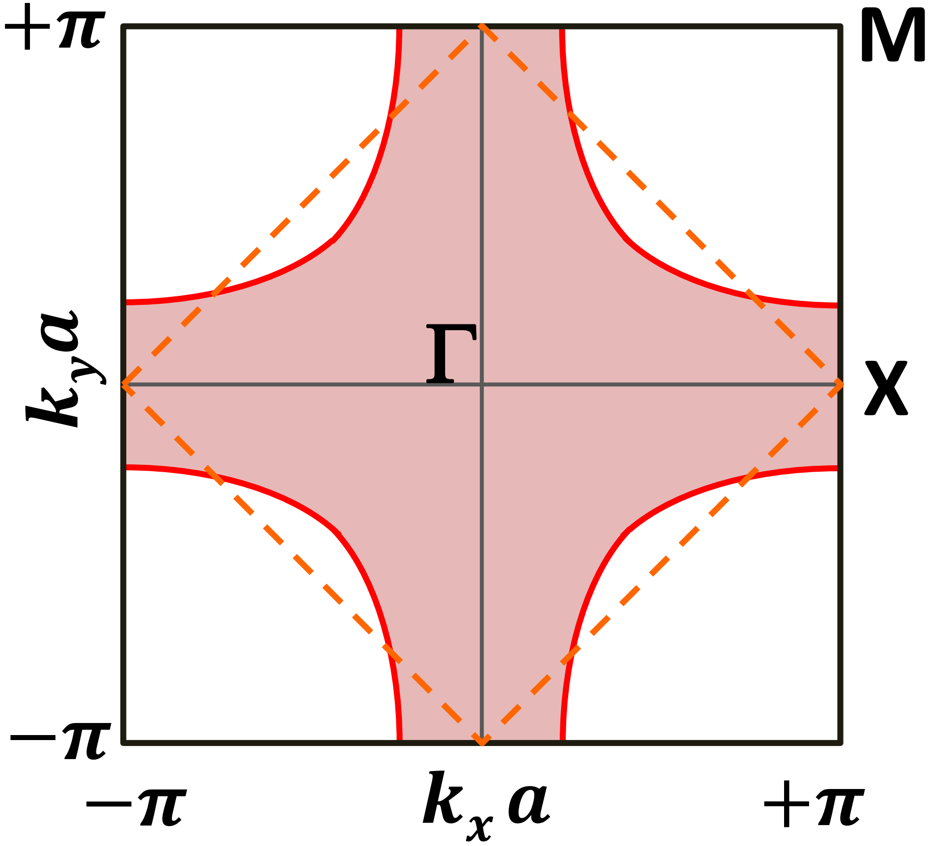

next-nearest
neighbor hopping t'

- **tight-binding band structure:**

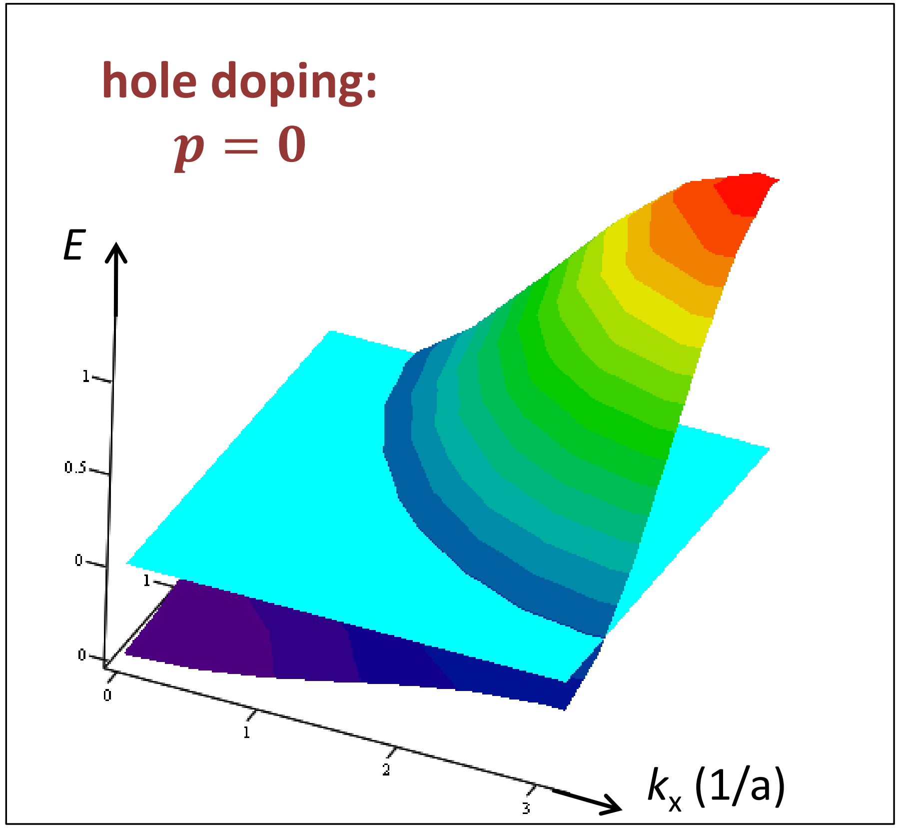

ξ, EF

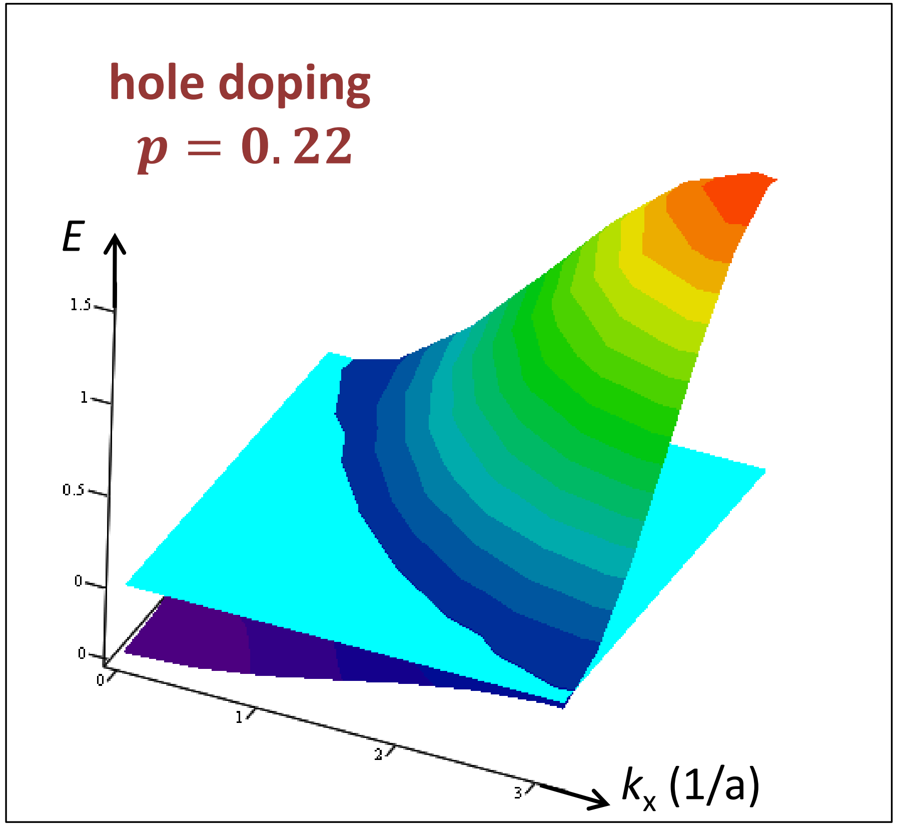

ξ, EF

Summary of Lecture No. 13 (1)

Discovery of high temperature superconductivity in cuprates by Bednorz and Müller (1986)

- completely unexpected (oxides)
- hype in superconductivity research (simple cooling by LN_2)
- no complete understanding until today

Crystal structure

- layered, ***anisotropic materials***
- stack sequence of perovskite, rock-salt, and fluorite blocks
- common structural unit: ***CuO_2 planes***
- other layers important for charge doping and degree of anisotropy → ***intrinsic modulation doping***

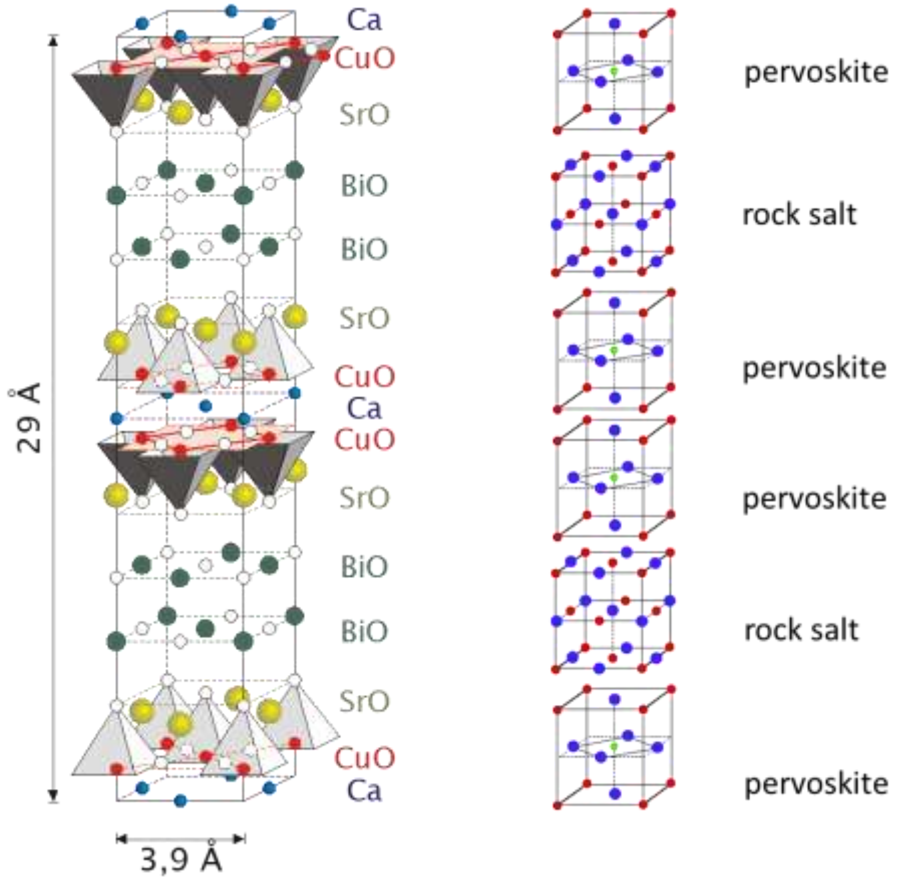

Summary of Lecture No. 13 (2)

Electronic structure

- naively expected: odd number of charge carriers per unit cell → half-filled band → metallic behavior
- experimentally measured: antiferromagnetic insulators in undoped state
- explanation of discrepancy: strong electronic correlations result in splitting of band into empty UHB and full LHB
- origin of antiferromagnetism: 180° superexchange between Cu spins via full oxygen orbitals
- electron doping: additional electron in Cu 3d orbital → removes hole spin, dilution of afm spin lattice
- hole doping: hole in O 2p orbital → adds hole spin on O site → frustration of afm spin lattice

Fermi surface

- simple guess by 2D tight-binding model with nearest and next-nearest neighbor hopping

Walther Meißner Institut

BAdW | BAYERISCHE AKADEMIE DER WISSENSCHAFTEN

Technische Universität München

Superconductivity and Low Temperature Physics I

Lecture No. 14
03 February 2022

R. Gross

7 High Temperature Superconductivity

7.3 Electronic Structure

- **Angle-Resolved Photoelectron Spectroscopy (ARPES)**

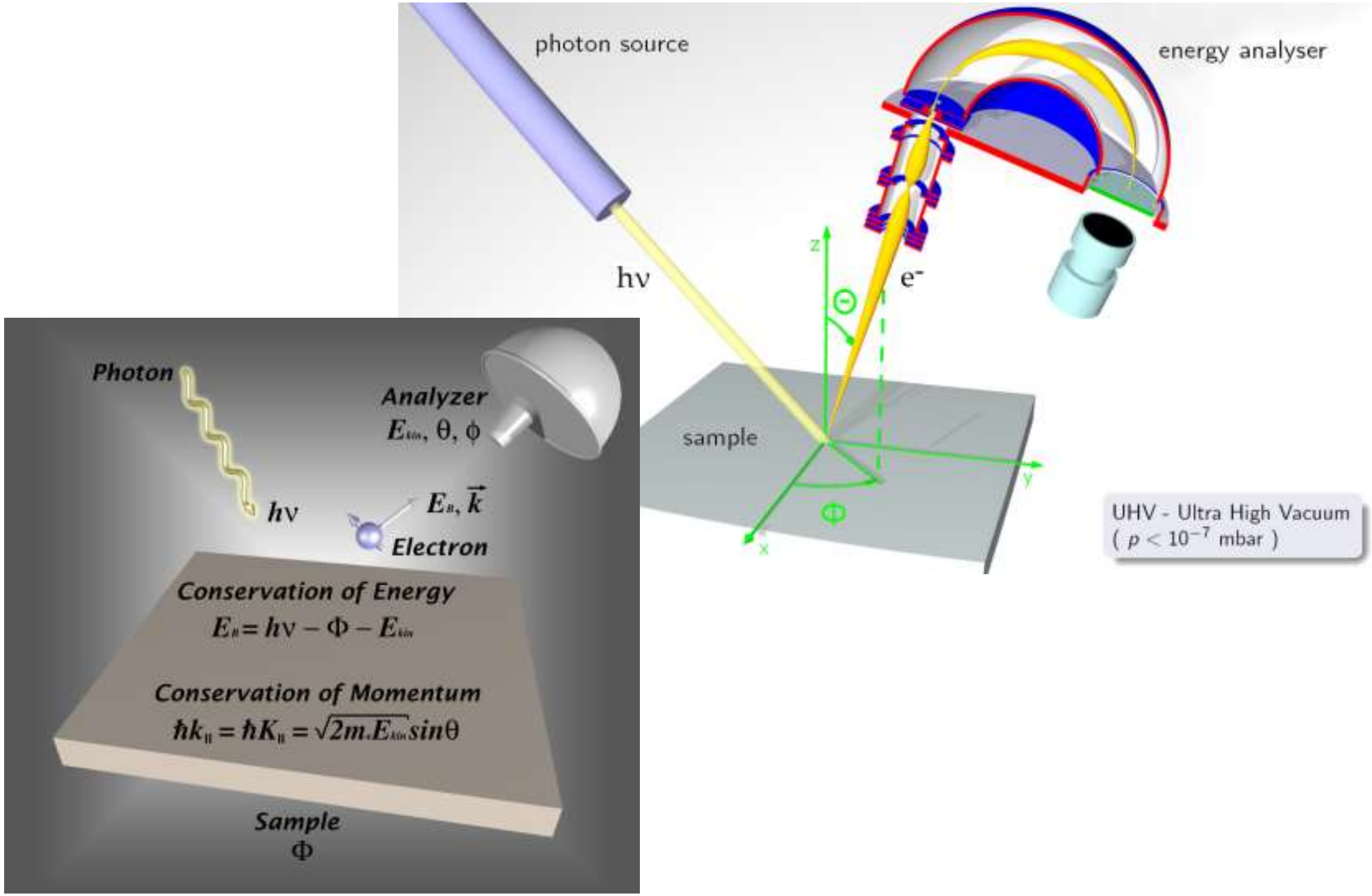

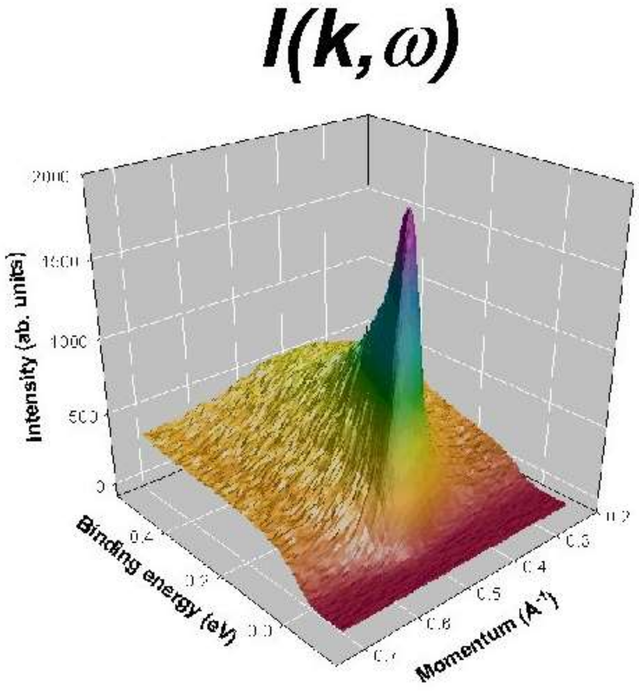

- **Angle-Resolved Photoelectron Spectroscopy (ARPES)**

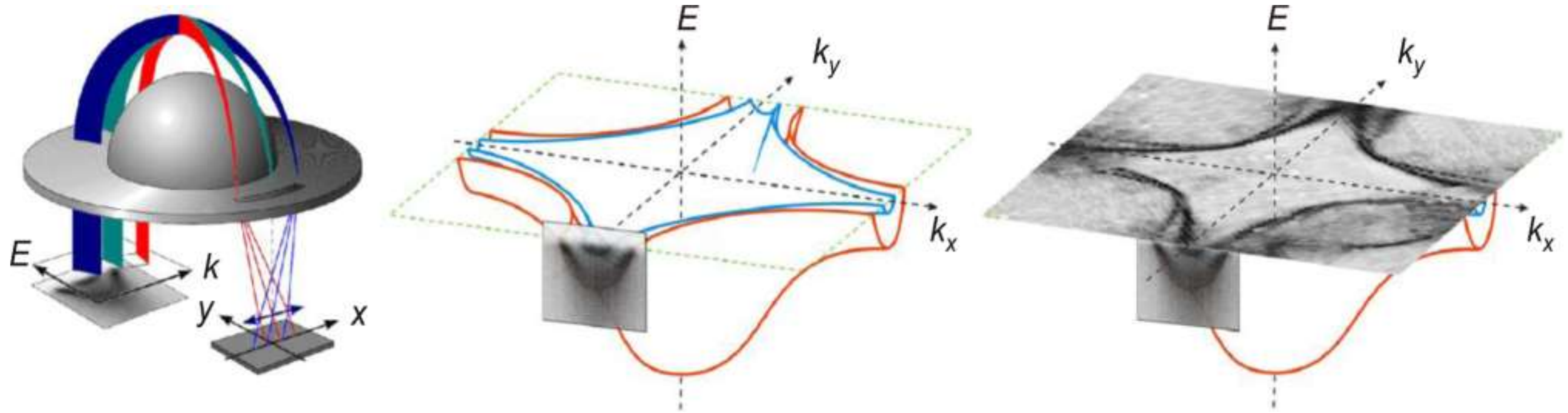

The detector of a modern photoelectron analyzer (left) acts as a **window into the 3D energy-momentum space** of a 2D metal (center). By moving this “window” in (ω, k)-space, a full distribution of electrons and its cross-section at the Fermi level — the Fermi surface (right) can be obtained. Shown are the electronic structure and spectra of high-temperature superconductor Bi-2212.

ARPES experiment in fermiology of quasi-2D metals
A. A. Kordyuk
Low Temp. Phys. **40**, 286-296 (2014)

- **Angle-resolved photoemission spectroscopy (ARPES)**

$(Bi,Pb)_2Sr_2CaCu_2O_{8+\delta}$

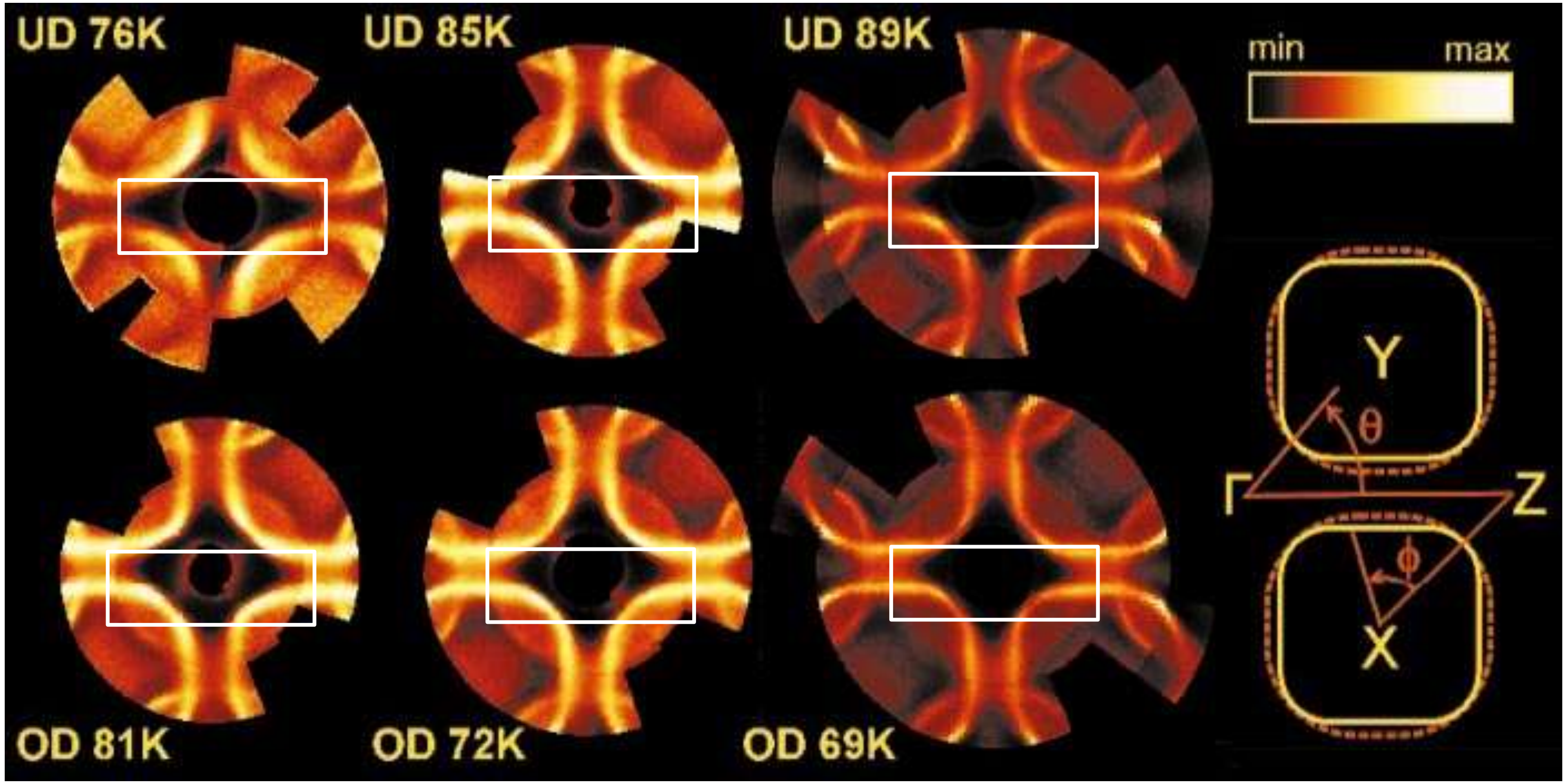

Doping dependence of the Fermi surface in $(Bi,Pb)_2Sr_2CaCu_2O_{8+\delta}$
A. A. Kordyuk, S. V. Borisenko, M. S. Golden, S. Legner, K. A. Nenkov, M. Knupfer, J. Fink, H. Berger, L. Forro, R. Follath
Phys. Rev. B **66**, 014502 (2002)

- **Angle-resolved photoemission spectroscopy (ARPES)**

$(Bi,Pb)_2Sr_2CaCu_2O_{8+d}$

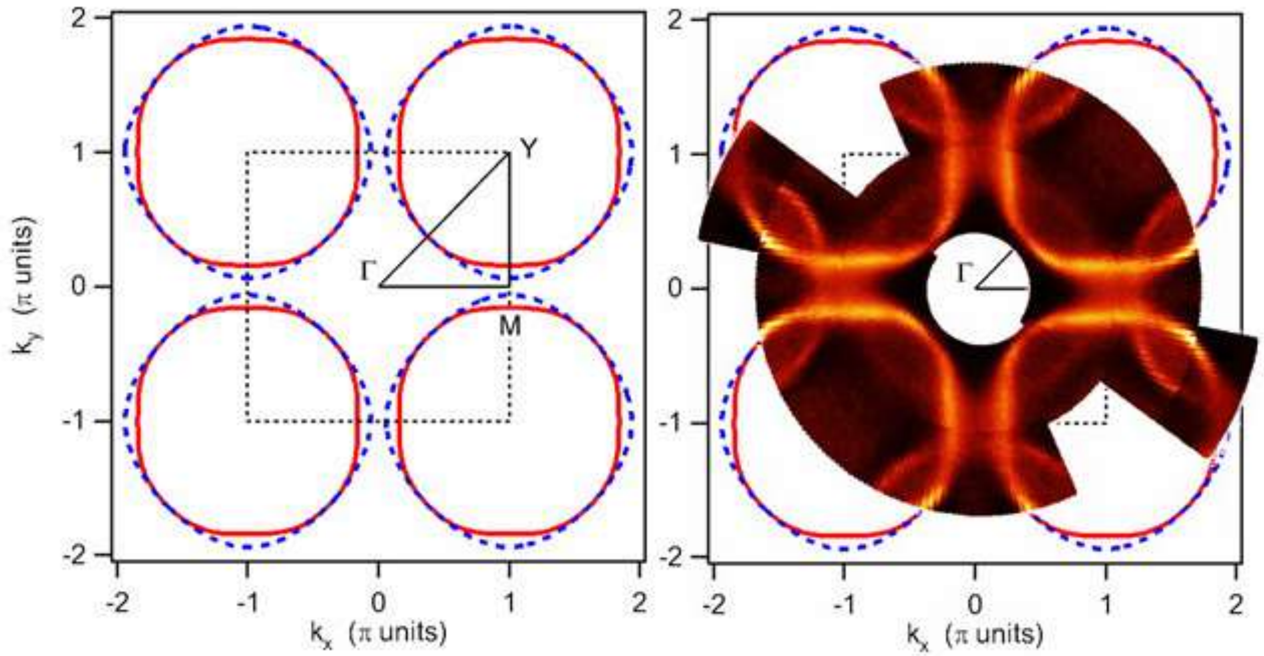

The Fermi surface of bi-layer BSCCO, calculated (left) and measured by ARPES (right). The dashed rectangle represents the first Brillouin zone.

Measuring the gap in angle-resolved photoemission experiments on cuprates
A. A. Kordyuk, S. V. Borisenko, M. Knupfer, and J. Fink
Phys. Rev. B **67**, 064504 – Published 25 February 2003

7.3 Electronic Structure

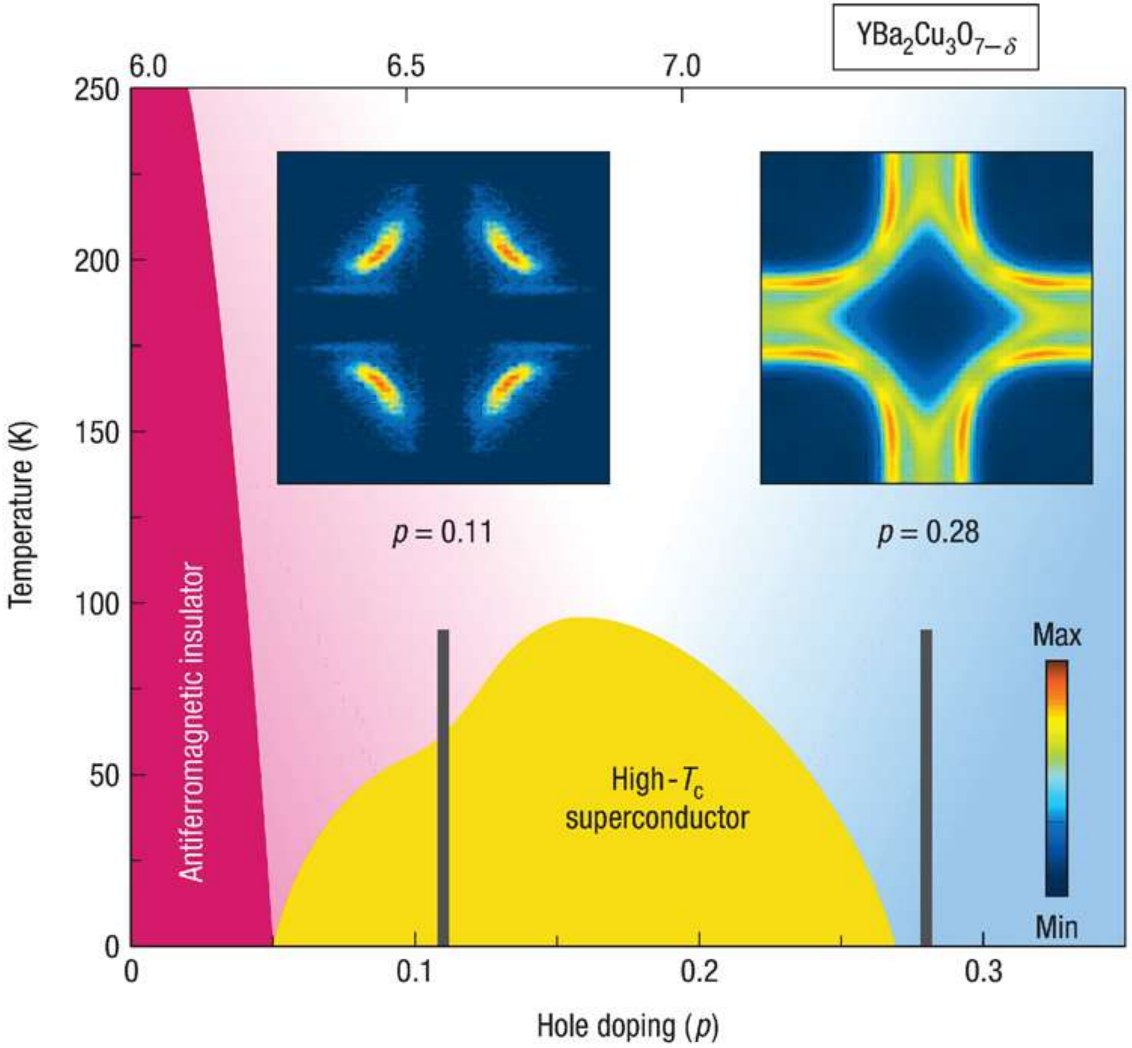

Schematic phase diagram of YBCO. The hole doping p per planar copper and the corresponding oxygen content (7-δ), are indicated on the bottom and top axes. The ARPES Fermi surface for under- and overdoped YBCO is also shown (according to A. Damascelli et al.)

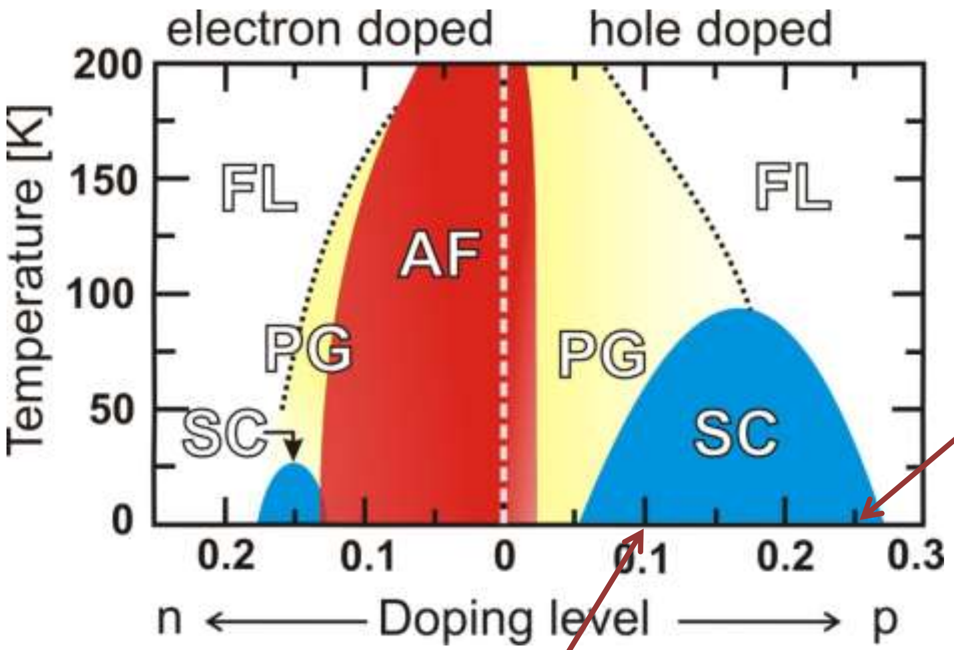

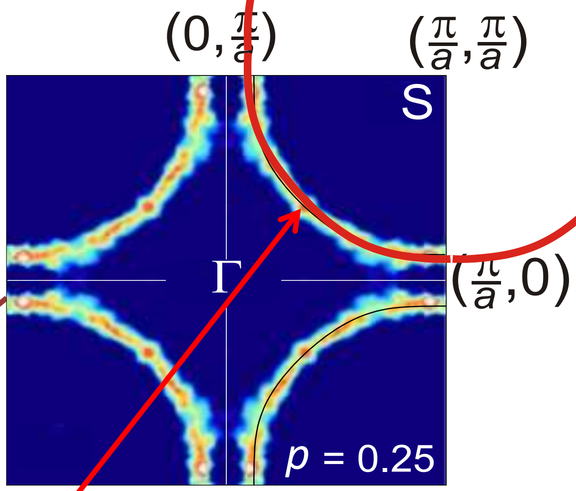

M. Plate et al., *PRL* 95, 077001 (2005)

SdH: Tl-2201 ($p \approx 0.25$)
B. Vignolle et al., *Nature* 455, 952 (2008)

ARPES:

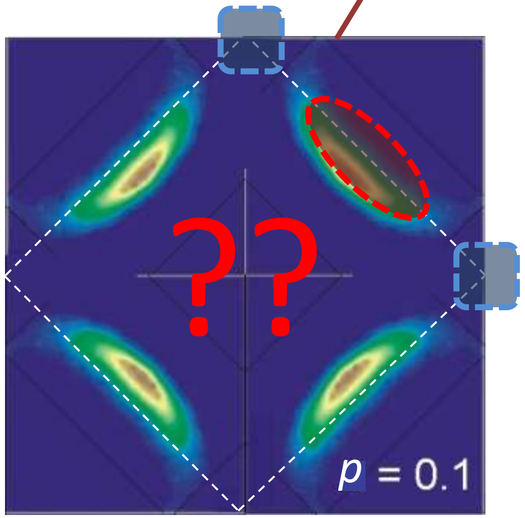

K. Shen et al., *Science* 307, 901 (2005)

1st Shubnikov – de Haas oscillations
$YBa_2Cu_3O_{6.5}$ ($p \approx 0.1$)
N. Doiron-Leyraud *et al.*, *Nature* 447, 565 (2007)
D. LeBoeuf *et al.*, *Nature* 450, 522 (2007)

small closed Fermi surface

$YBa_2Cu_4O_8$ ($p \approx 0.12$)
E. Yelland et al., *PRL* 100, 047003 (2008)
A. Bangura et al., *PRL* 100, 047004 (2008)

- Magnetic quantum oscillations (dHvA, SdH effects)

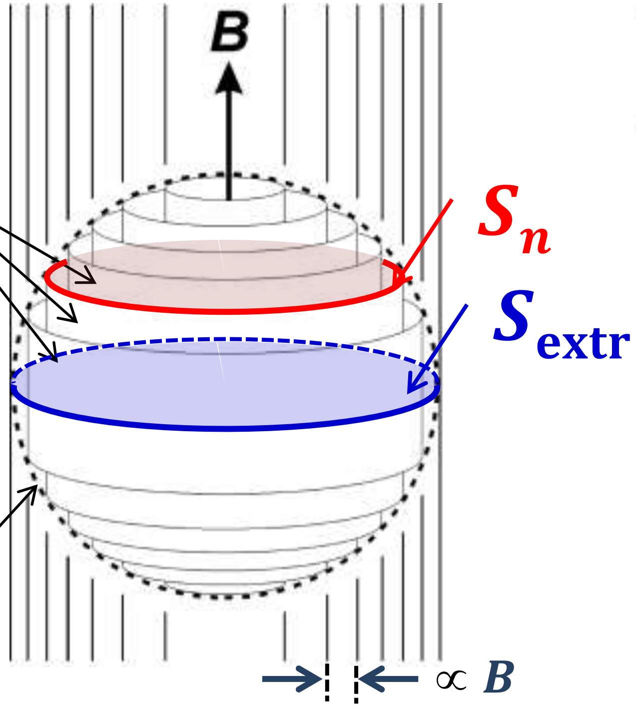

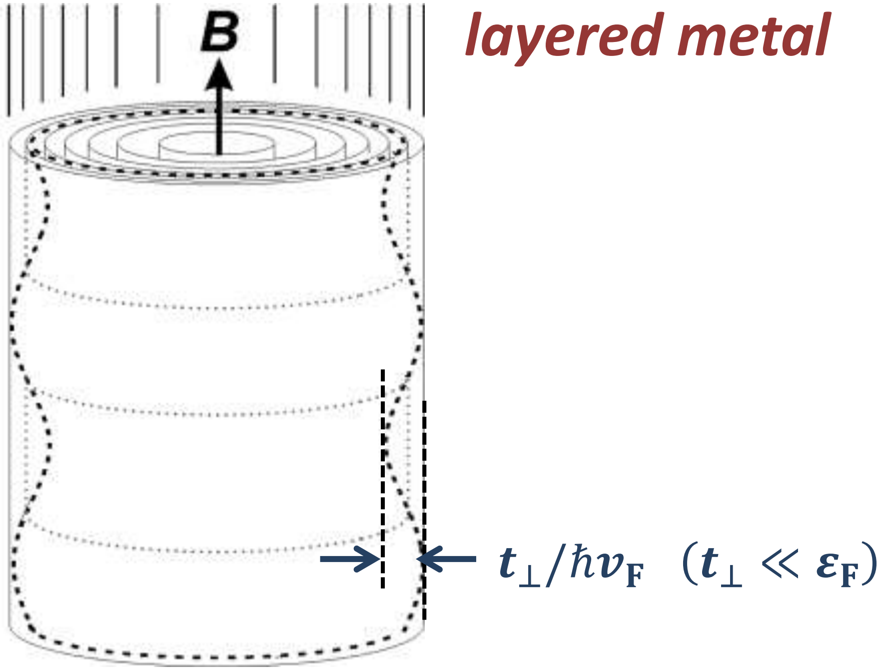

Onsager relation:

$$S_{n,\perp} = (n+\gamma)\frac{2\pi e}{\hbar} B$$

$$\Delta S = S_{n+1,\perp} - S_{n,\perp} = \frac{2\pi e}{\hbar} B$$

L. Onsager, Phil. Mag. 43, 1006 (1952)

$$F = \left(\frac{1}{B_n} - \frac{1}{B_{n+1}}\right)^{-1} = \frac{\hbar}{2\pi e} S_{\text{extr}}$$

physical properties show periodic oscillation on $1/B$ scale

- resistance: *Shubnikov – de Haas effect*
- magnetization: *de Haas – van Alphen effect*

7.3.1 Fermi Surface

- Magnetic quantum oscillations (dHvA, SdH effects)

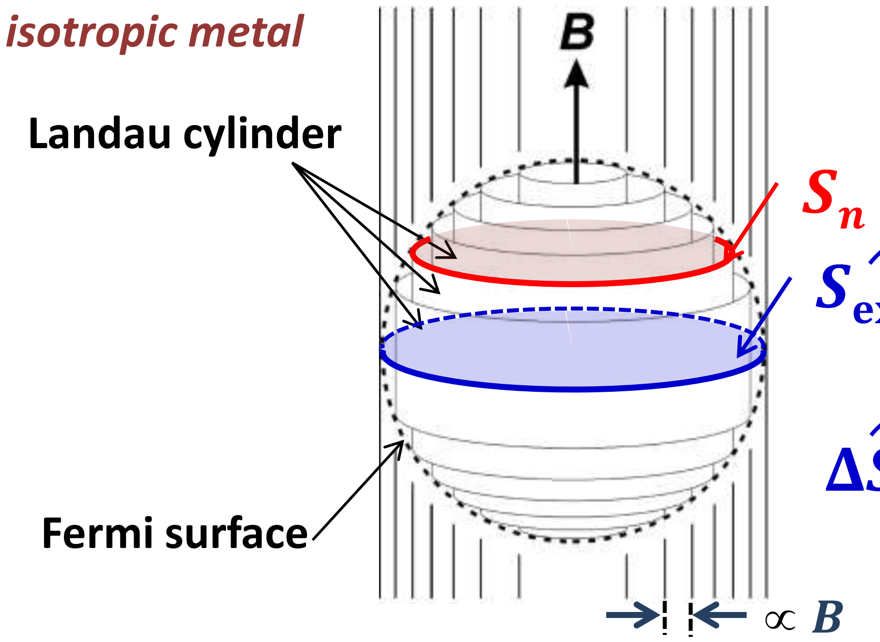

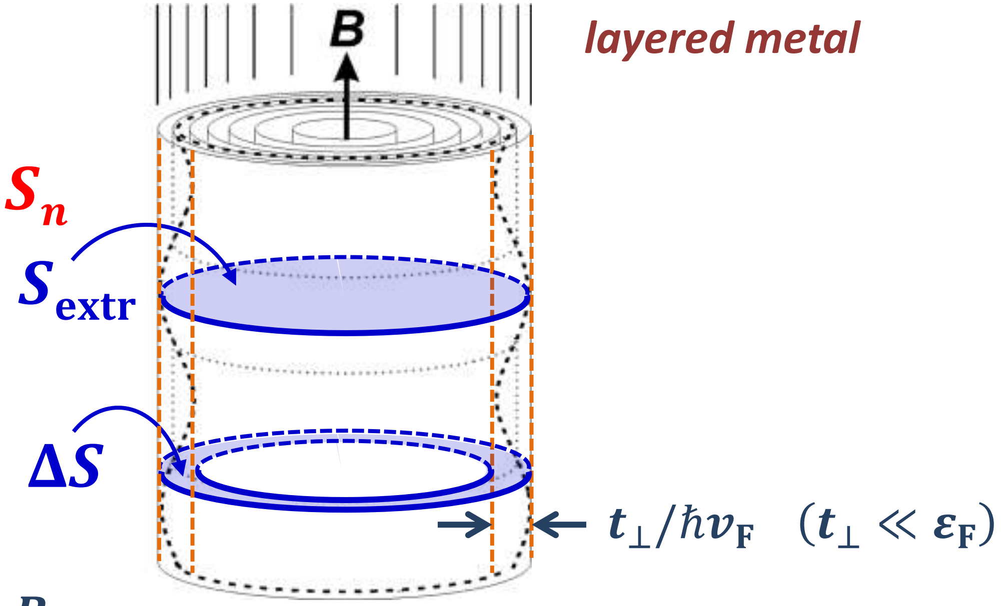

I. Lifshitz & A. Kosevich (including relaxation and dephasing: finite T, finite τ, Zeeman splitting)

damping factors $\quad S_{\mathrm{extr}} \quad \Delta S, t_\perp$

$$\tilde{A} \propto R_T R_D R_S \cos\left(2\pi \frac{F}{B} + \phi\right) \cos\left(2\pi \frac{\Delta F}{2B} + \phi'\right)$$

cyclotron mass m_c *scattering time τ* *g-factor*

7.3.1 Fermi Surface

- **Shubnikov – de Haas oscillations in $YBa_2Cu_3O_{6.5}$**

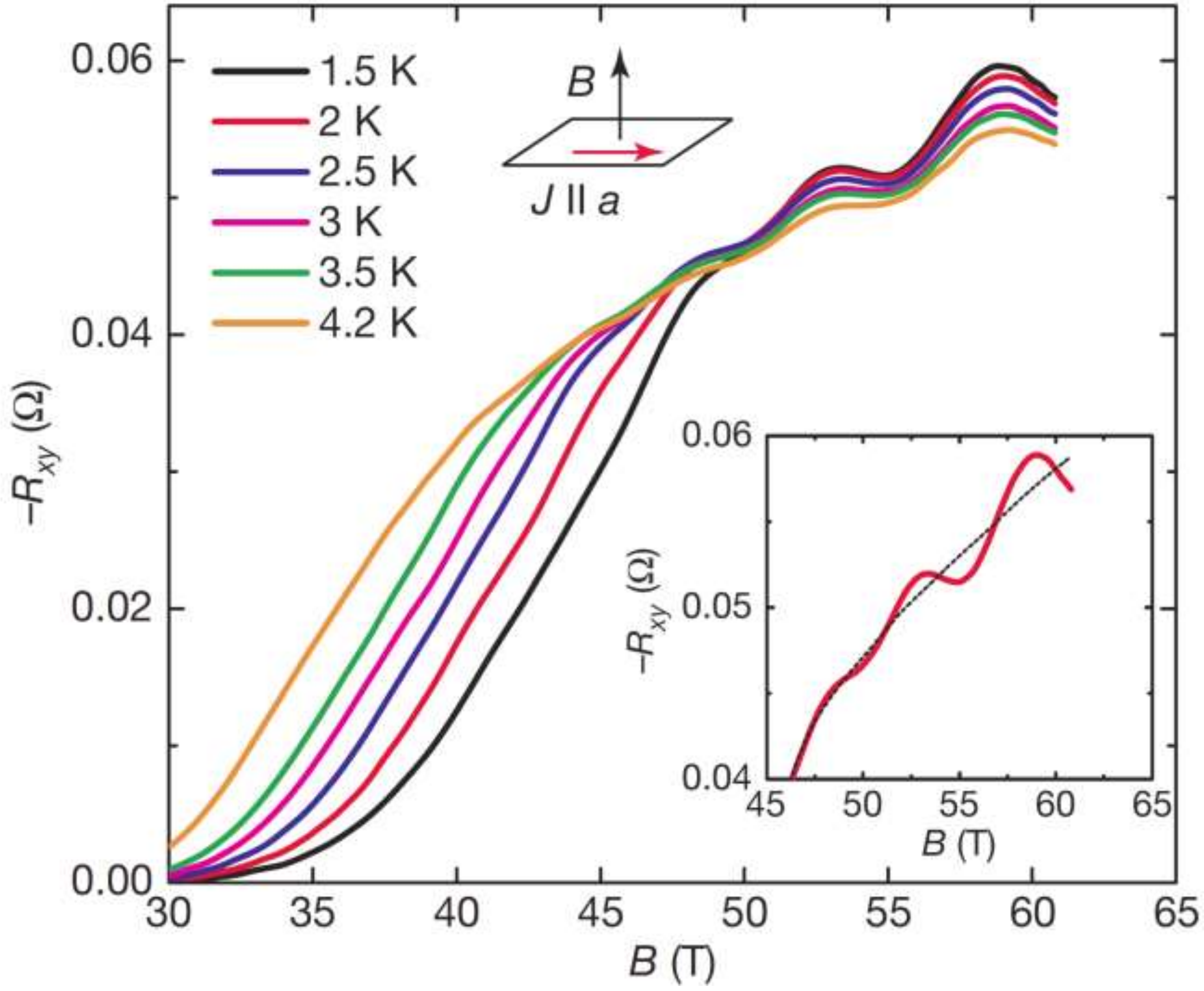

$$F = 530\ \mathrm{T}$$

small Fermi pocket:

$$S_{\mathrm{FS}} = 0.019 S_{\mathrm{BZ}}$$

$$F = \left(\frac{1}{B_n} - \frac{1}{B_{n+1}}\right)^{-1} = \frac{\hbar}{2\pi e} S_{\mathrm{extr}}$$

N. Doiron-Leyraud et al., *Nature* 447, 565 (2007)

7.3.1 Fermi Surface

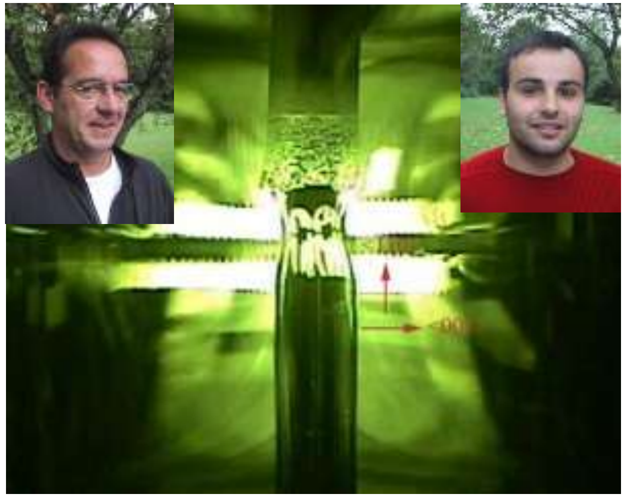

Travelling Solvent Floating Zone

X-ray,
thermal treatment,
SQUID,
magnetotransport
(low-field)

c-axis

experimental techniques
samples

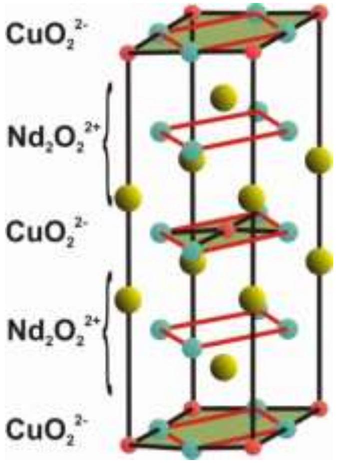

Nd_2CuO_4

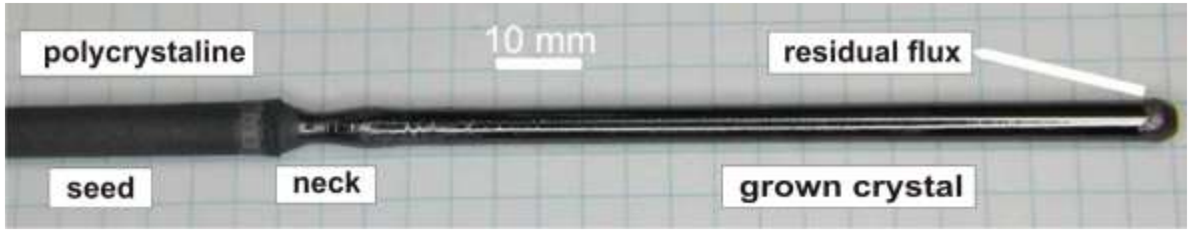

$Nd_{2-x}Ce_xCuO_4$
$Pr_{2-x}Ce_xCuO_4$

- Experimental techniques – high fields

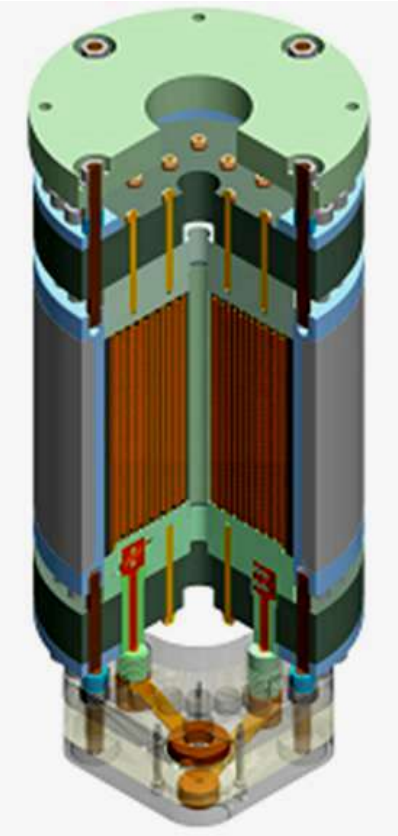

I, *H* || *c*-axis

pulsed fields at the Dresden High Magnetic Field Lab

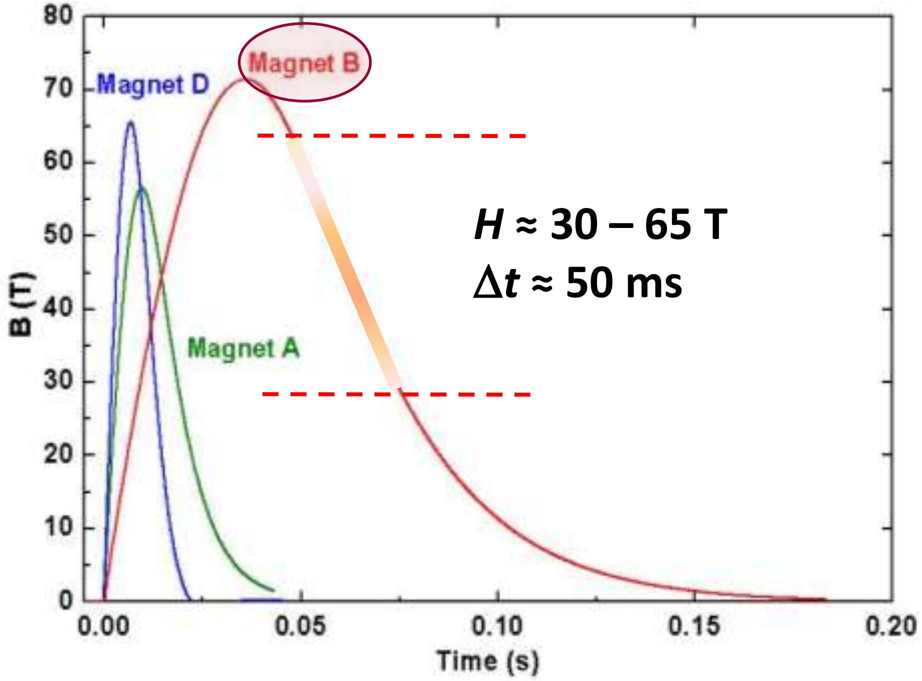

$H \approx 30 - 65$ T
$\Delta t \approx 50$ ms

7.3.1 Fermi Surface

- **c-axis magnetoresistance of NCCO**

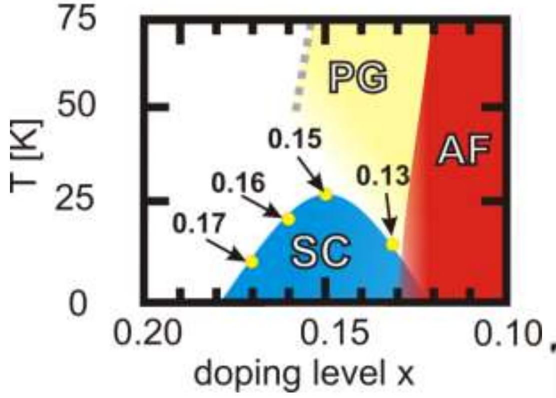

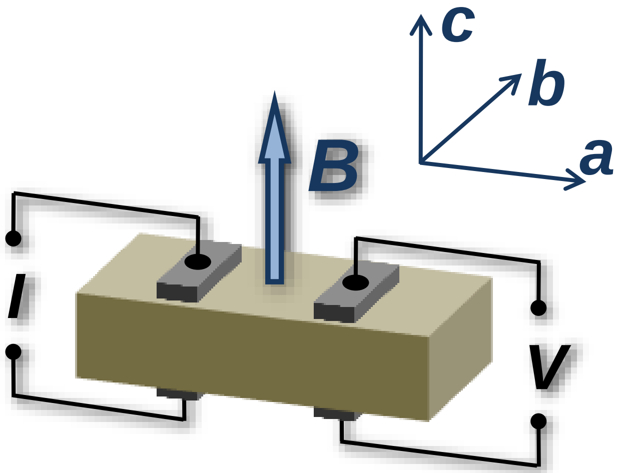

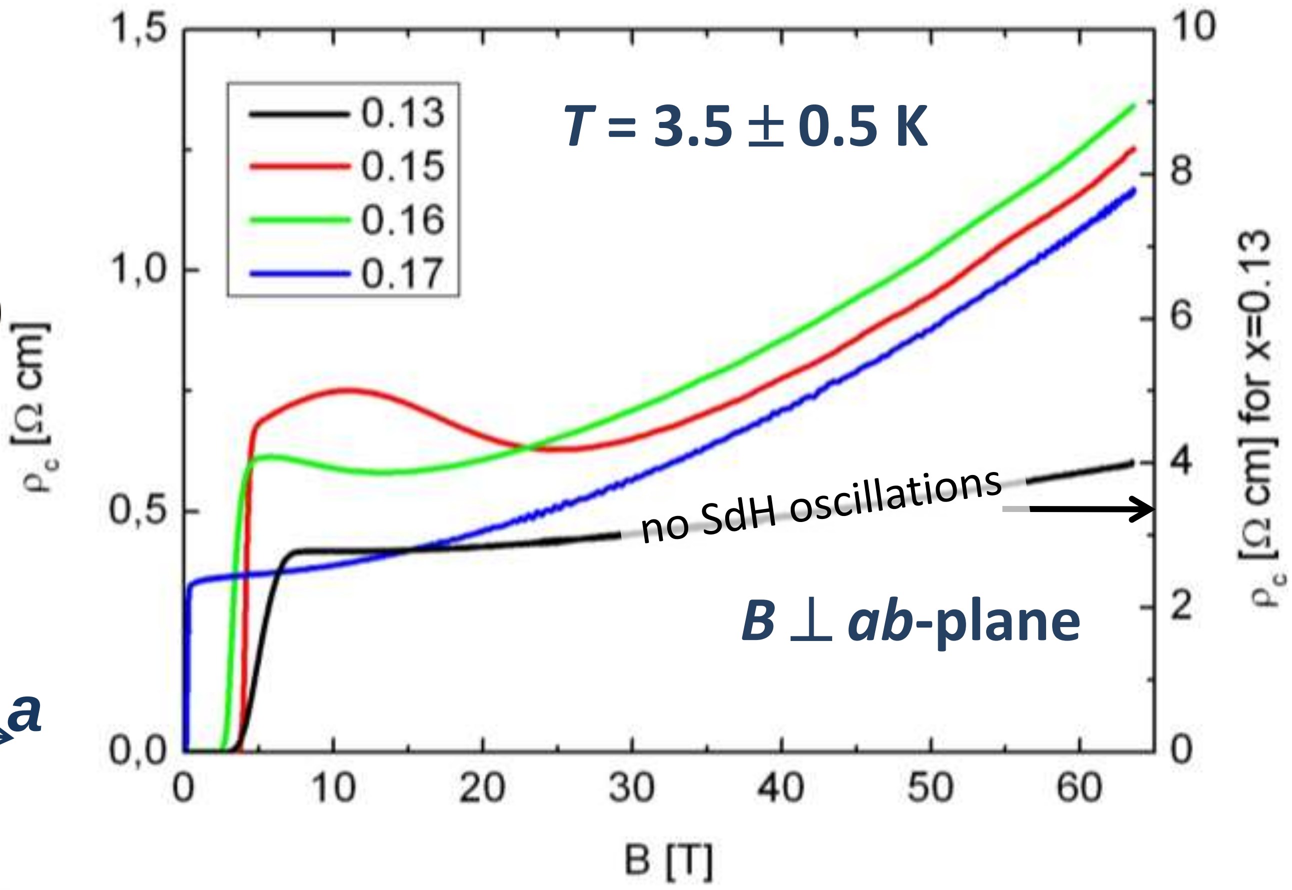

T. Helm, M.V. Kartsovnik, M. Bartkowiak, N. Bittner, M. Lambacher, A. Erb, J. Wosnitza, R. Gross, **Phys. Rev. Lett. 103, 157002 (2009).**

7.3.1 Fermi Surface

- SdH oscillations in $Nd_{2-x}Ce_xCuO_4$

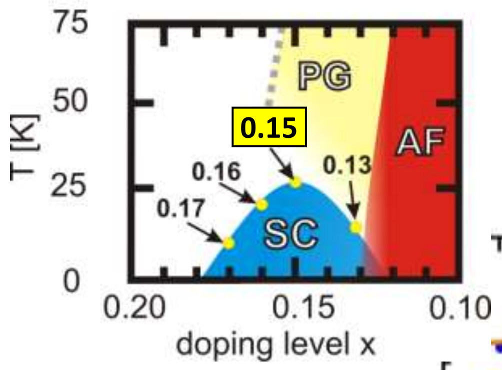

x = 0.15
optimal doping

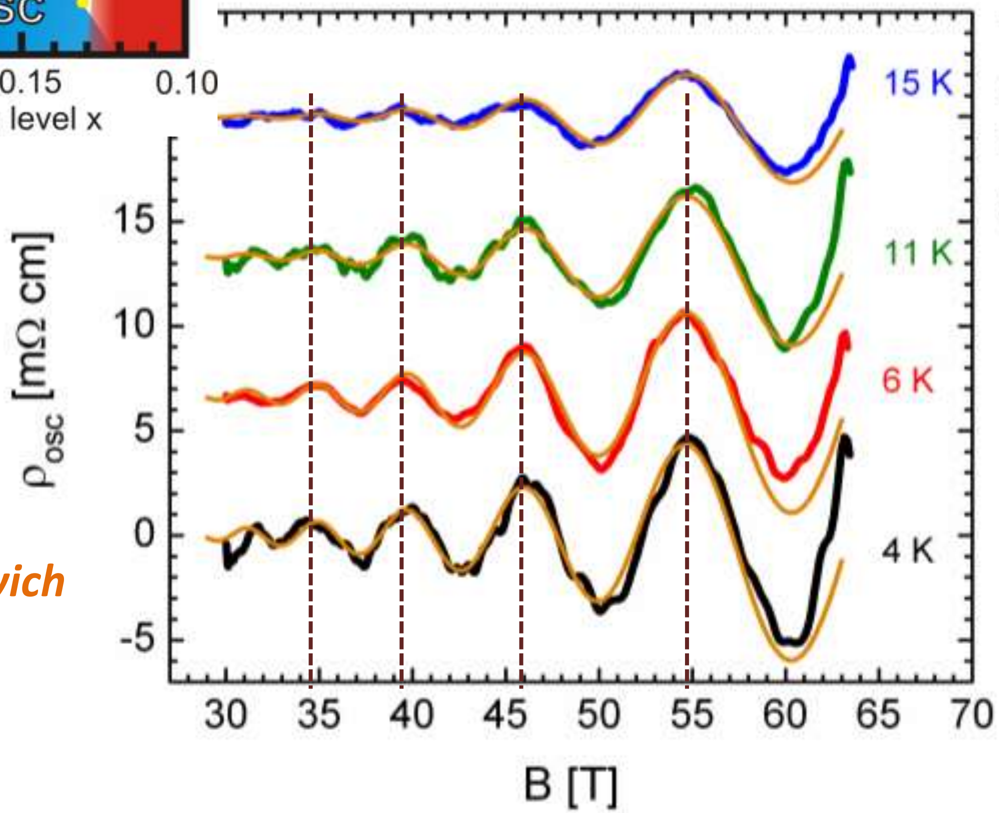

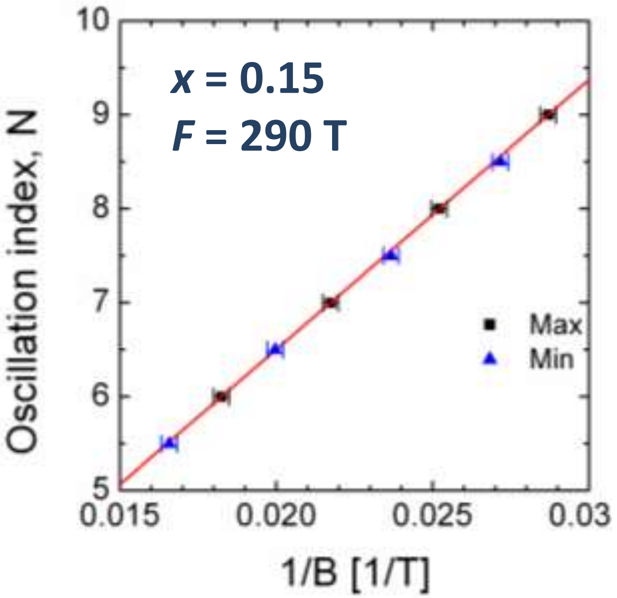

Lifshitz-Kosevich formula

$$F = 290\ \mathrm{T}$$
$$\Rightarrow S_{\mathrm{FS}} = 2\pi eF/\hbar = 0.011 S_{\mathrm{BZ}}$$

$$\Delta\rho_{osc}(T) \rightarrow m_c = 0.6 \pm 0.05\, m_e$$

$$\Delta\rho_{osc}(B) \rightarrow \tau \approx 0.8 \times 10^{-13}\ \mathrm{s}$$

$$\Rightarrow \langle \ell \rangle \approx 14\ \mathrm{nm}$$

T. Helm et al., Phys. Rev. Lett. 103, 157002 (2009).

7.3.1 Fermi Surface

- SdH oscillations in $Nd_{2-x}Ce_xCuO_4$

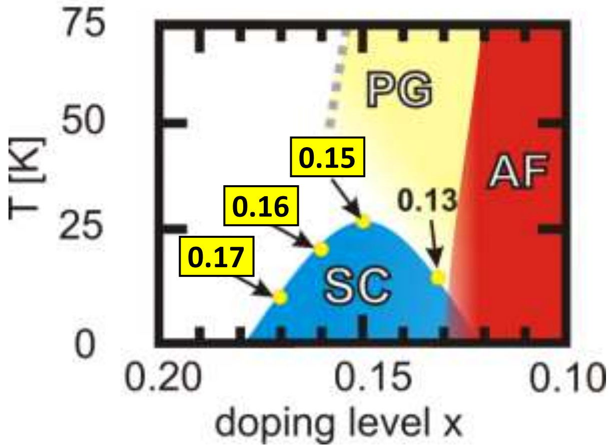

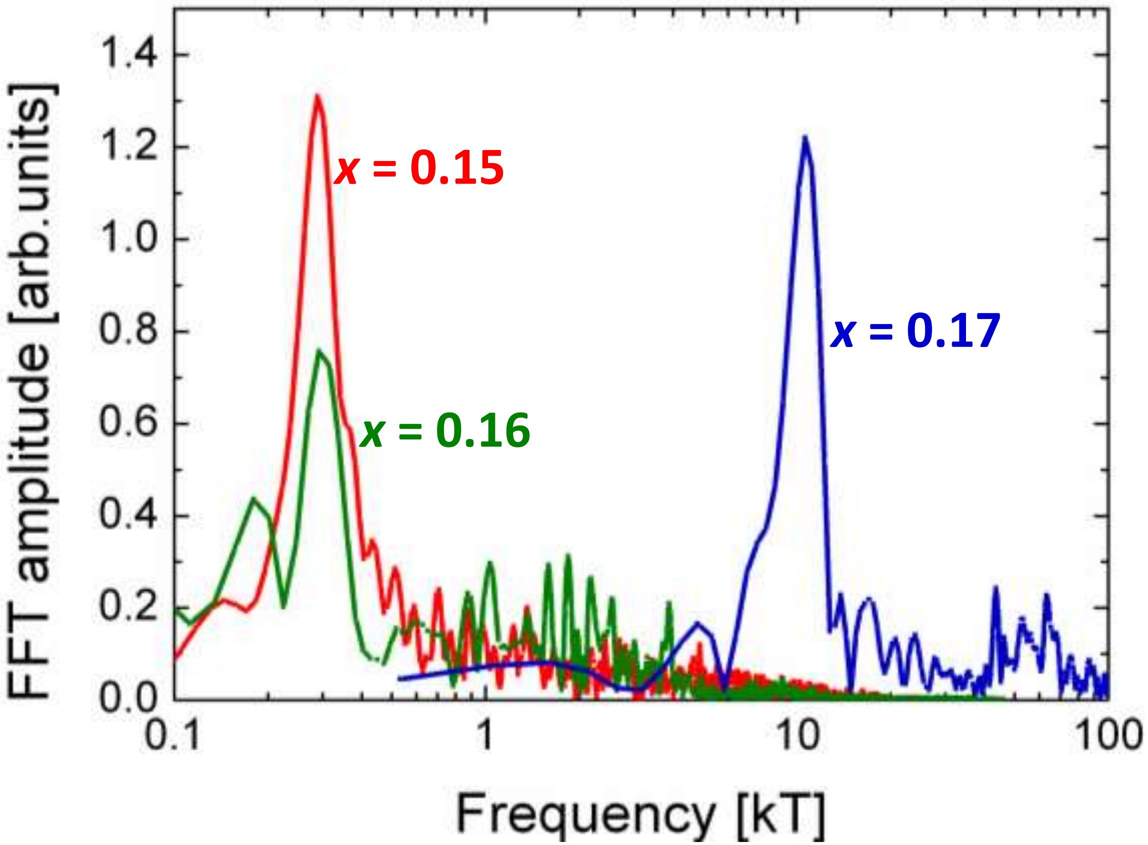

Fermi surface for x = 0.15 and 0.16 appears to be very different from that for x = 0.17

T. Helm et al., Phys. Rev. Lett. 103, 157002 (2009).

7.3.1 Fermi Surface

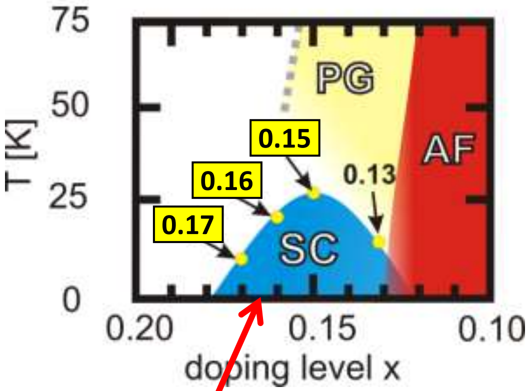

quantum phase transition ?

Fermi surface reconstruction

J. Lin & A.J. Millis, *PRB* 72, 214506 (2007)

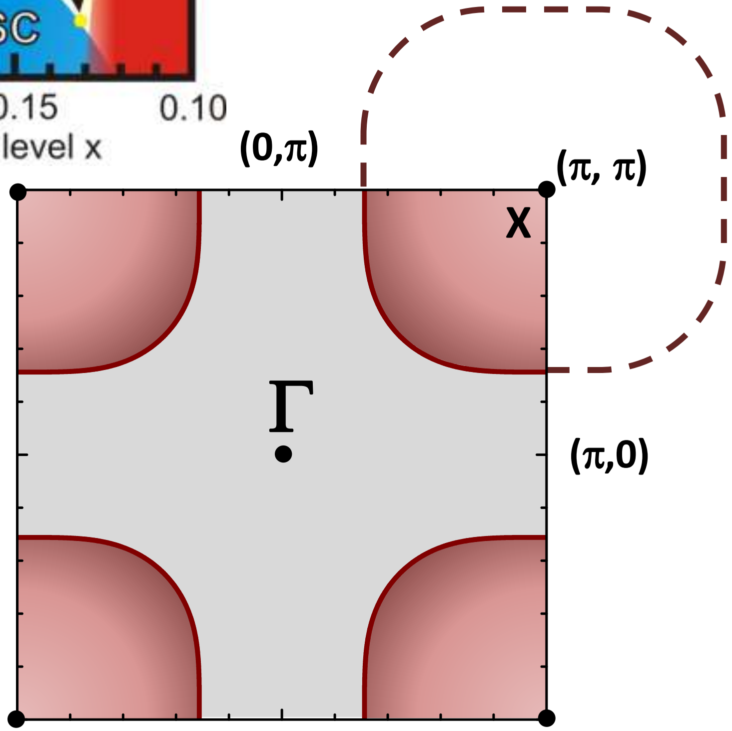

$x = 0.17$

S_h = 41.5% of S_{BZ}

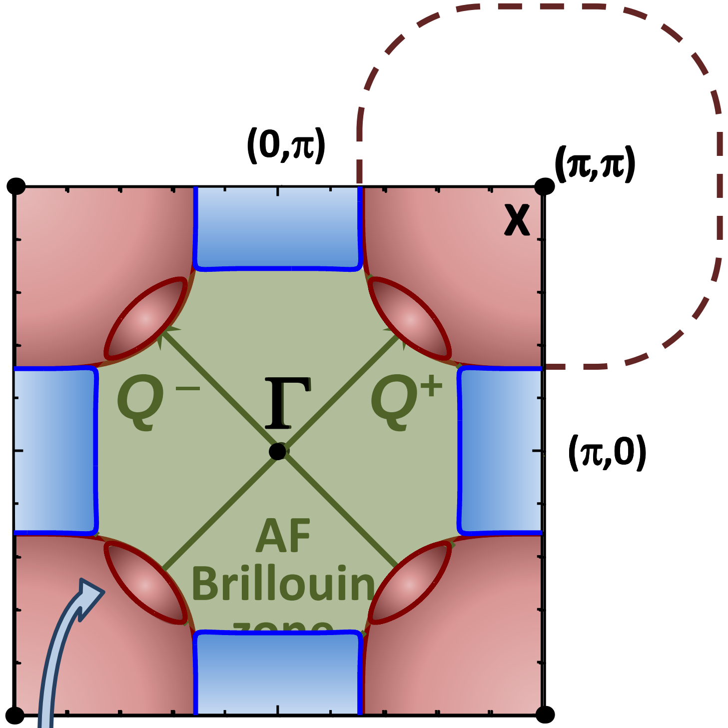

$x = 0.15$ and $x = 0.16$

$S_h \approx$ 1.1% of S_{BZ}

$\Delta_{0.15} \approx$ 64 meV, $\Delta_{0.16} \approx$ 36 meV

T. Helm et al., Phys. Rev. Lett. 103, 157002 (2009).

7.3.1 Fermi Surface

original FS:

reconstructed FS:

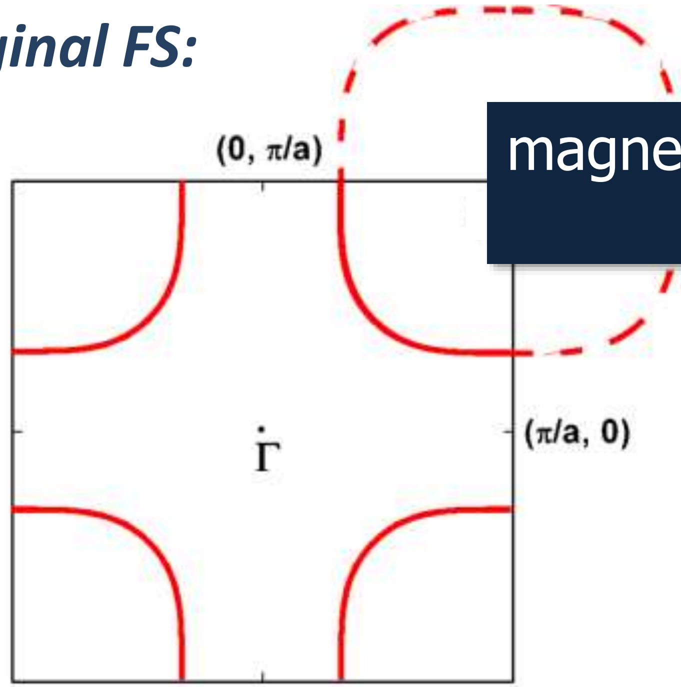

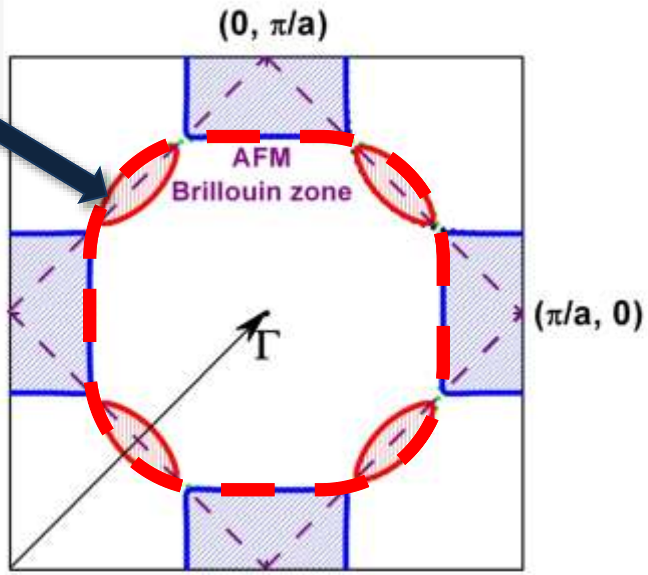

$x = 0.17$

$x = 0.15$ and $x = 0.16$

small Fermi pockets are present even at $x = 0.17$!!

7.4 Symmetry of Pair Wavefunction (cf. 4.1.3)

– **important**: pair consistst of two fermions ➔ ***total wavefunction must be antisymmetric: minus sign for particle exchange***

$$\Psi(\mathbf{r_1},\boldsymbol{\sigma_1},\mathbf{r_2},\boldsymbol{\sigma_2}) = \underbrace{\frac{1}{\sqrt{V}}\,\mathrm{e}^{i\,\mathbf{K_s}\cdot\mathbf{R_s}}}_{\text{center of mass motion, we assume } \mathbf{K}_s = 0}\;\underbrace{f(\mathbf{k},\mathbf{r})}_{\text{orbital part}}\;\underbrace{\chi(\boldsymbol{\sigma_1},\boldsymbol{\sigma_2})}_{\text{spin part}} = -\Psi(\mathbf{r_2},\boldsymbol{\sigma_2},\mathbf{r_1},\boldsymbol{\sigma_1})$$

$$\mathbf{R_s} = (\mathbf{r_1}+\mathbf{r_2})/2$$
$$\mathbf{r} = (\mathbf{r_1}-\mathbf{r_2})$$
$$\mathbf{K_s} = (\mathbf{k_1}+\mathbf{k_2})/2$$
$$\mathbf{k} = (\mathbf{k_1}-\mathbf{k_2})$$

– possible ***spin wavefunctions*** $\chi(\boldsymbol{\sigma_1},\boldsymbol{\sigma_2})$ for electron pairs

$$S = \begin{cases} 0 \quad m_s = 0 \qquad \chi^a = \frac{1}{\sqrt{2}}(\uparrow\downarrow - \downarrow\uparrow) \\ 1 \quad m_s = \begin{cases} -1 & \chi^s = \downarrow\downarrow \\ 0 & \chi^s = \frac{1}{\sqrt{2}}(\uparrow\downarrow + \downarrow\uparrow) \\ +1 & \chi^s = \uparrow\uparrow \end{cases} \end{cases}$$

→**singlet pairing**, antisymmetric spin wavefunction
symmetric orbital function:
L = 0, 2, … (s, d, ….)

→**triplet pairing**, symmetric spin wavefunction
antisymmetric orbital function:
L = 1, 3, … (p, f, ….)

7.4 Symmetry of Pair Wavefunction (cf. 4.1.3)

- isotropic interaction: $V_{\mathbf{k},\mathbf{k}'} = -V_0$

  → interaction only depends on $|\mathbf{k}|$
  → in agreement with angular momentum $L = 0$ (s – wave superconductor)

  – corresponding spin wavefunction must by antisymmetric

  → **spin singlet Cooper pairs ($S = 0$)**

  – resulting Cooper pair: $(\mathbf{k}\uparrow, -\mathbf{k}\downarrow)$ spin singlet Cooper pair ($L = 0, S = 0$)

- **spin triplet Cooper pairs ($S = 1$):**
  - realized in superfluid ^{3}He: $L = 1, S = 1$ (p – wave pairing)
  - evidence for $L = 1, S = 1$ also for some heavy Fermion superconductors (e.g. UPt_3)

$L = 0$, $S = 0$

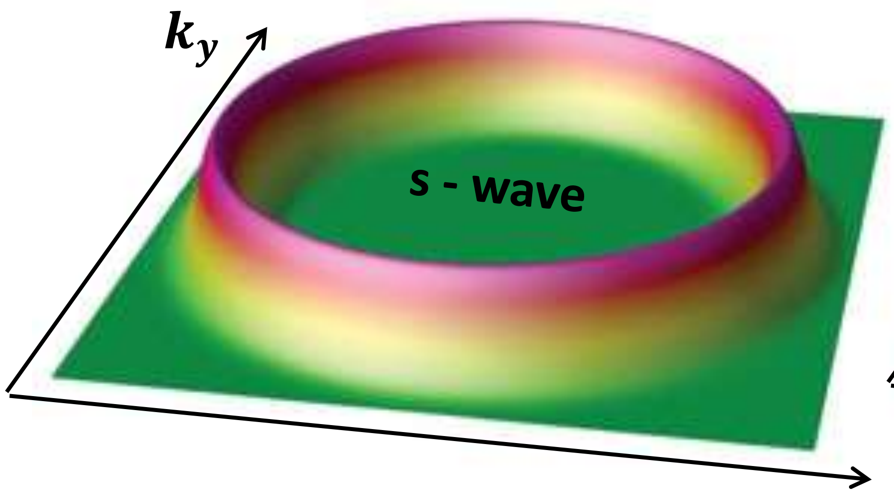

$$\Delta(\mathbf{k}) = \Delta_m$$

$L = 2$, $S = 0$

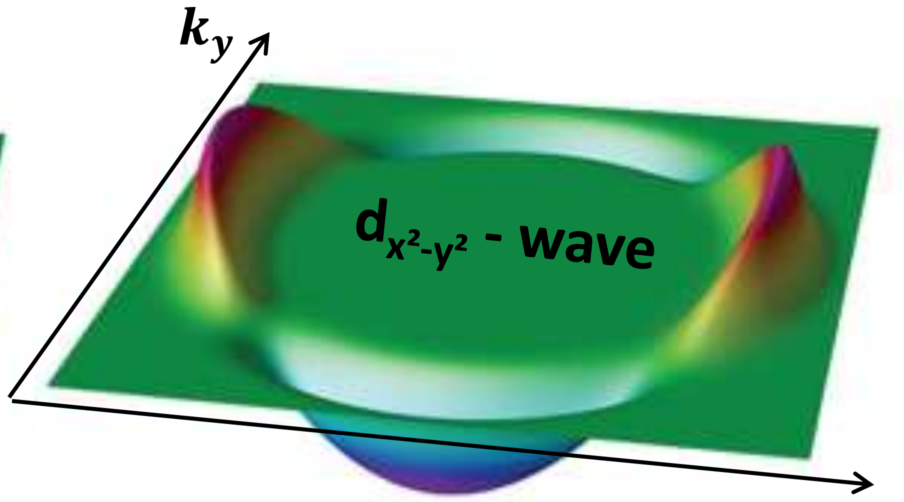

$$\Delta(\mathbf{k}) = \frac{\Delta_m}{2}\left(\cos k_y a - \cos k_x a\right)$$

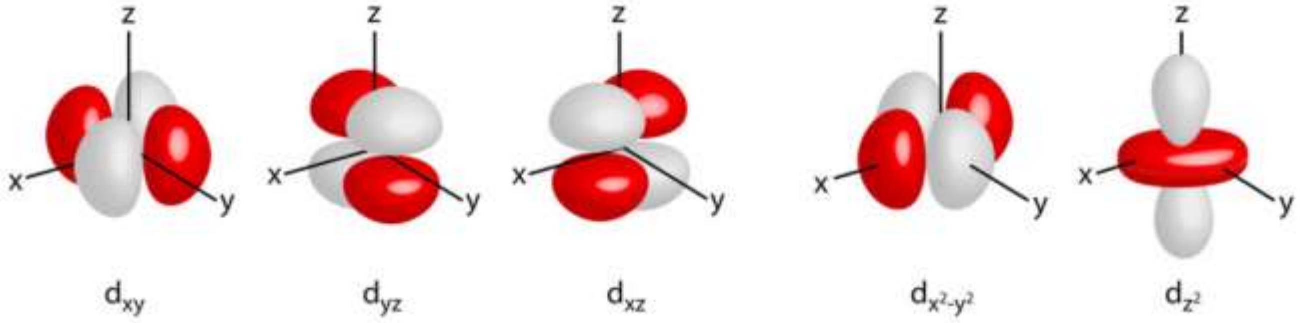

[Superconductivity gets an iron boost]
Igor I. Mazin
Nature **464**, 183-186(11 March 2010)

7.4 Symmetry of Pair Wavefunction

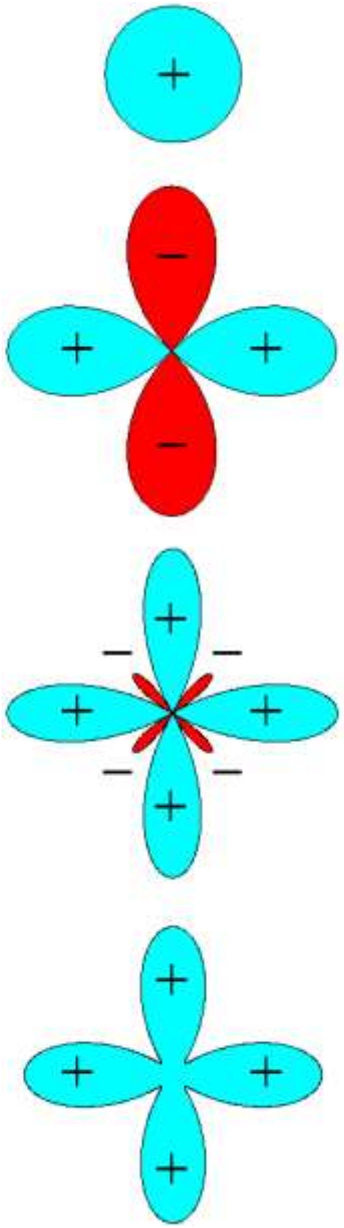

isotropic *s*-wave:
$\Delta(\theta) = \Delta_0$
no nodes

BCS-type superconductors

Nb, Hg, Pb, Nb_3Ge

d-wave:
$\Delta(\theta) = \Delta_0 \cos(2\theta)$
4 nodes

hole-doped cuprates

$La_{2-x}Sr_xCuO_{4-\delta}$

$YBa_2Cu_3O_{7-\delta}$

extended *s*-wave:
$\Delta(\theta) = \Delta_0 \left[\cos(4\theta) + \alpha\right]$
$\alpha < 1$
8 nodes

?

electron-doped cuprates

$(Nd,Pr,La)_{2-x}Ce_xCuO_{4-y}$

anisotropic *s*-wave:
$\Delta(\theta) = \Delta_0 \left[\cos(4\theta) + \alpha\right]$
$\alpha \geq 1$
no nodes

7.4 Symmetry of Pair Wavefunction

- ***why are cuprates d-wave superconductors ?***

quasi free electron gas

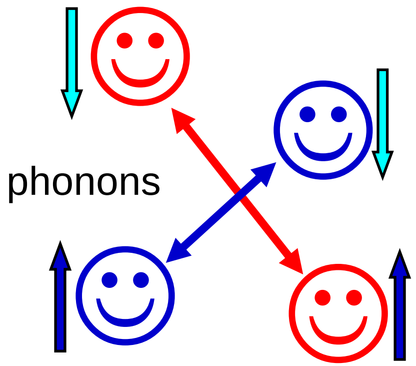

strongly correlated electrons
(on-site Coulomb repulsion U)

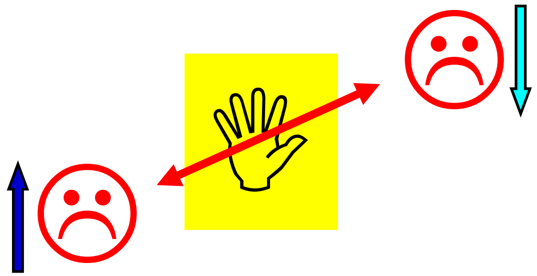

electrons avoid to come close to each other → d-wave pair function

probability amplitude

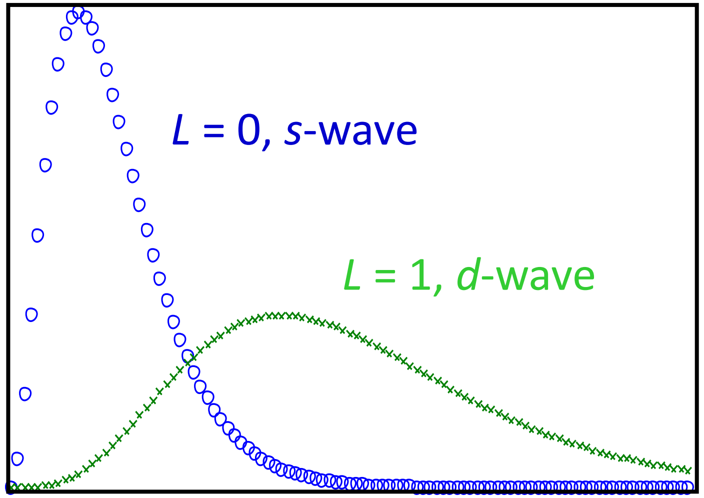

distance r

	L	parity	spin state (S)
s	0	even	singlet ($S = 0$)
p	1	odd	triplet ($S = 1$)
d	2	even	singlet ($S = 0$)

7.4 Symmetry of Pair Wavefunction

- experimental study of the symmetry of the pair wave function

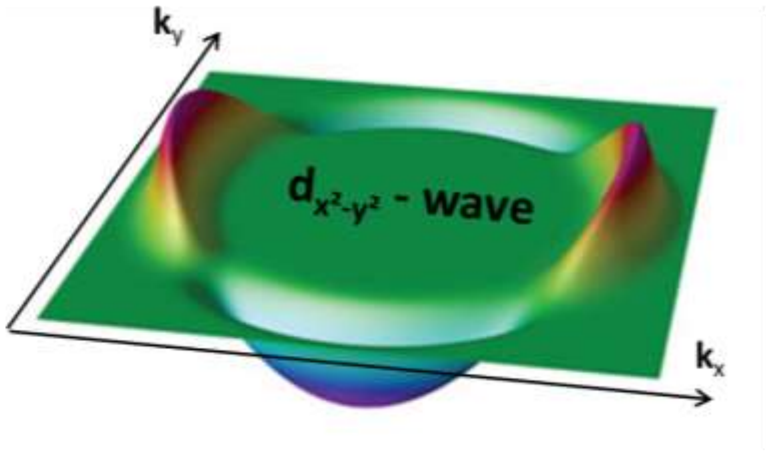

- ***phase sensitive measurements***

  - OP changes sign in different *k*-directions
  - realize interference experiment which is phase sensitive

- ***amplitude sensitive measurements***

  - OP disappears for certain *k*-directions: ***nodes***
    → low-lying quasiparticle excitations
  - measure quantities which depend on quasipartice excitation spectrum
    → specific heat, London penetration depth, Raman response, ….
    → exponential laws change into power laws due to nodes

7.4 Symmetry of Pair Wavefunction

- **London penetration depth**: $\lambda_{\mathrm{L}}^2(T) = \dfrac{m_s}{\mu_0 n_s(T) q_s^2} \propto \dfrac{1}{n_s(T)}$

two fluid model: $\dfrac{n_s(T)}{n_s(0)} = 1 - \dfrac{n_{\mathrm{qp}}(T)/2}{n_s(0)} = \left(\dfrac{\lambda_{\mathrm{L}}(0)}{\lambda_{\mathrm{L}}(T)}\right)^2 = \Bigg(1 + \underbrace{\dfrac{\Delta\lambda_{\mathrm{L}}(T)}{\lambda_{\mathrm{L}}(0)}}_{\ll 1 \text{ @ low } T \Rightarrow (1+x)^{-2} \approx 1-2x}\Bigg)^{-2} \simeq 1 - 2\dfrac{\Delta\lambda_{\mathrm{L}}(T)}{\lambda_{\mathrm{L}}(0)}$

total electron density $n = 2n_s(0)$

with $\Delta\lambda_{\mathrm{L}}(T) = \lambda_{\mathrm{L}}(T) - \lambda_{\mathrm{L}}(0)$

$$\Rightarrow \quad 2\frac{\Delta\lambda_{\mathrm{L}}(T)}{\lambda_{\mathrm{L}}(0)} \approx \frac{n_{\mathrm{qp}}(T)}{2n_s(0)} = \frac{2[n_s(0) - n_s(T)]}{2n_s(0)} = 1 - \frac{2n_s(T)}{n} = 1 - 2\int_{\Delta}^{\infty}\left(-\frac{\partial f}{\partial E_{\mathbf{k}}}\right)\frac{D_s(E_{\mathbf{k}})}{D_n(E_{\mathbf{k}})}\,\mathrm{d}E_{\mathbf{k}}$$

$$D_s(E_{\mathbf{k}}) = D_n(E_{\mathbf{k}})\frac{E_{\mathbf{k}}}{\sqrt{E_{\mathbf{k}}^2 - \Delta_{\mathbf{k}}^2}}$$

$\mathbf{k}$-dependence of the OP matters

7.4 Symmetry of Pair Wavefunction

- **London penetration depth:**

$L = 0, S = 0$

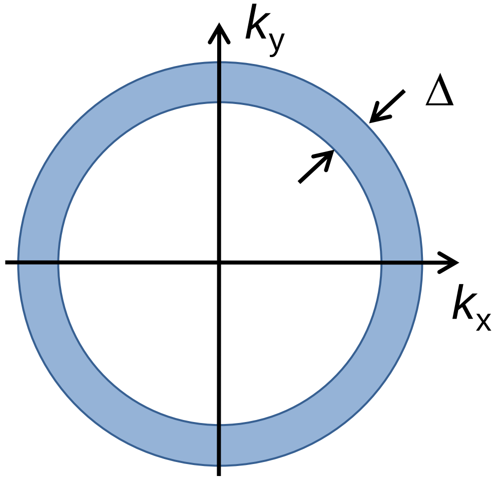

- OP is finite for all $\mathbf{k}$-directions
- at low T:

$$\frac{\Delta\lambda_L(T)}{\lambda_L(0)} \simeq \sqrt{\frac{\pi\Delta}{2k_B T}}\,\exp\left(-\frac{\Delta}{k_B T}\right)$$

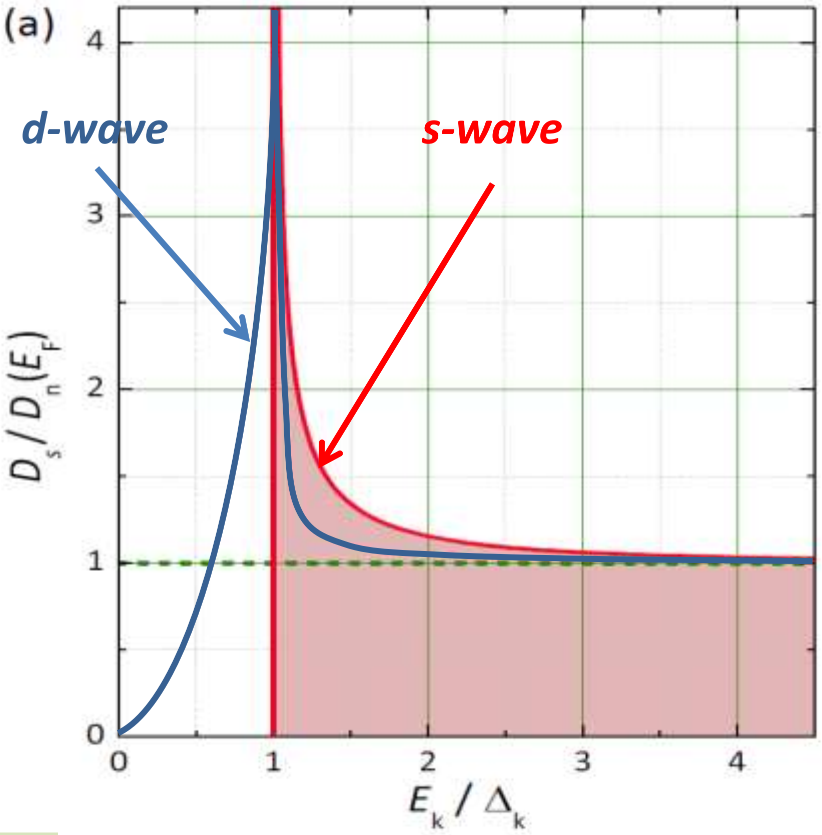

$L = 2, S = 0$

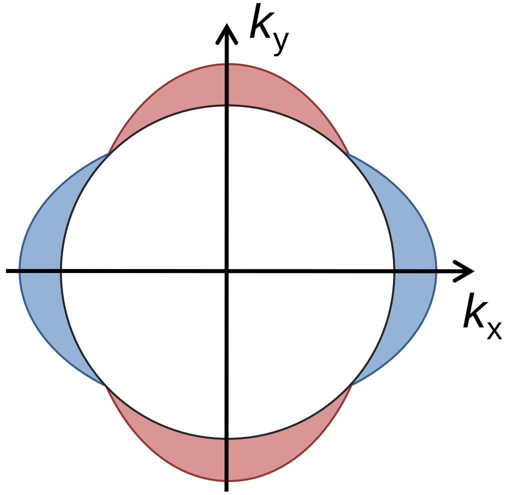

- OP disappears on line nodes
- at low T:

$$\frac{\Delta\lambda_L(T)}{\lambda_L(0)} \simeq \ln 2\,\frac{k_B T}{\Delta}$$

$L = 0, S = 0$

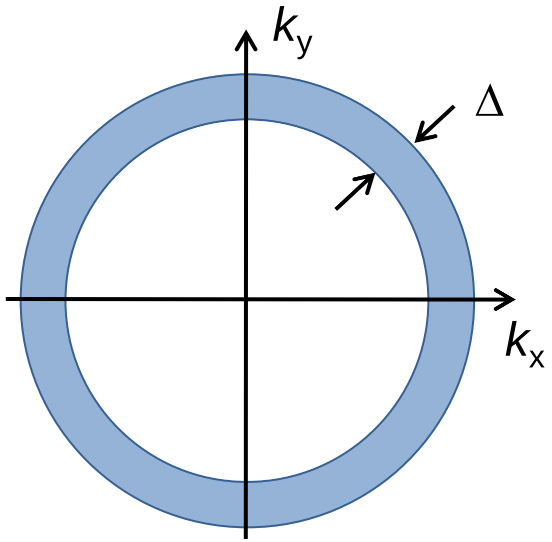

- OP is finite for all $\mathbf{k}$-directions
- at low T: $n_{\mathrm{qp}}(T) \propto \exp(-\Delta/k_\mathrm{B}T)$

$L = 2, S = 0$

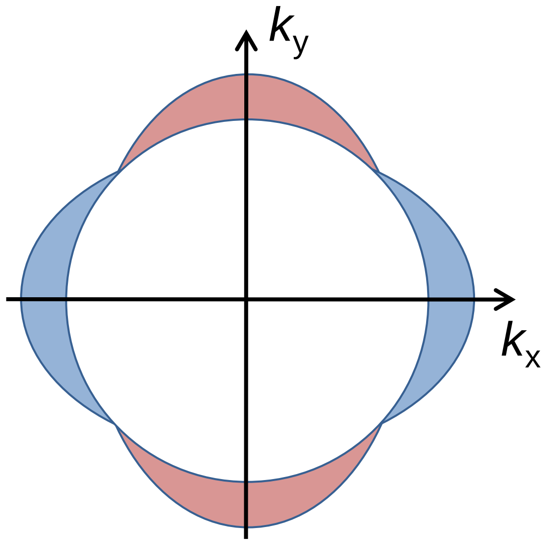

- OP disappears on line nodes
- at low T: $n_{\mathrm{qp}}(T) \propto T$

- **London penetration depth**:

  - *s*-wave pairing: $\lambda_\mathrm{L}(T) - \lambda_\mathrm{L}(0) \propto \exp\left(-\frac{\Delta}{k_\mathrm{B}T}\right)$

  - *d*-wave pairing: $\lambda_\mathrm{L}(T) - \lambda_\mathrm{L}(0) \propto T$

$$\lambda_\mathrm{L}^2(T) = \frac{m_s}{\mu_0 n_s(T) q_s^2} \propto \frac{1}{n_s(T)}$$

BCS-theory:

$$\frac{\Delta\lambda_\mathrm{L}(T)}{\lambda_\mathrm{L}(0)} \simeq 3.33\left(\frac{T}{T_c}\right)^{1/2} \exp\left(-1.76\frac{T}{T_c}\right)$$

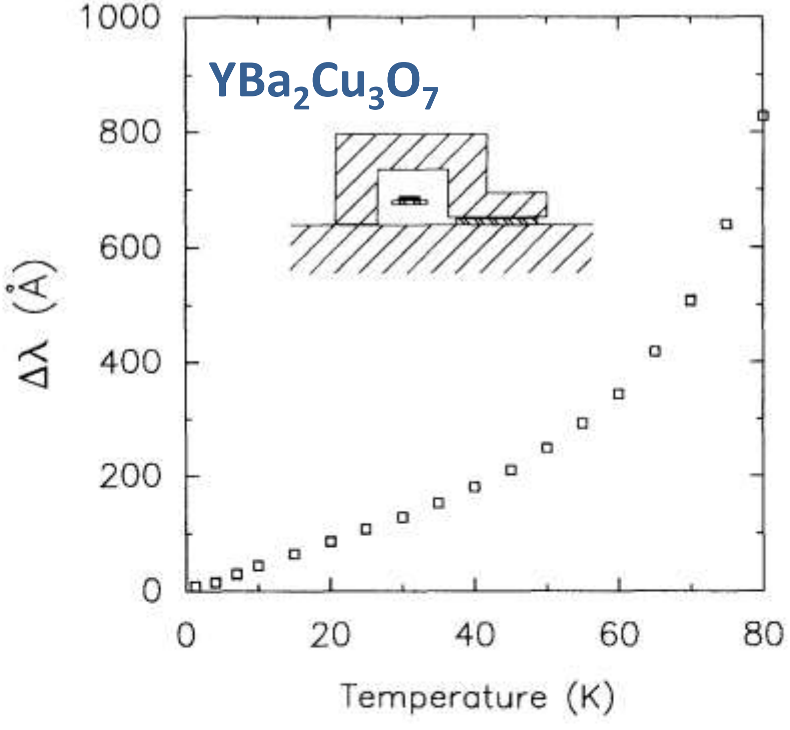

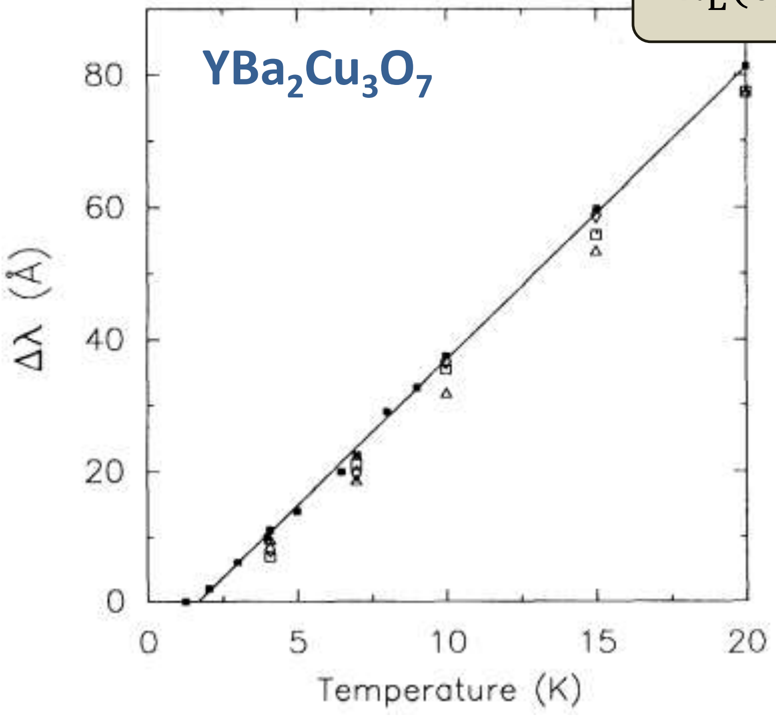

W.N. Hardy *et al.*, Phys. Rev. Lett. **70**, 3999–4002 (1993)

7.4 Symmetry of Pair Wavefunction

VOLUME 83, NUMBER 13 PHYSICAL REVIEW LETTERS 27 SEPTEMBER 1999

Anomalous Low Temperature Behavior of Superconducting $Nd_{1.85}Ce_{0.15}CuO_{4-y}$

L. Alff,[1] S. Meyer,[1] S. Kleefisch,[1] U. Schoop,[1] A. Marx,[1] H. Sato,[2] M. Naito,[2] and R. Gross[1]

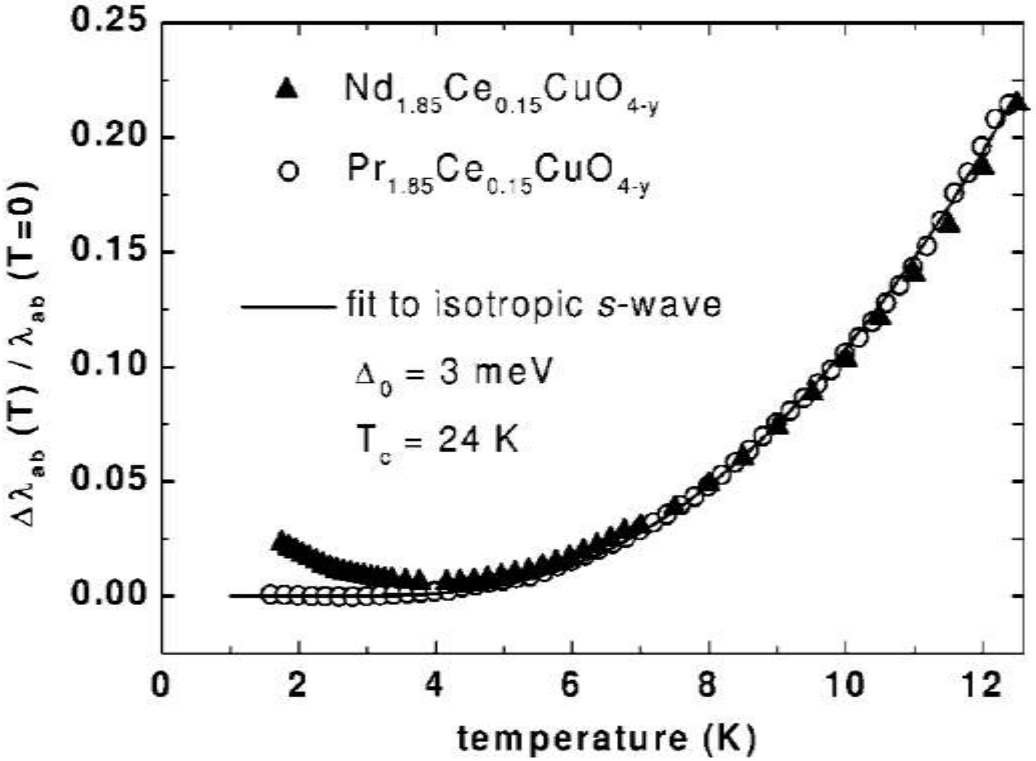

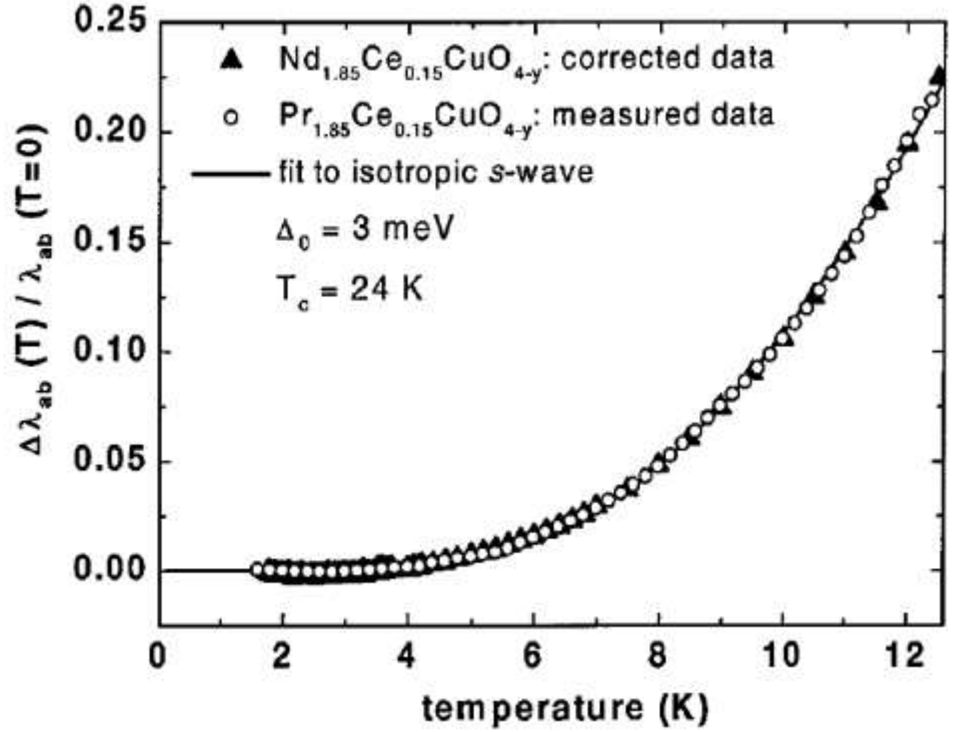

7.4 Symmetry of Pair Wavefunction

- **ARPES can measure $|\Delta|$ as function of k**:

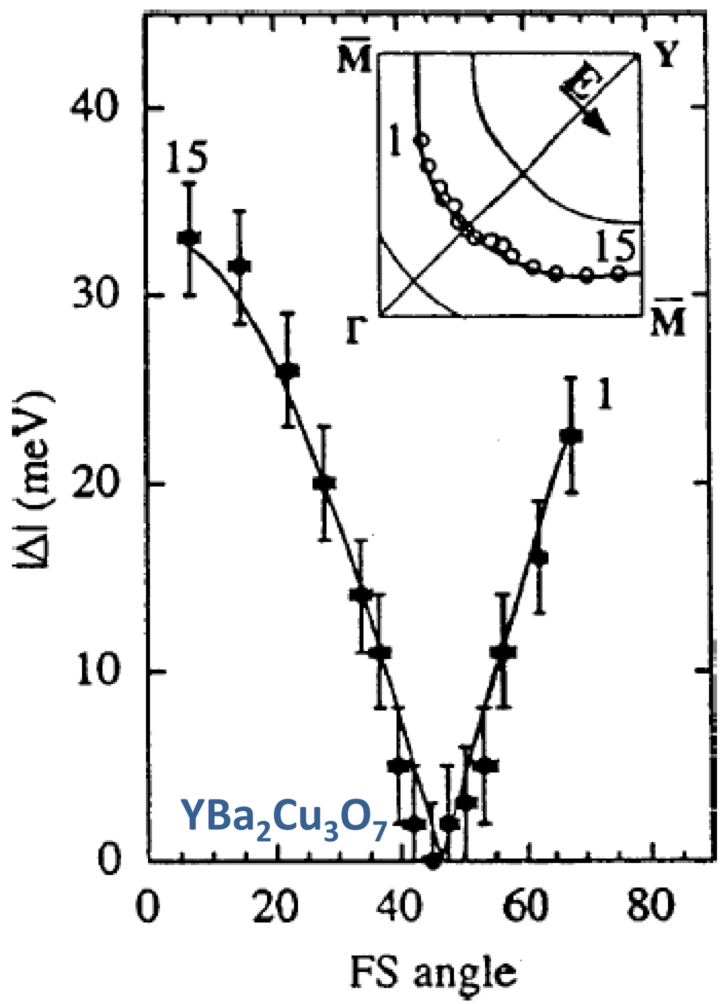

angle dependence follows $\left|d_{x^2-y^2}\right|$

- experiment cannot distinguish between:

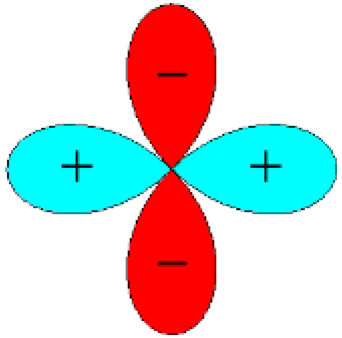

d-wave OP

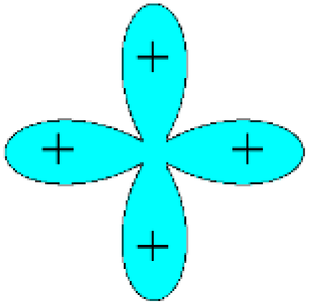

anisotropic
s-wave OP

- **Raman scattering**

Conventional superconductors

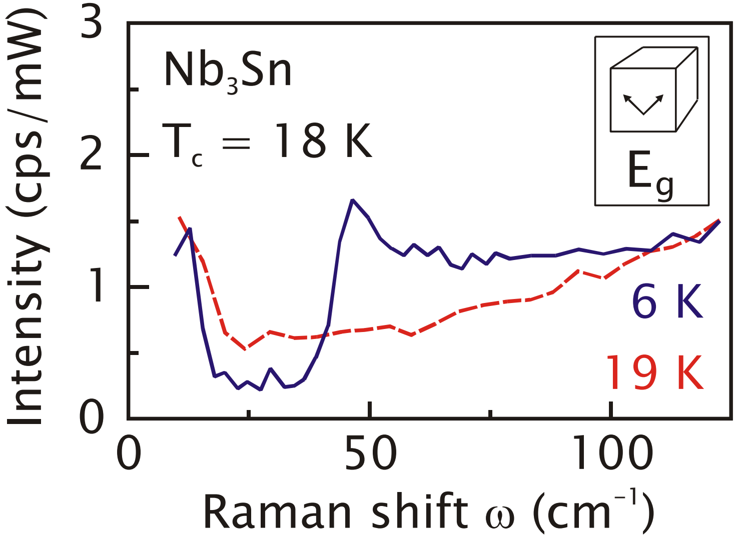

Hackl et al., Physica C **162-164**, 431 (1989)

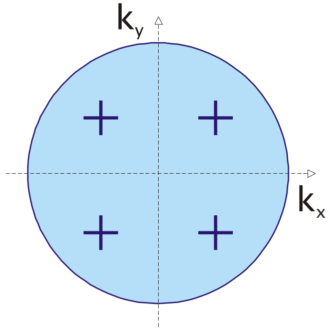

Cuprate superconductors

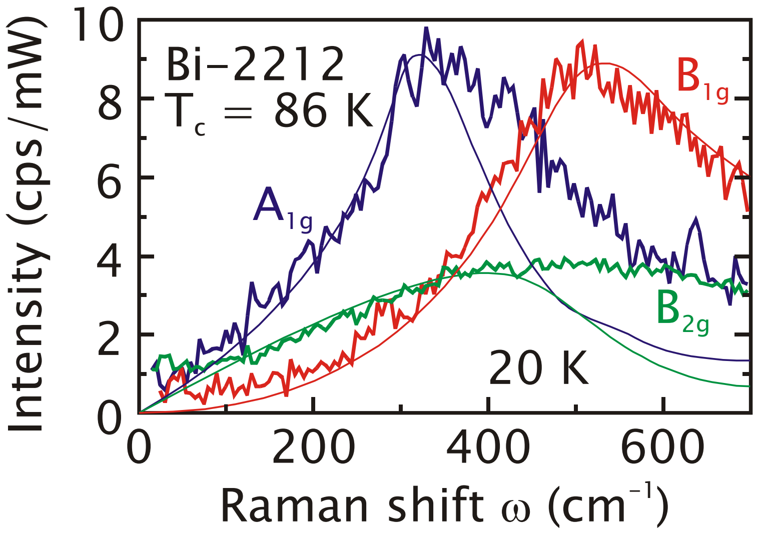

Devereaux et al., PRL **72**, 3291 (1994)

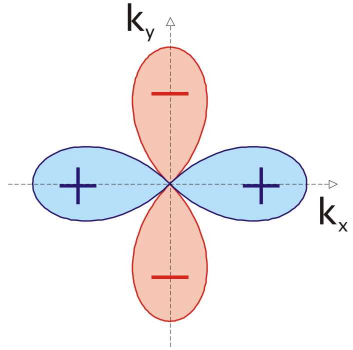

7.4 Symmetry of Pair Wavefunction

- phase sensitive experiments using superconducting loops

$$\Psi(x) = \Psi(x + n \cdot 2\pi)$$

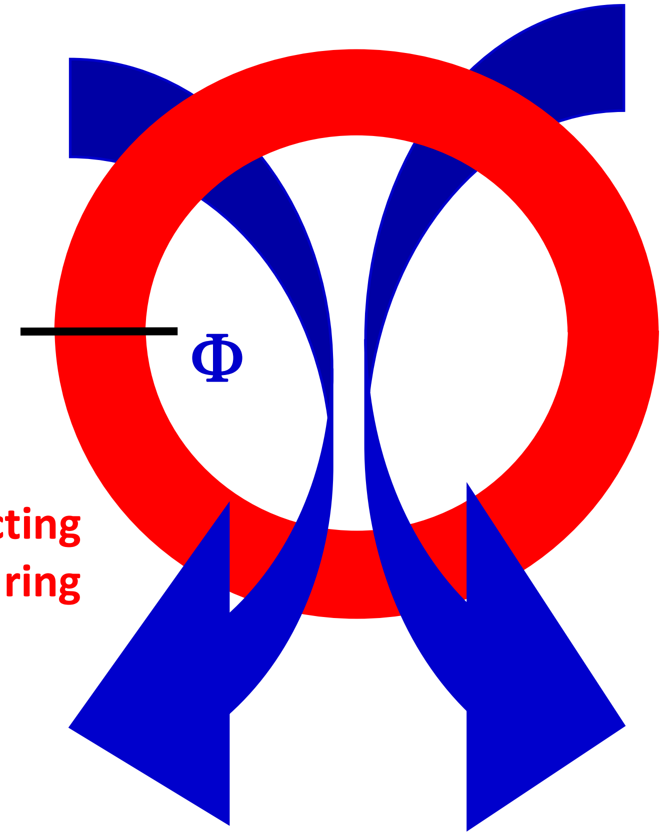

superconducting ring

magnetic flux

$$\Phi = n \cdot \Phi_0$$

$$(-1)^m \Psi(x) = \Psi(x + n \cdot 2\pi)$$

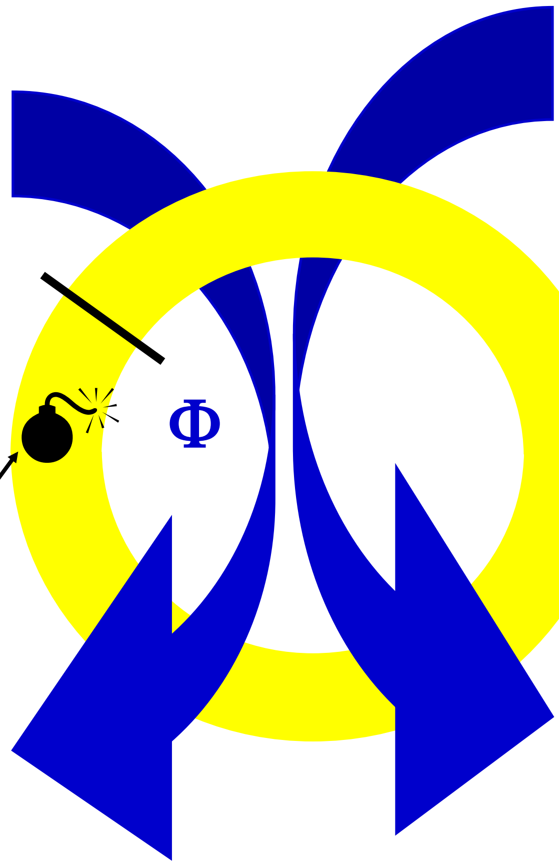

$$\Phi = \frac{2n+1}{2} \cdot \Phi_0$$

7.4 Symmetry of Pair Wavefunction

- **tri-crystal experiments**: epitaxial YBCO film on $SrTiO_3$ tricystal substrate

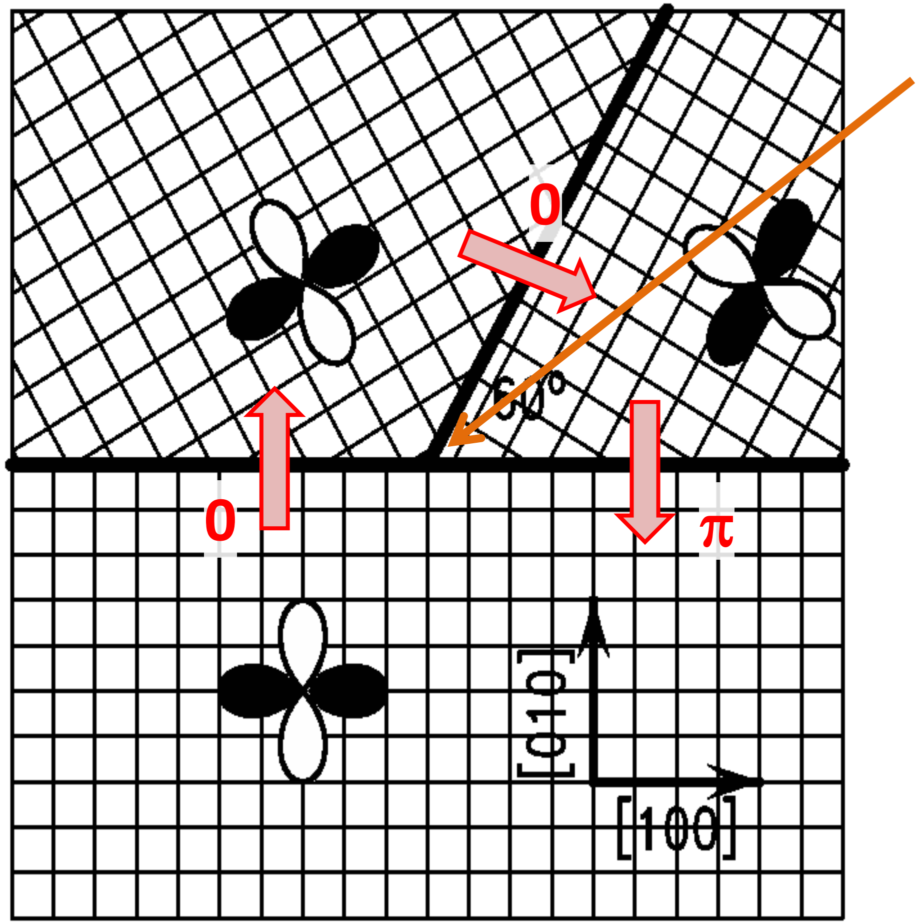

spontaneous magnetic flux $\Phi_0/2$ at tricystal intersection

measurement of flux by scanning SQUID

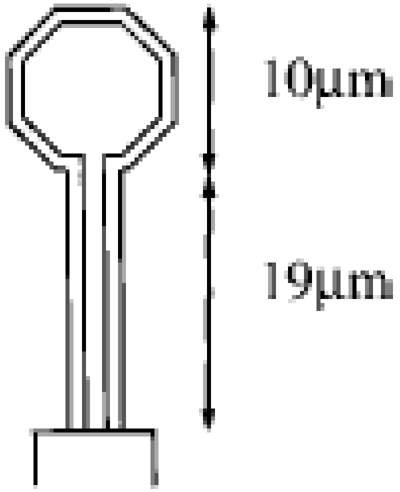

- $YBa_2Cu_3O_7$, hole doped HTS

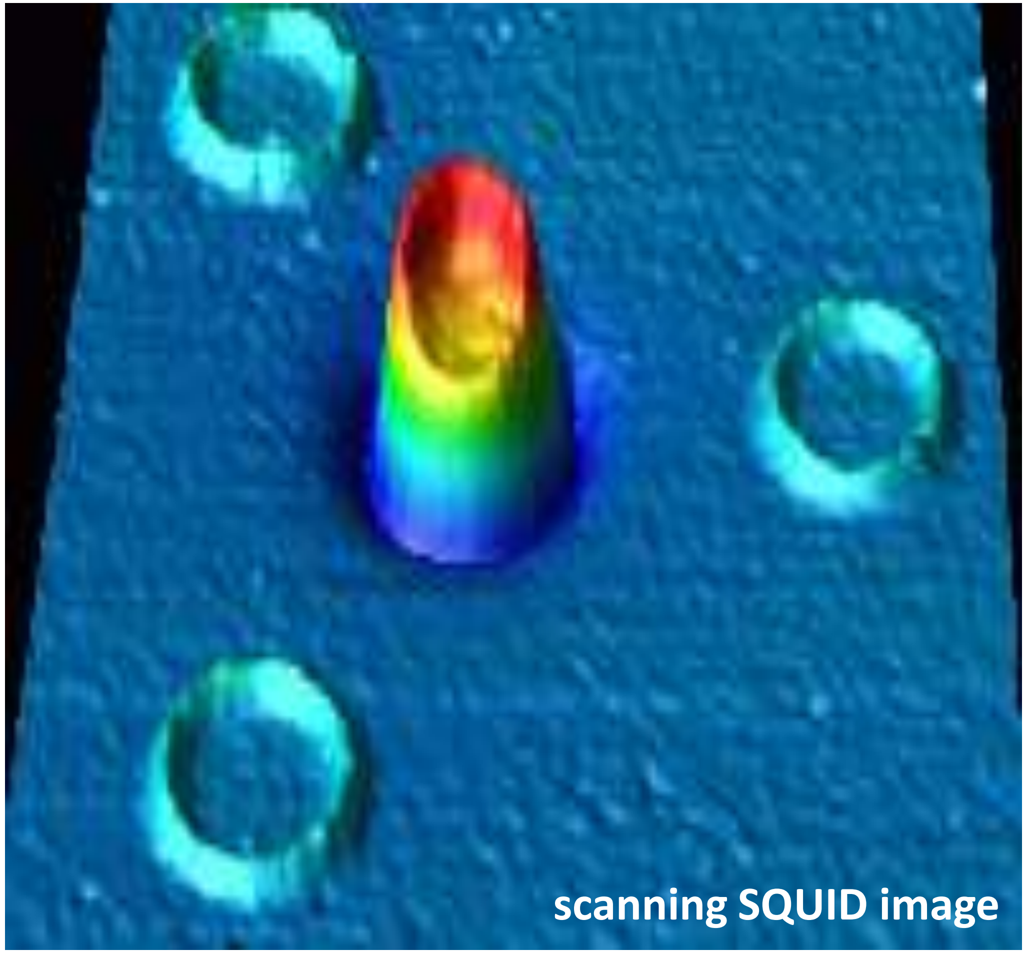

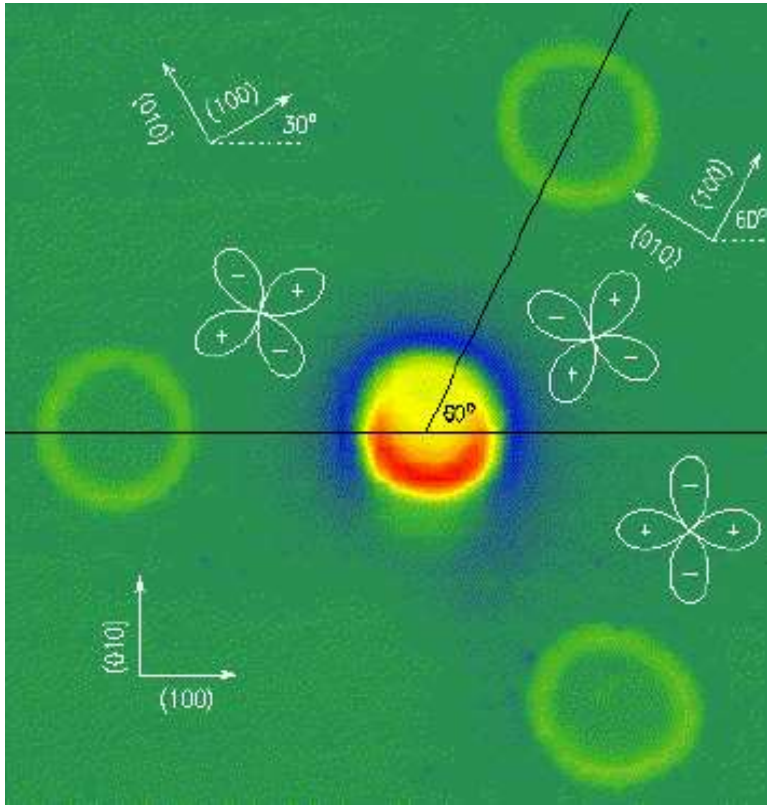

half-integer flux quantization in odd-number π-junction ring

$$\Phi = \Phi_0 \cdot (0.505 \pm 0.02)$$

C.C. Tsuei et al., Phys. Rev. Lett. **73**, 593 (1994)
J. R. Kirtley et al., Nature **373**, 225 (1995)

- **tricrystal experiment for electron doped HTS**

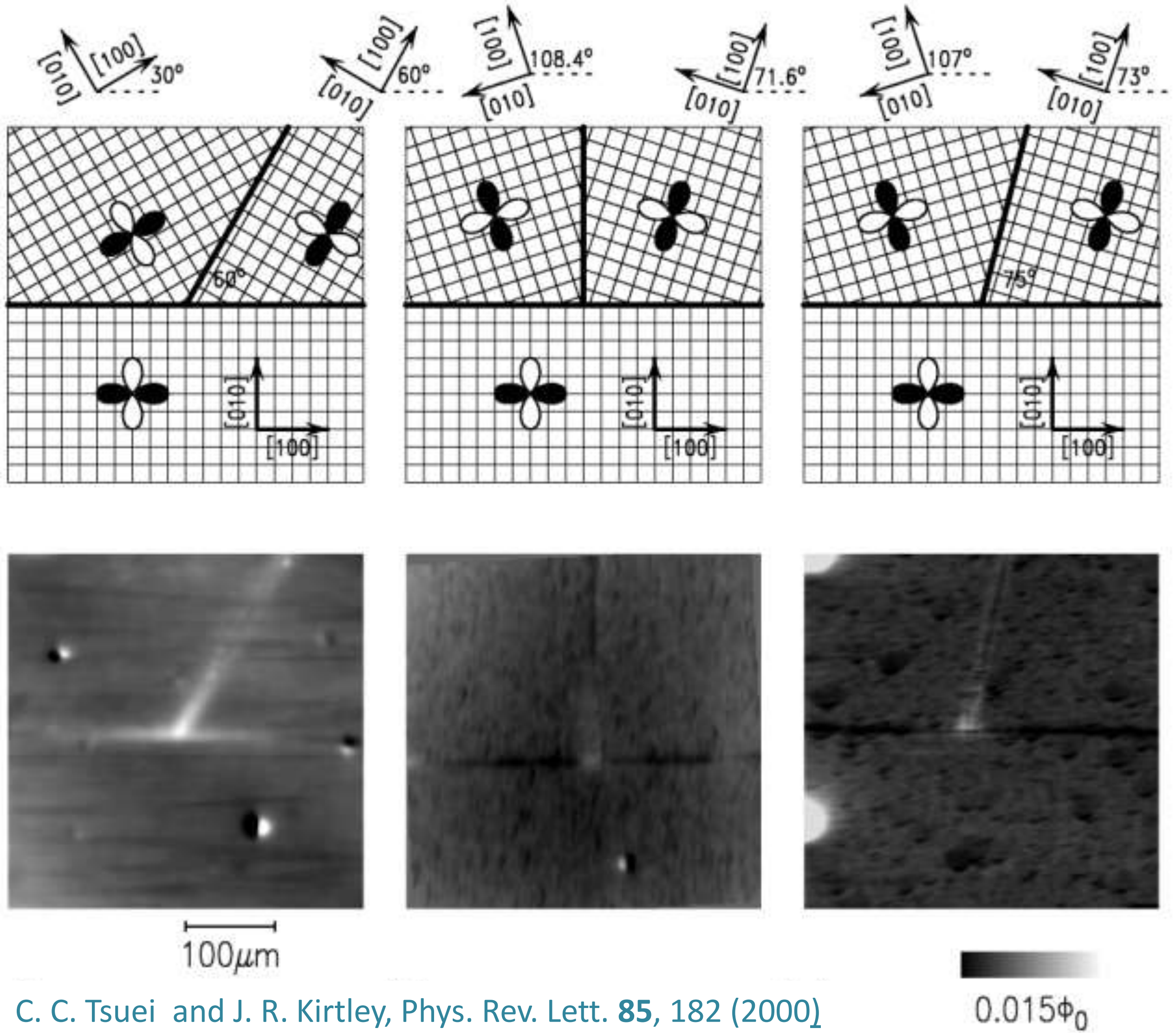

$(Nd,Pr)_{1.85}Ce_{0.15}CuO_{4-y}$

$$\boxed{\begin{array}{c}\Phi = (0.57 + 0.24 - 0.17) \cdot \Phi_0 \\ (0.4\,\Phi_0\text{-}0.81\,\Phi_0)\end{array}}$$

C. C. Tsuei and J. R. Kirtley, Phys. Rev. Lett. **85**, 182 (2000)

half-integer or fractional quantization!

7.4 Symmetry of Pair Wavefunction

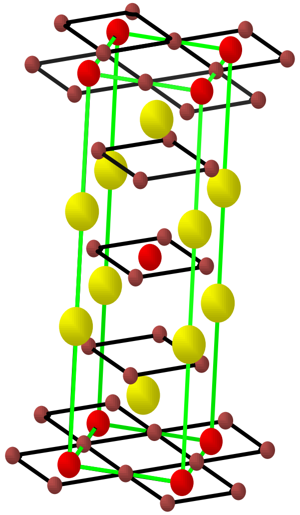

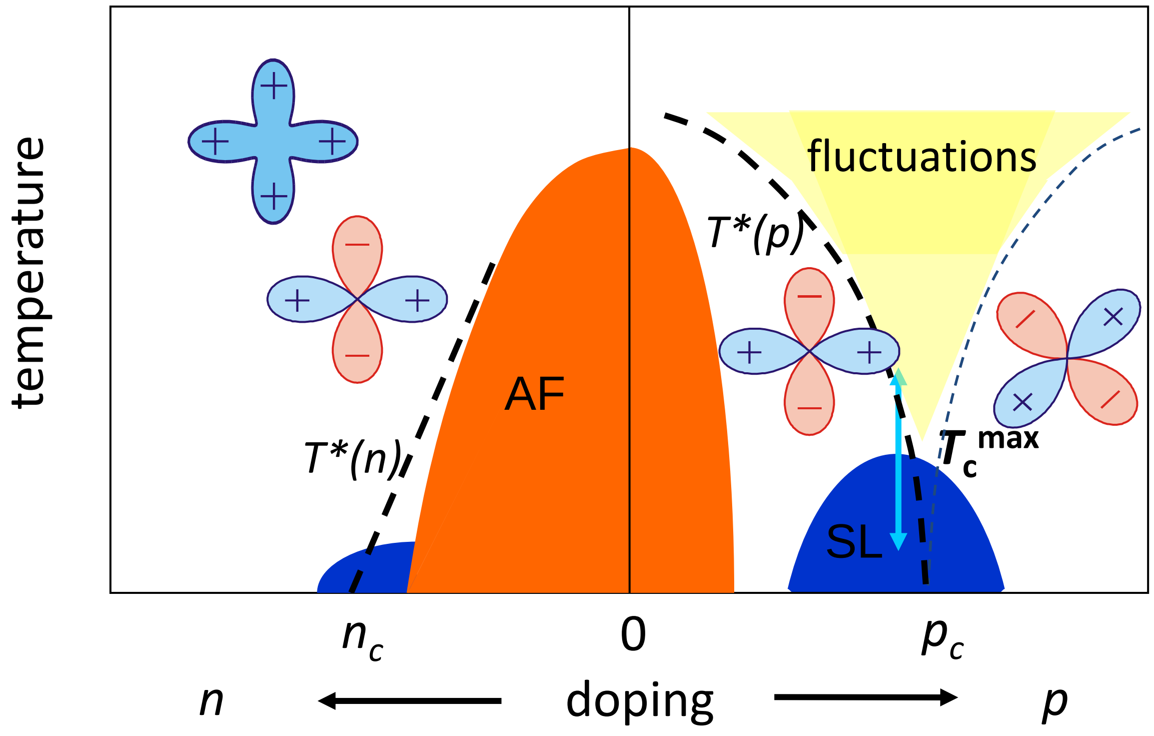

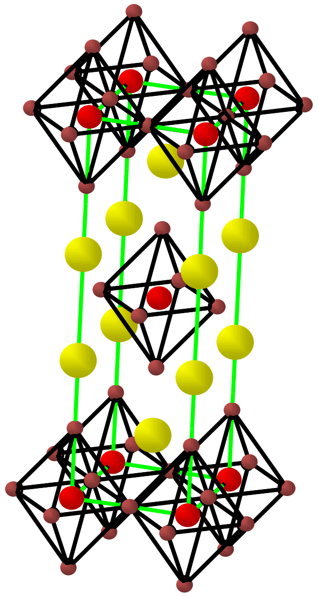

- **Tunneling spectroscopy**

bicrystal grain boundary junctions

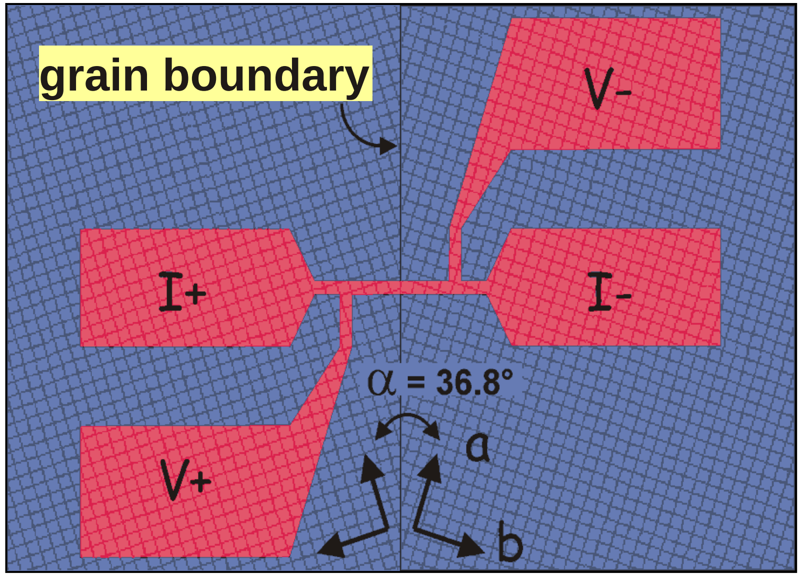

bicrystal-substrate ($SrTiO_3$)

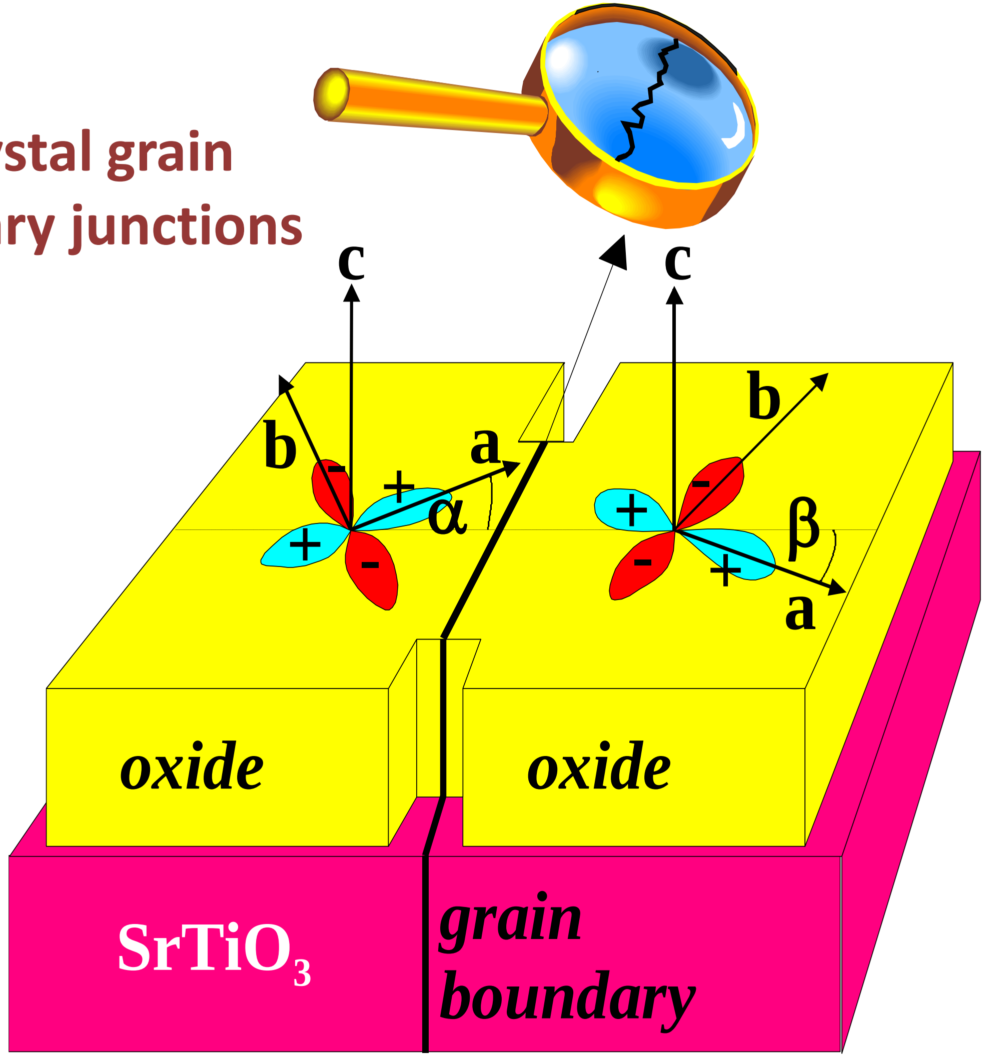

R. Gross et al., Phys. Rev. Lett. 64, 228 (1990)
Nature 322, 818 (1988)

7.4 Symmetry of Pair Wavefunction

- grain boundary junctions

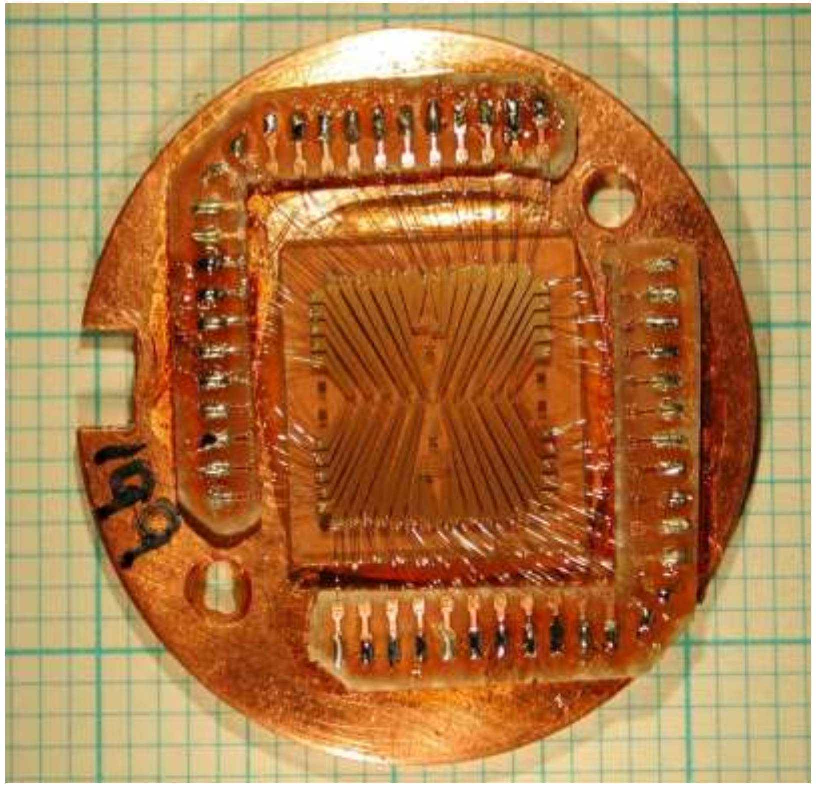

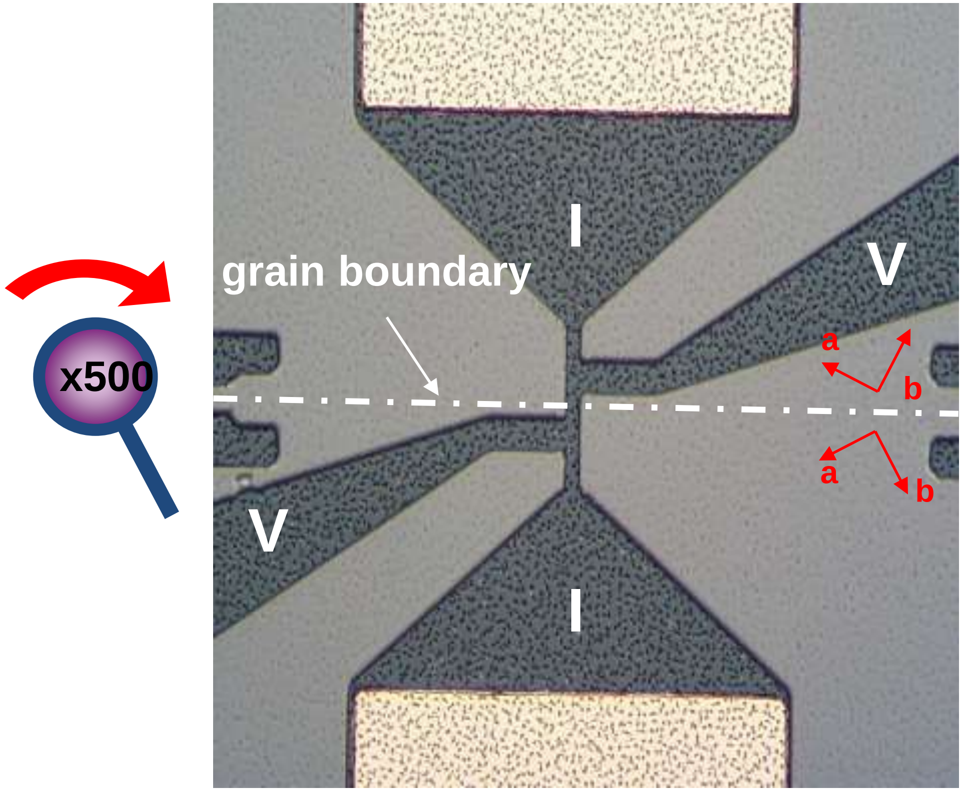

- $La_{2-x}Ce_xCuO_4$ on $SrTiO_3$
- optical lithography

- **Andreev reflection**

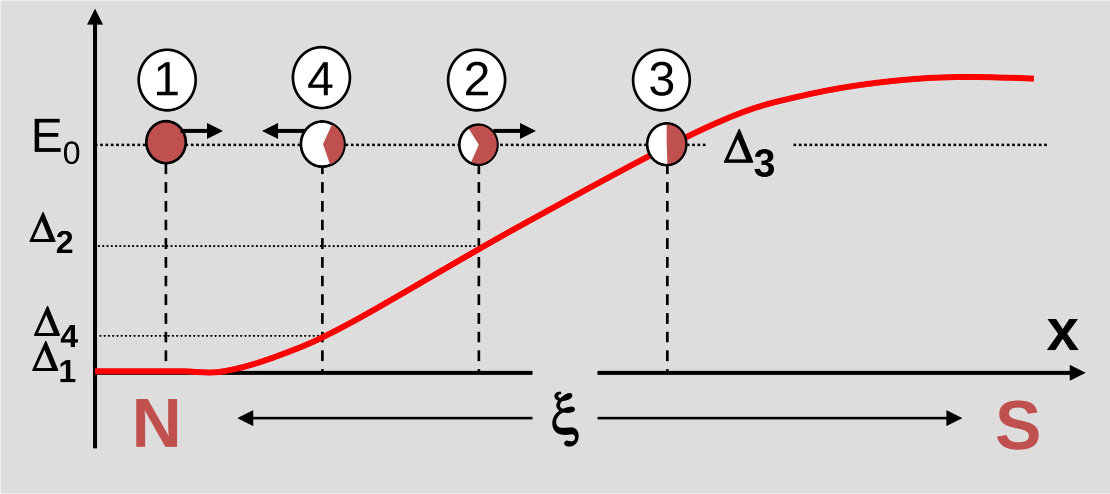

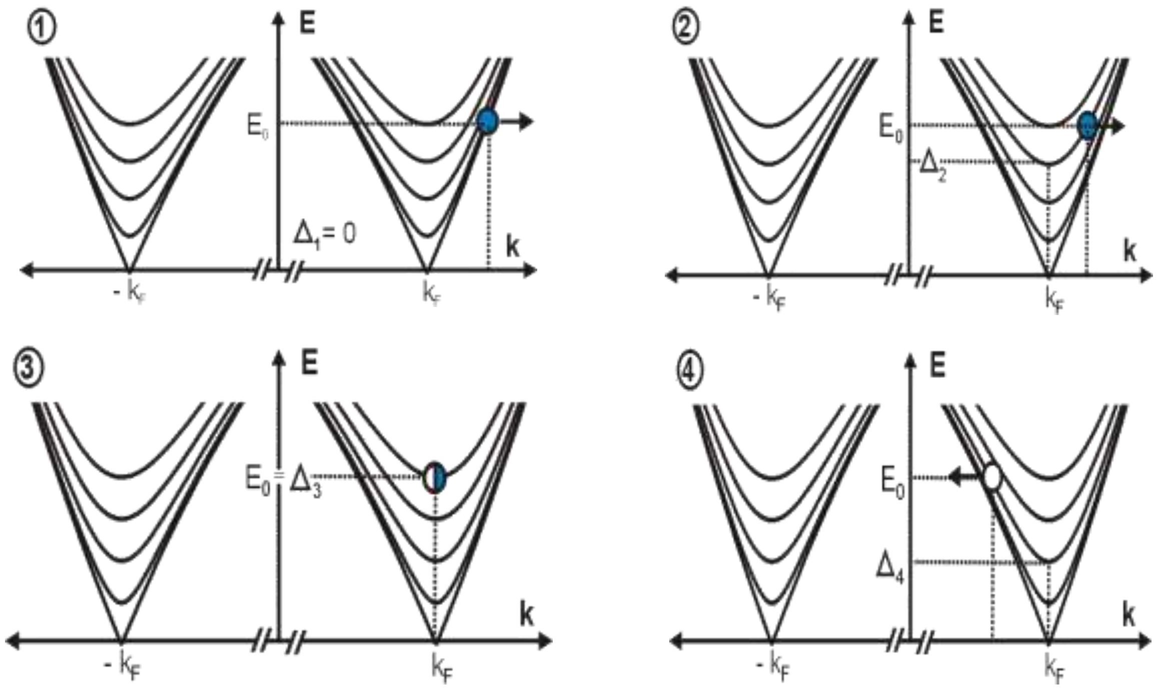

- **Andreev bound states**

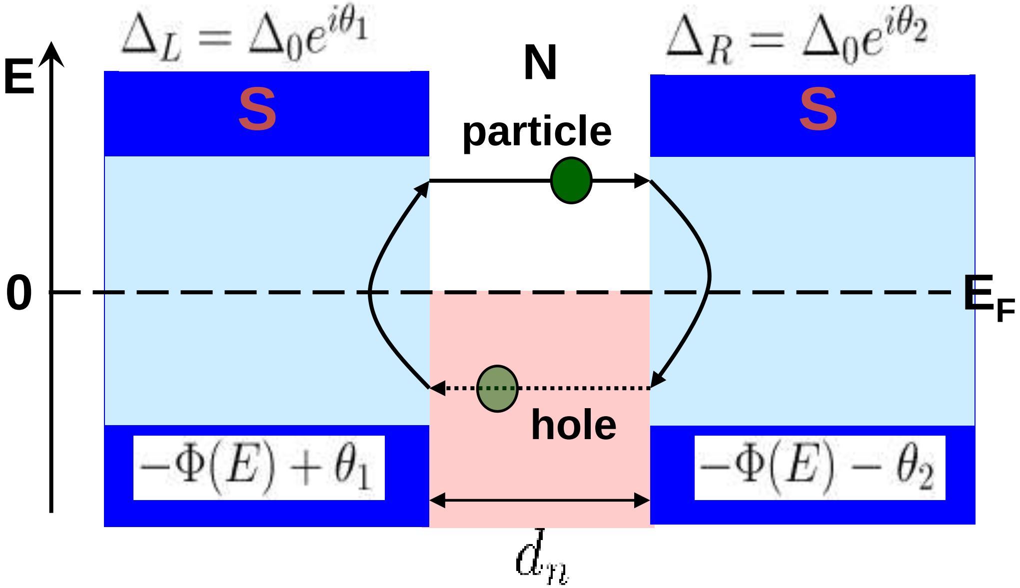

$$\Phi(E) = \arctan\left(\sqrt{\left(\frac{\Delta}{E}\right)^2 - 1}\right)$$

$$\theta_d(E) = \frac{d_n E}{\hbar v_F}$$

quantum condition:

$$-2\Phi(E) + (\theta_1 - \theta_2) + 2\theta_d(E) = n2\pi$$

special case

$$\theta_1 - \theta_2 = \pi$$

bound state at ε_F

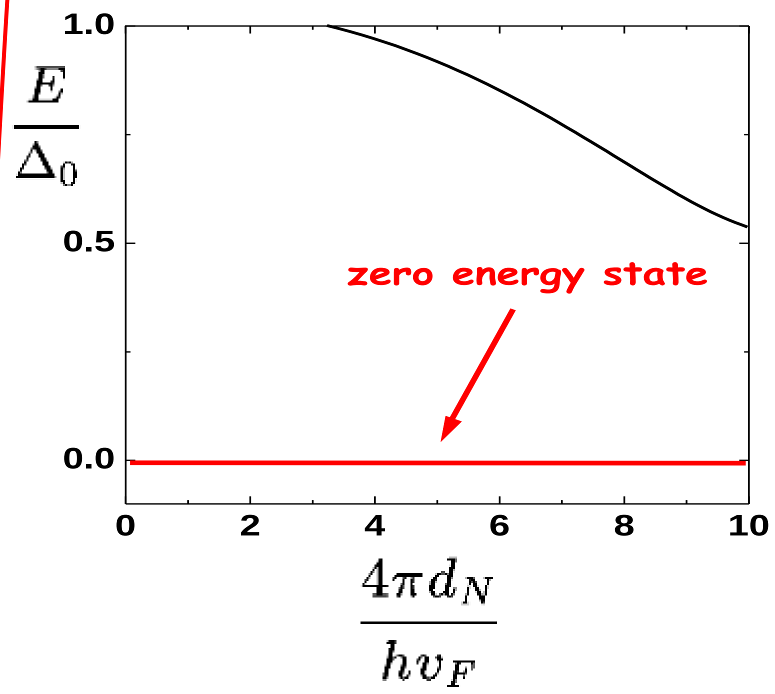

- **midgap surface states**

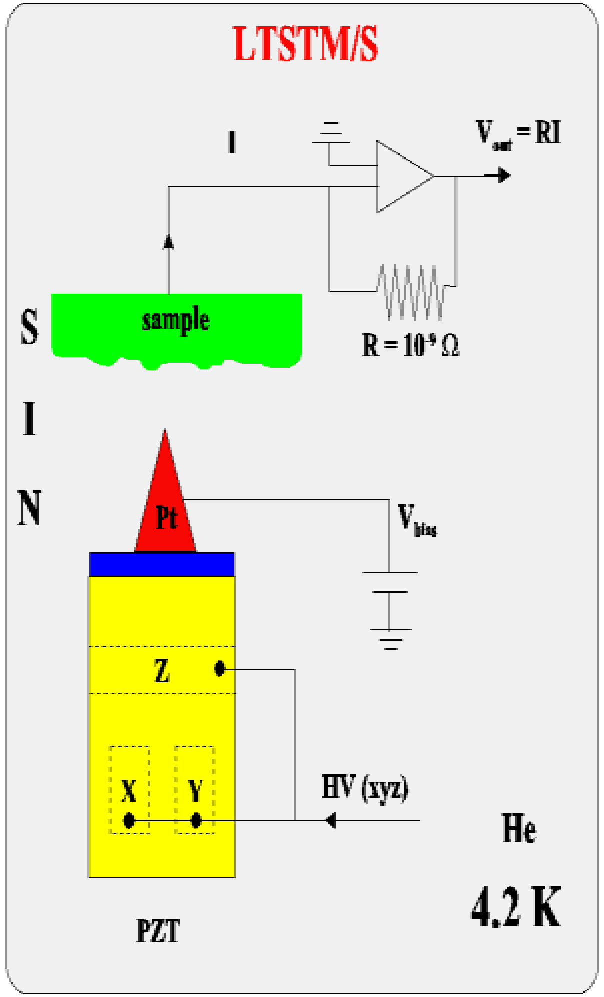

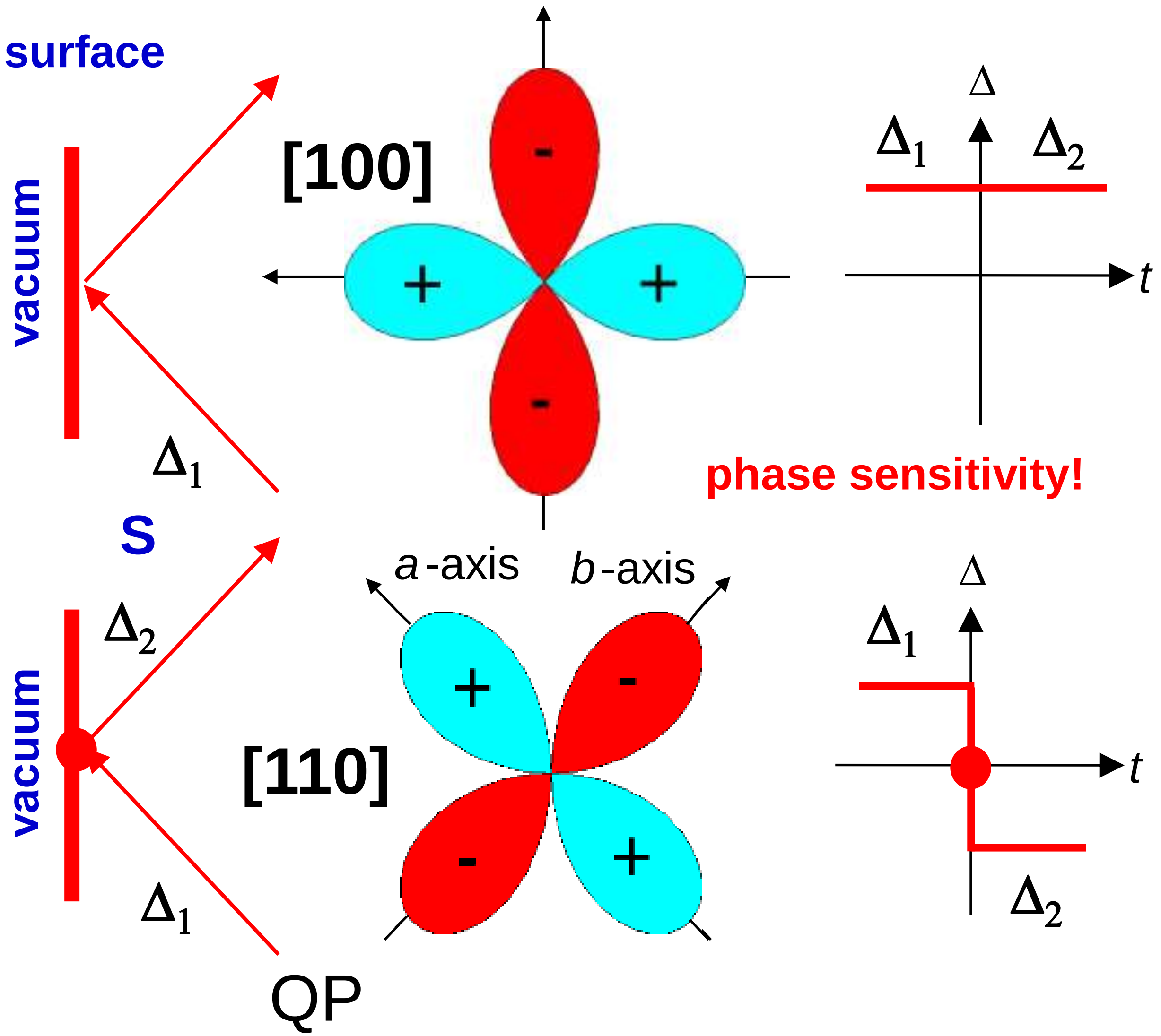

C. R. Hu, Phys. Rev. Lett. **72**, 1526 (1994)

7.4 Symmetry of Pair Wavefunction

- **tunneling spectrosocpy in superconductors**

$$\rho_{BCS}(E) = \Re\left(\frac{|E|}{\sqrt{E^2 - |\Delta_s|^2}}\right)$$

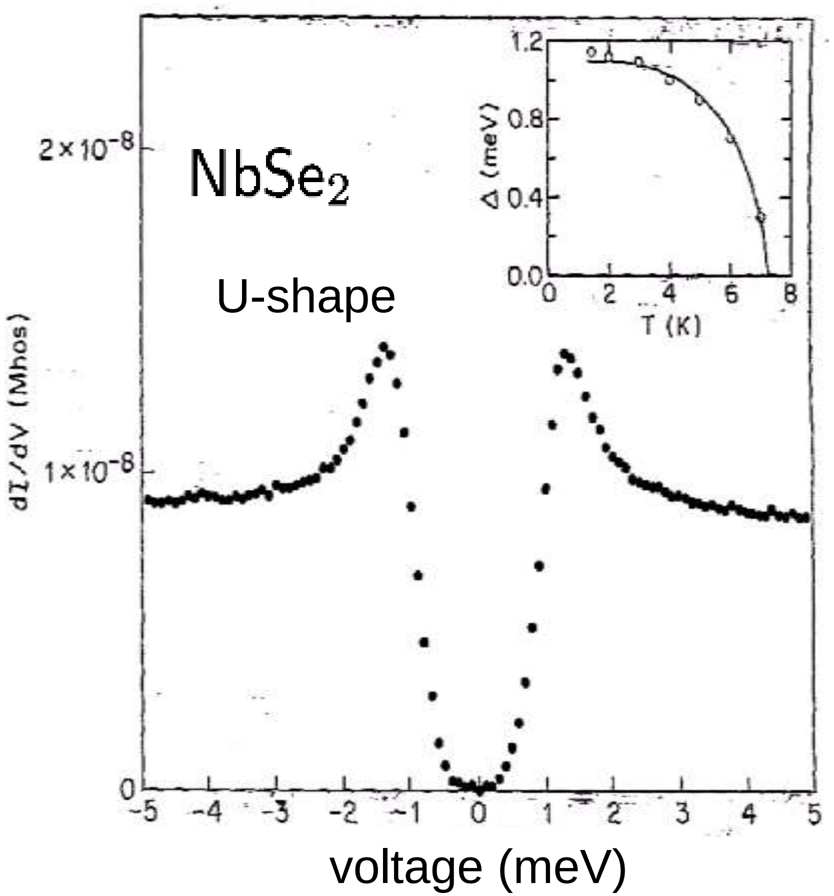

H. F. Hess et al., Phys. Rev. Lett. **62**, 214 (1989)

high temperature superconductors

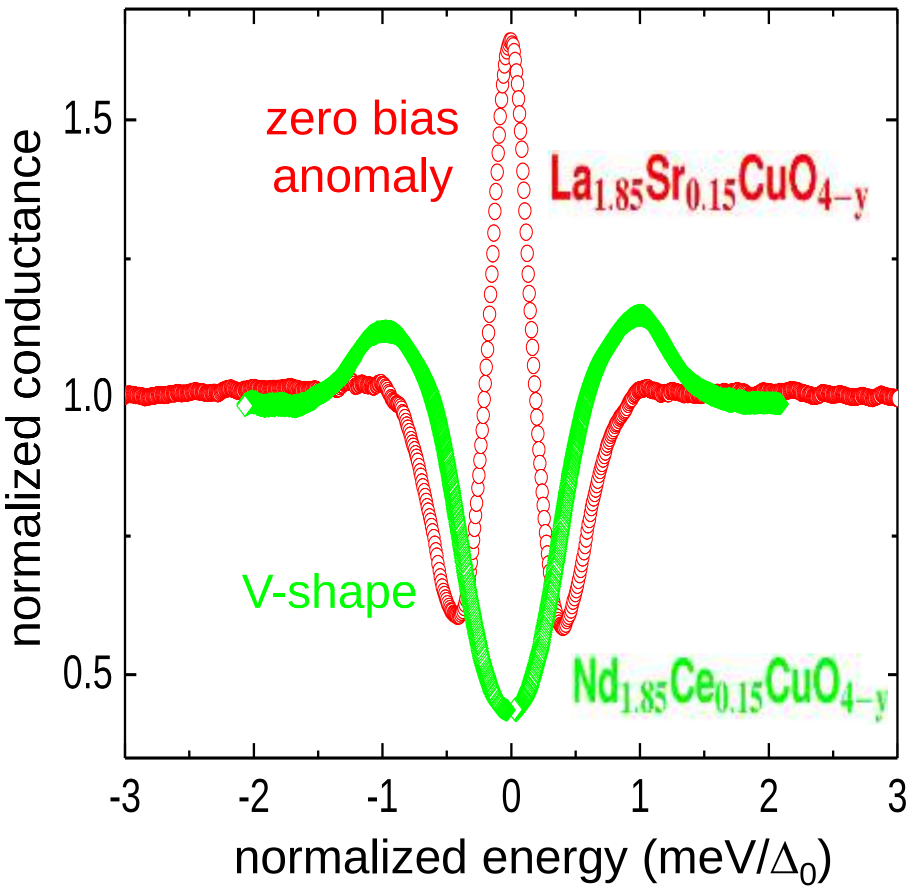

L. Alff et al., Phys. Rev. B **58**, 11197 (1998)

- **LT-STS hole doped HTS: S-I-N**

S-I-N junction

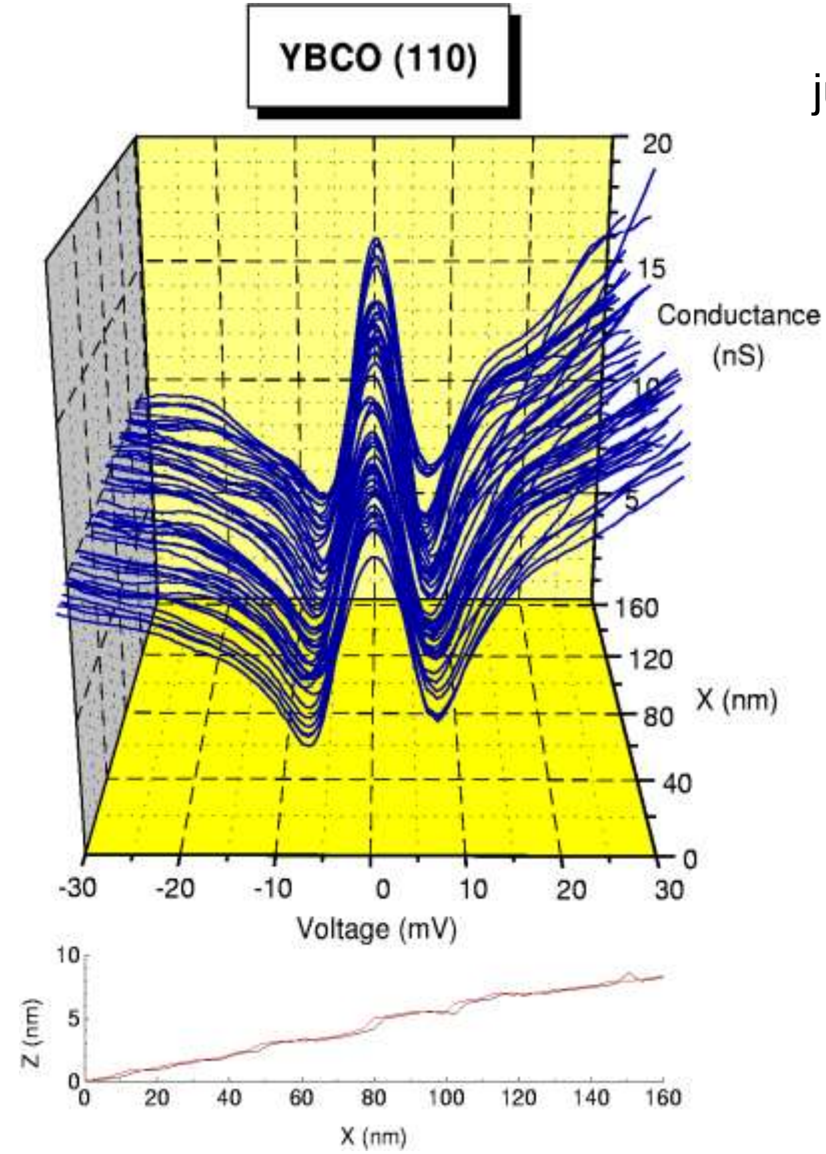

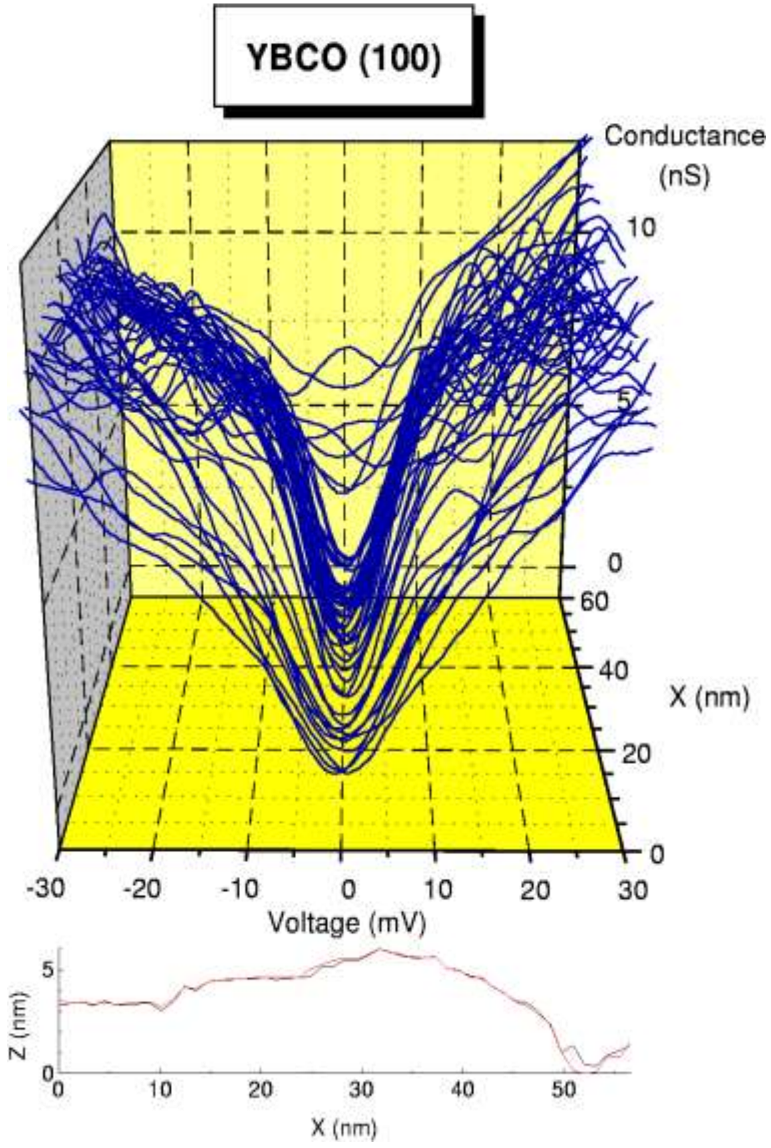

L. Alff et al.,
Phys. Rev. B **55**, R14757 (1997)

7.4 Symmetry of Pair Wavefunction

- **temperature dependence of zero bias anomaly**

bicrystal grain boundary junction

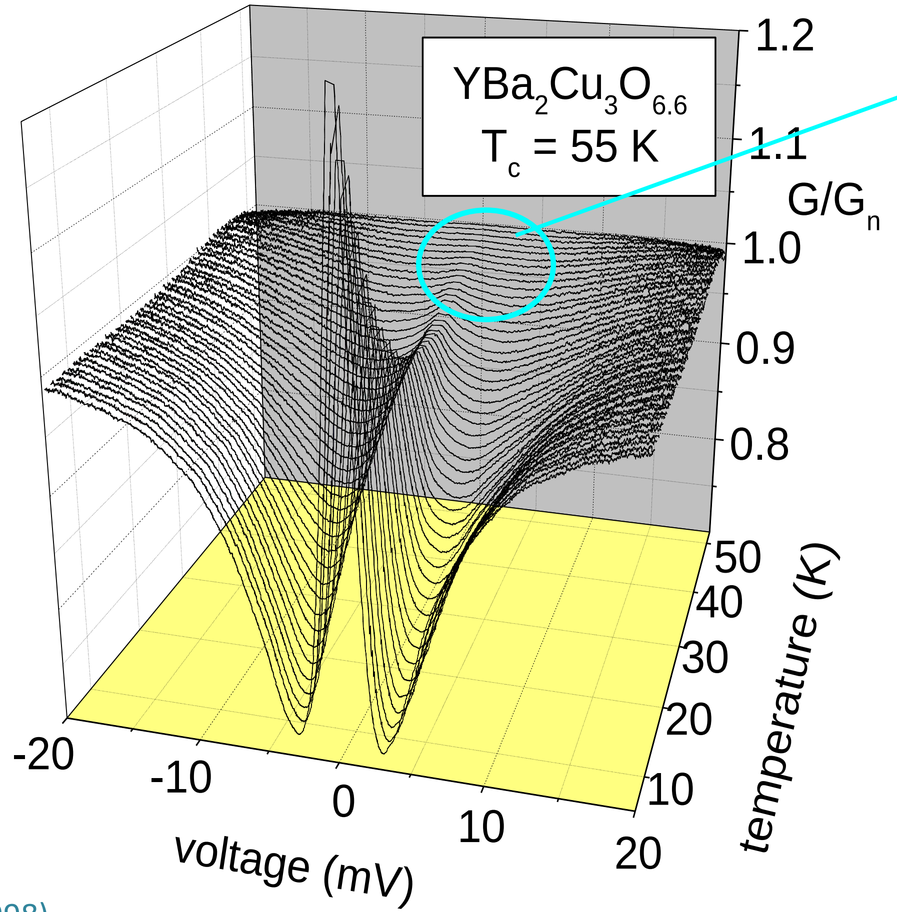

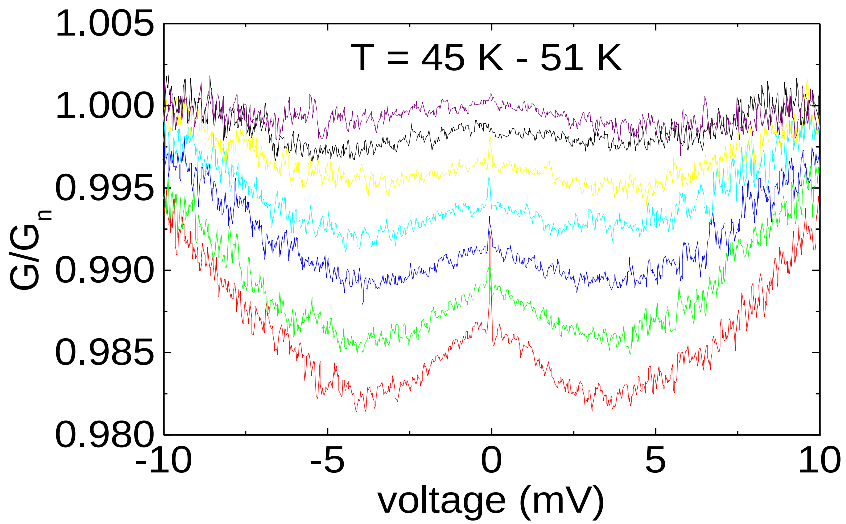

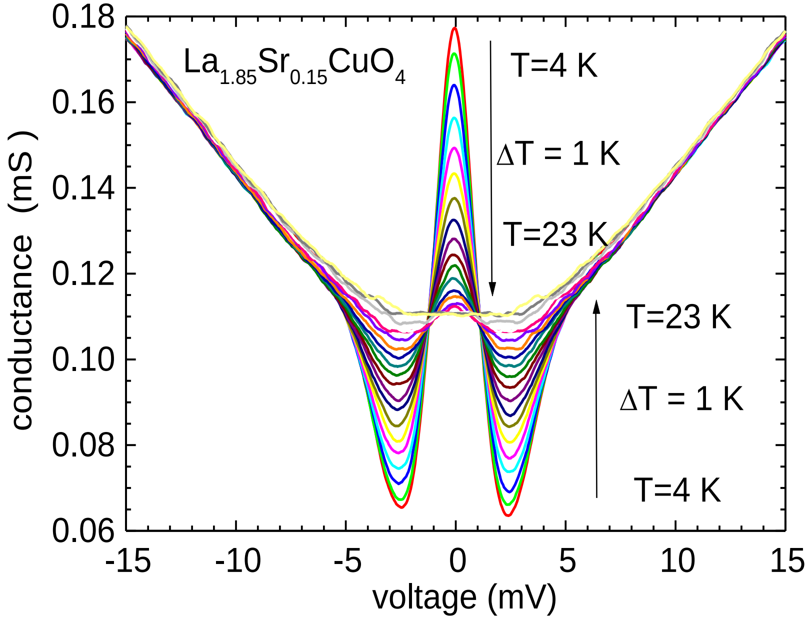

L. Alff et al., Eur. Phys. J. B **5**, 423 (1998)
L. Alff et al., Phys. Rev. B **58**, 11197 (1998)

- **LT-STS electron doped HTS: S-I-N**

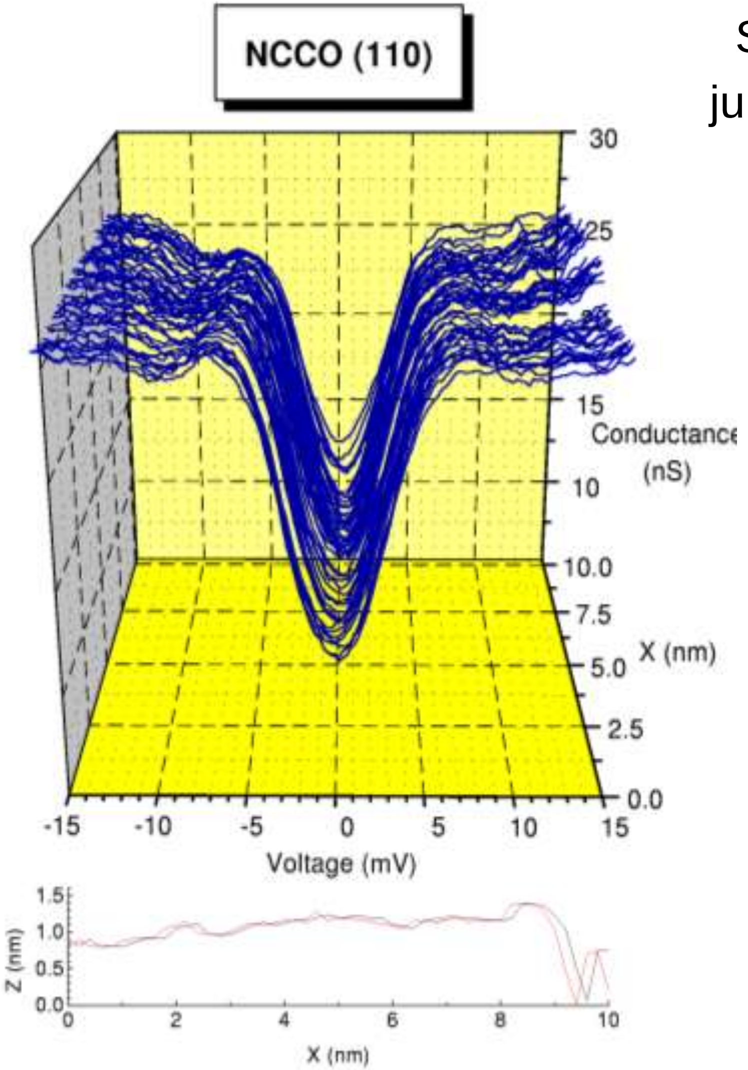

S-I-N
junction

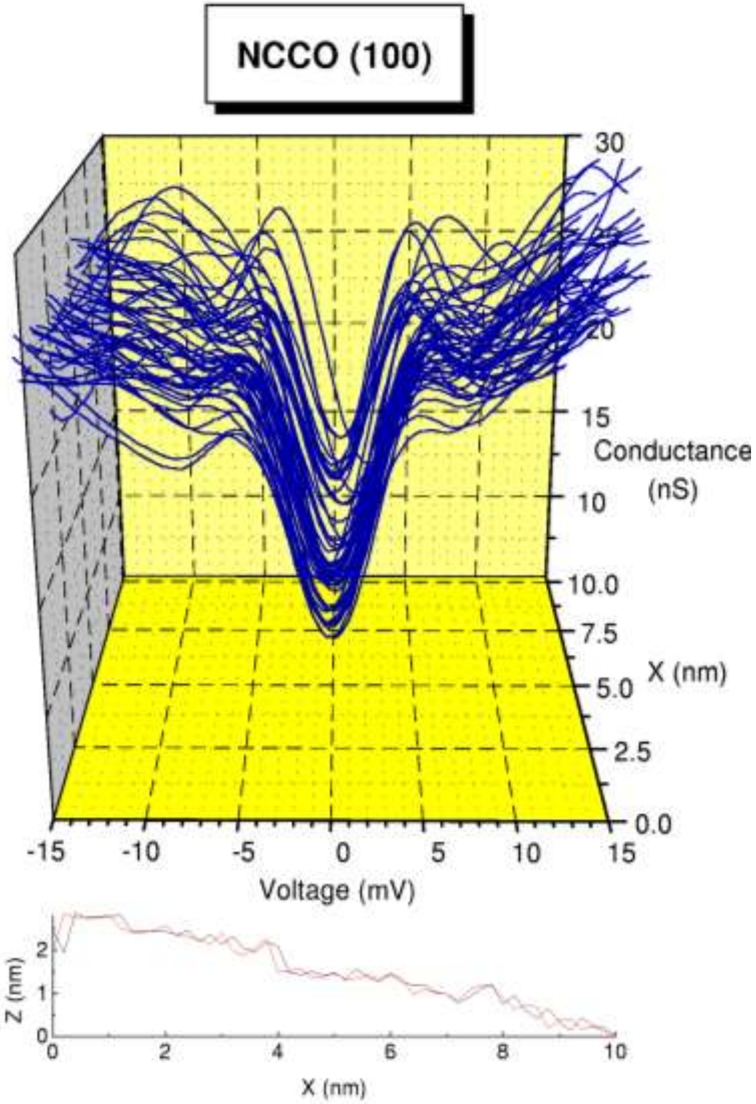

L. Alff et al.,
Physica C **282-287**, 1485 (1997)

Summary of Lecture No. 14 (1)

Determination of the Fermi Surface

- ARPES is powerful tool but at the same time is very surface sensitive
  ➔ requires very clean surfaces, UHV environment, stability of surfaces
- Quantum oscillations of the magnetization (de Haas – van Alphen effect) and the resistance (Shubnikov – de Haas effect)
  ➔ requires very pure single crystals, high magnetic fields and low temperatures

Symmetry of the Order Parameter

- Determination by amplitude and phase sensitive measurements
  - Phase sensitive measurements probe the change of sign of the wavefunction in different k-directions
  - Amplitude sensitive measurements probe the change of the quasiparticle excitation spectrum due to nodes in the order parameter
- London penetration depth: $\lambda_\mathrm{L}(T) \propto \exp(-\Delta/k_\mathrm{B}T)$ for s-wave superconductors and $\lambda_\mathrm{L}(T) \propto T$ for d-wave superconductors
- Phase sensitive experiments based on tricrystals
- **most cuprate superconductors are d-wave superconductors**

Walther Meißner Institut

BAdW | BAYERISCHE AKADEMIE DER WISSENSCHAFTEN

Technische Universität München

Superconductivity and Low Temperature Physics I

Lecture No. 15
10 February 2022

R. Gross

7 High Temperature Superconductivity

7.5 Superconducting Properties

- **cuprate superconductors are $\boldsymbol{d}$-wave spin singlet superconductors**
  - fluxoid quantization: $\Phi_0 = h/2e$,
  - Josephson frequency: $\omega_J = 2eV/\hbar$,
  - Knight-shift compatible with spin-singlet pairing
  - $d_{x^2-y^2}$ orbital OP symmetry proven by phase sensitive experiments

- **pairing mechanism still unclear**
  - no smoking gun experiment for nature of exchange boson (as isotop effect for metallic SC)
  - since parent state is AFM insulator, antiferromagnetic spin fluctuations are likely candidate

  (other candidates: electron-phonon coupling, charge density fluctuations, orbital currents, …)

- **development of adequate theory is difficult**
  - free electron gas/Fermi liquid is not a good starting point
  - strong electronic correlations play a role
  - no clear separation of energy scales (Fermi energy, Debye energy, superconducting energy gap)
  - competing ordering processes (e.g. CDW, SDW)

7.5 Superconducting Properties

Größe	Einheit	YBCO	Nb_3Sn	Al	Anmerkung
T_c	K	93	18	1.19	
$\Delta(0)$	meV	30	4.3	0.18	
$2\Delta(0)/k_B T_c$		7.4	5.4	3.5	
ξ_{BCS}	nm	1.3	10	170	
B_{cth}	T	1.1	0.9	0.01	
$B_{c1,\Vert c}$	T	0.05	0.75	–	$\mathbf{B} \Vert c$
$B_{c1,\Vert ab}$	T	0.009	0.75	–	$\mathbf{B} \Vert ab$
$\lambda_{L,\Vert c}$	nm	140	80	50	$\mathbf{J}_s \Vert c$
$\lambda_{L,\Vert ab}$	nm	900	80	50	$\mathbf{J}_s \Vert ab$
$B_{c2,\Vert c}$	T	160	25	–	$\mathbf{B} \Vert c$
$B_{c2,\Vert ab}$	T	1000	25	–	$\mathbf{B} \Vert ab$
ξ_{ab}	nm	1.4	4	170	$\mathbf{B} \Vert c$
ξ_c	nm	0.2	4	170	$\mathbf{B} \Vert ab$
κ_c		100	20	0.3	$\mathbf{B} \Vert c$

- small BCS coherence length:

$$\xi_{\text{BCS}} = \frac{\hbar v_{\text{F}}}{\pi \Delta_0}$$

a. $v_{\text{F}} \simeq 2 \times 10^5$ m/s is small due to small carrier density (0.16 holes per unit cell) and large effective mass $m^* \simeq 4\, m_e$

b. Δ_0 is large (about 30 meV)

- high upper critical field:

$$B_{c2} = \frac{\Phi_0}{\pi \xi_{\text{GL}}^2}$$

cuprate superconductors are strongly anisotropic

7.5.1 Anisotropy

$Bi_2Sr_2Ca_1Cu_2O_8$ = Bi-2212 (≈ 90 K)

- cuprate superconductors consist of conducting CuO_2 planes separated by isolating intermediate layers
- large anisotropy of electrical resistivity

  e.g. Bi-2212: $\frac{\rho_c}{\rho_{ab}} \simeq 10^5$
- large anisotropy of superconducting properties, e.g. $B_{c1}, B_{c2}, \lambda_{\mathrm{L}}, \xi_{\mathrm{GL}}$

how to describe anisotropic superconductors?

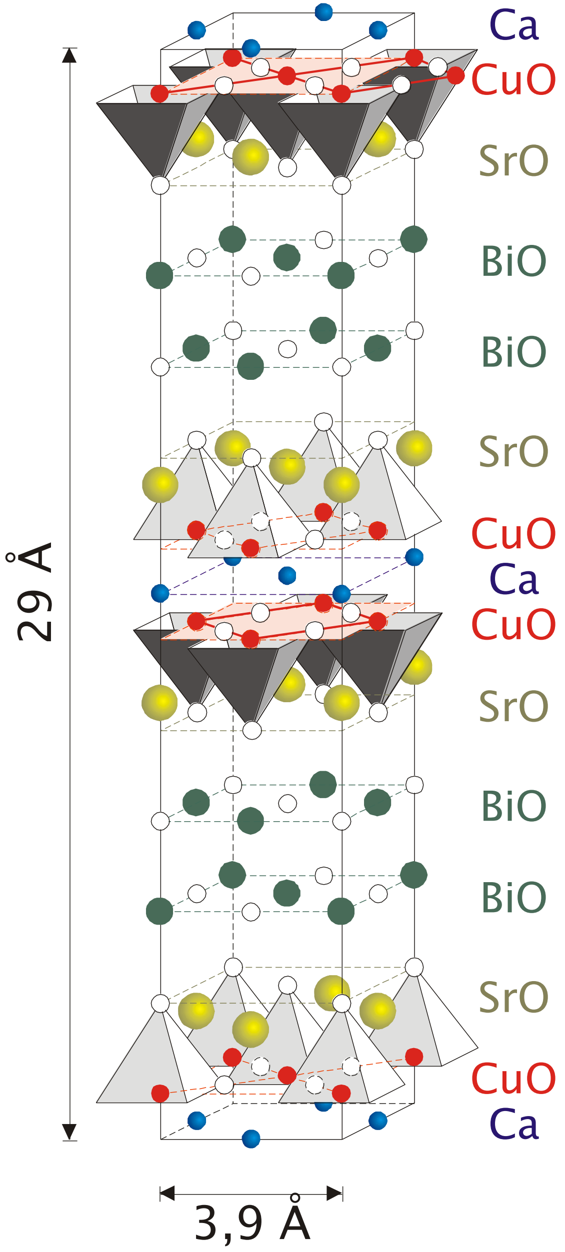

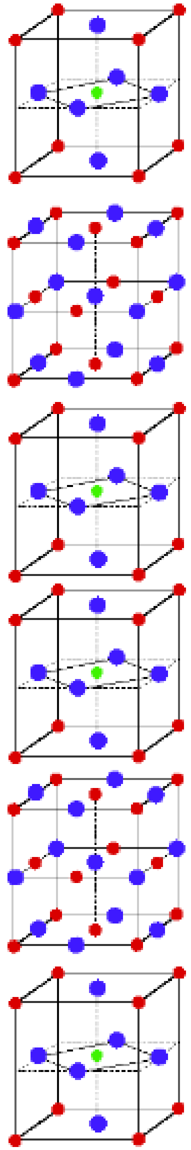

7.5.1 Anisotropy

- **generalized Ginzburg-Landau theory**

– free enthalpy density for $\mathbf{B}_{\text{ext}} = \mu_0 \mathbf{H}_{\text{ext}} = 0$ (cf. 3.3)

$$\Delta g = g_s - g_n = \alpha|\Psi|^2 + \frac{1}{2}\beta|\Psi|^4 + \cdots + \underbrace{\frac{1}{2m_s}\left|\frac{\hbar}{\imath}\nabla\Psi(\mathbf{r})\right|^2}$$

additional term due to spatial inhomogeneities of order parameter

– **Lawrence-Doniach Model** for anisotropic SCs

➢ associate an order parameter Ψ_n to each superconducting layer (can be several CuO2 planes)

➢ replace gradient perpendicular to layer structure by differences: $\left|\frac{\partial\Psi}{\partial z}\right| \Rightarrow \frac{|\Psi_n - \Psi_{n-1}|}{s}$

$$\Delta g = \sum_n \alpha|\Psi_n|^2 + \frac{1}{2}\beta|\Psi_n|^4 + \ldots + \frac{\hbar^2}{2m_{ab}}\left(\left|\frac{\partial\Psi_n(\mathbf{r})}{\partial x}\right|^2 + \left|\frac{\partial\Psi_n(\mathbf{r})}{\partial y}\right|^2\right) + \frac{\hbar^2}{2m_c s^2}|\Psi_n - \Psi_{n-1}|^2$$

with $\Psi_n = |\Psi_n| \mathrm{e}^{\imath\theta_n}$

7.5.1 Anisotropy

- **Lawrence-Doniach Model**

simplification: we assume that $|\Psi_n|$ is the same for each layer

$$\frac{\hbar^2}{2m_c s^2}|\Psi_n - \Psi_{n-1}|^2 = \frac{\hbar^2}{2m_c s^2}|\Psi_n|^2\,[1-\cos(\theta_n-\theta_{n-1})] = \underbrace{E_{J,n}[1-\cos(\theta_n-\theta_{n-1})]}$$

corresponds to Josephson coupling between layer n and $n-1$

anisotropic cuprate superconductors can be modelled as a stack of Josephson coupled 2D superconducting sheets described by $\Psi_n = |\Psi_n|e^{\imath\theta_n}$

$$\Delta g = \sum_n \alpha|\Psi_n|^2 + \frac{1}{2}\beta|\Psi_n|^4 + \ldots + \frac{\hbar^2}{2m_{ab}}\left(\left|\frac{\partial\Psi_n(\mathbf{r})}{\partial x}\right|^2 + \left|\frac{\partial\Psi_n(\mathbf{r})}{\partial y}\right|^2\right) + \frac{\hbar^2}{2m_c s^2}|\Psi_n|^2[1-\cos(\theta_n-\theta_{n-1})]$$

7.5.1 Anisotropy

- **anisotropic Ginzburg-Landau Model**

  - for length scales large compared to s we can replace differences by a gradient: $\frac{|\Psi_n - \Psi_{n-1}|}{s} \simeq \left|\frac{\partial \Psi_n}{\partial z}\right|$
  - to account for the anisotropy, we use anisotropic mass

$$\Delta g = \sum_n \alpha |\Psi_n|^2 + \frac{1}{2}\beta|\Psi_n|^4 + \ldots + \frac{\hbar^2}{2m_{ab}}\left(\left|\frac{\partial \Psi_n(\mathbf{r})}{\partial x}\right|^2 + \left|\frac{\partial \Psi_n(\mathbf{r})}{\partial y}\right|^2\right) + \frac{\hbar^2}{2m_c}\left|\frac{\partial \Psi_n(\mathbf{r})}{\partial z}\right|^2$$

  - integration of Δg over volume and minimization of free enthalpy yields anisotropic GL equations

$$\left(\frac{\hbar}{\imath}\mathbf{\nabla} - q_s\,\mathbf{A}(\mathbf{r})\right)\underbrace{\left(\frac{1}{2m^*}\right)}\left(\frac{\hbar}{\imath}\mathbf{\nabla} - q_s\,\mathbf{A}(\mathbf{r})\right)\Psi(\mathbf{r}) + \alpha\Psi(\mathbf{r}) + \frac{1}{2}\beta|\Psi(\mathbf{r})|^2\Psi(\mathbf{r}) = 0$$

1st GL equation

anisotropic mass tensor with major axis values $1/m_{ab}$ and $1/m_c$

$m_c \gg m_{ab}$ as coupling between layers is weak

7.5.1 Anisotropy

- **Ginzburg-Landau coherence length**

$$\xi_{\mathrm{GL}}(T) = \sqrt{\frac{\hbar^2}{2m_s|\alpha(T)|}} \quad \begin{cases} \xi_{ab}(T) = \sqrt{\dfrac{\hbar^2}{2m_{ab}|\alpha(T)|}} \\ \xi_c(T) = \sqrt{\dfrac{\hbar^2}{2m_c|\alpha(T)|}} \end{cases}$$

as $m_c \gg m_{ab} \Rightarrow \xi_{ab} \gg \xi_c$

- **magnetic field penetration depth**

$$\lambda_{\mathrm{GL}}(T) = \sqrt{\frac{m_s}{\mu_0 n_s(T) q_s^2}} \quad \begin{cases} \lambda_{ab}(T) = \sqrt{\dfrac{m_{ab}}{\mu_0 n_s(0) q_s^2}} \\ \lambda_c(T) = \sqrt{\dfrac{m_c}{\mu_0 n_s(0) q_s^2}} \end{cases}$$

as $m_c \gg m_{ab} \Rightarrow \lambda_{ab} \ll \lambda_c$

7.5.1 Anisotropy

- cross-section of vortex core for vortex parallel to the CuO_2 plane (in b-direction)

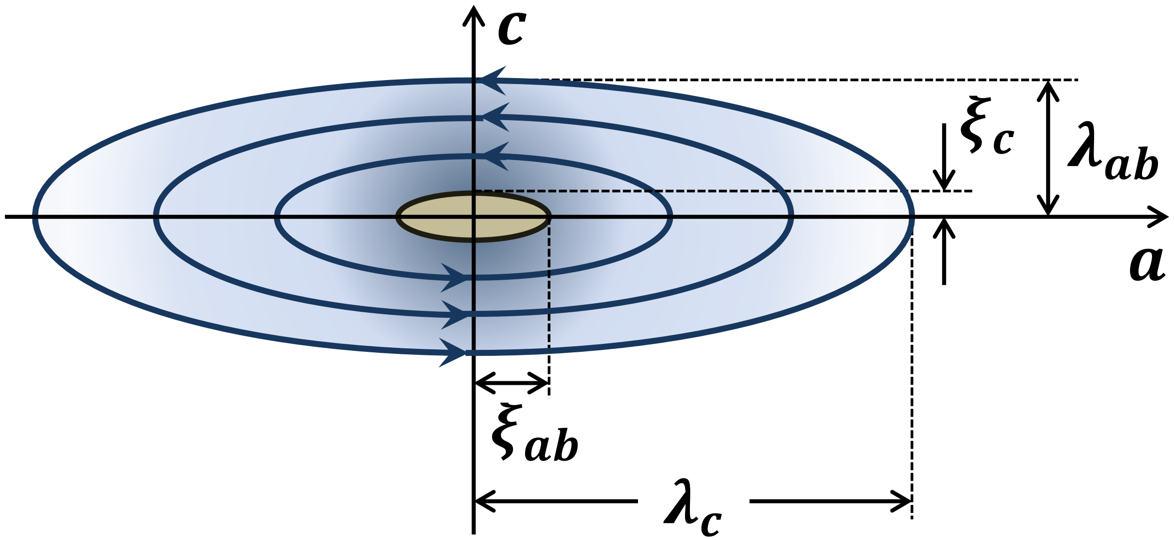

- **screening length in a-direction** (parallel to CuO_2 planes)

  screening length λ_c is large as screening currents are flowing in c-direction (perpendicular to CuO_2 planes)

- **screening length in c-direction** (perpendicular to CuO_2 planes)

  screening length λ_{ab} is small as screening currents are flowing in ab-plane (parallel to CuO_2 planes)

7.5.1 Anisotropy

- upper and lower critical field

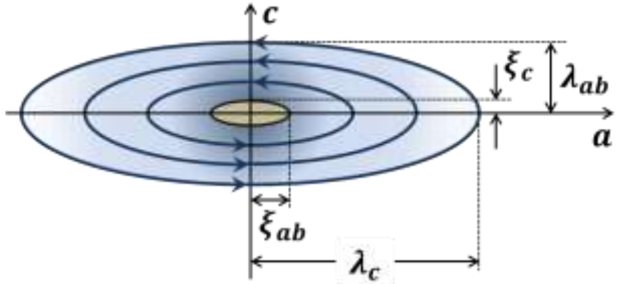

$$B_{c1}(T) = \frac{\Phi_0}{2\pi\lambda_L^2(T)}(\ln\kappa + 0.08) \quad \begin{cases} B_{c1,||ab} = \dfrac{\Phi_0}{2\pi\lambda_{ab}\lambda_c}(\ln\kappa_{ab} + 0.08) \\ B_{c1,||c} = \dfrac{\Phi_0}{2\pi\lambda_{ab}^2}(\ln\sqrt{\kappa_{ab}\kappa_c} + 0.08) \end{cases}$$

as $\lambda_{ab} \ll \lambda_c \Rightarrow B_{c1,||ab} \ll B_{c1,||c}$

$$B_{c2}(T) = \frac{\Phi_0}{2\pi\xi_{GL}^2(T)} \quad \begin{cases} B_{c2,||ab} = \dfrac{\Phi_0}{2\pi\xi_{ab}\xi_c} \\ B_{c2,||c} = \dfrac{\Phi_0}{2\pi\xi_{ab}^2} \end{cases}$$

as $\xi_{ab} \gg \xi_c \Rightarrow B_{c2,||ab} \gg B_{c2,||c}$

$$B_{cth}(T) = \frac{\Phi_0}{2\pi\sqrt{2}\ \xi_{GL}(T)\lambda_{GL}(T)} = \frac{\Phi_0}{2\pi\sqrt{2}\ \xi_{ab}(T)\lambda_{ab}(T)} = \frac{\Phi_0}{2\pi\sqrt{2}\ \xi_c(T)\lambda_c(T)}$$

7.5.1 Anisotropy

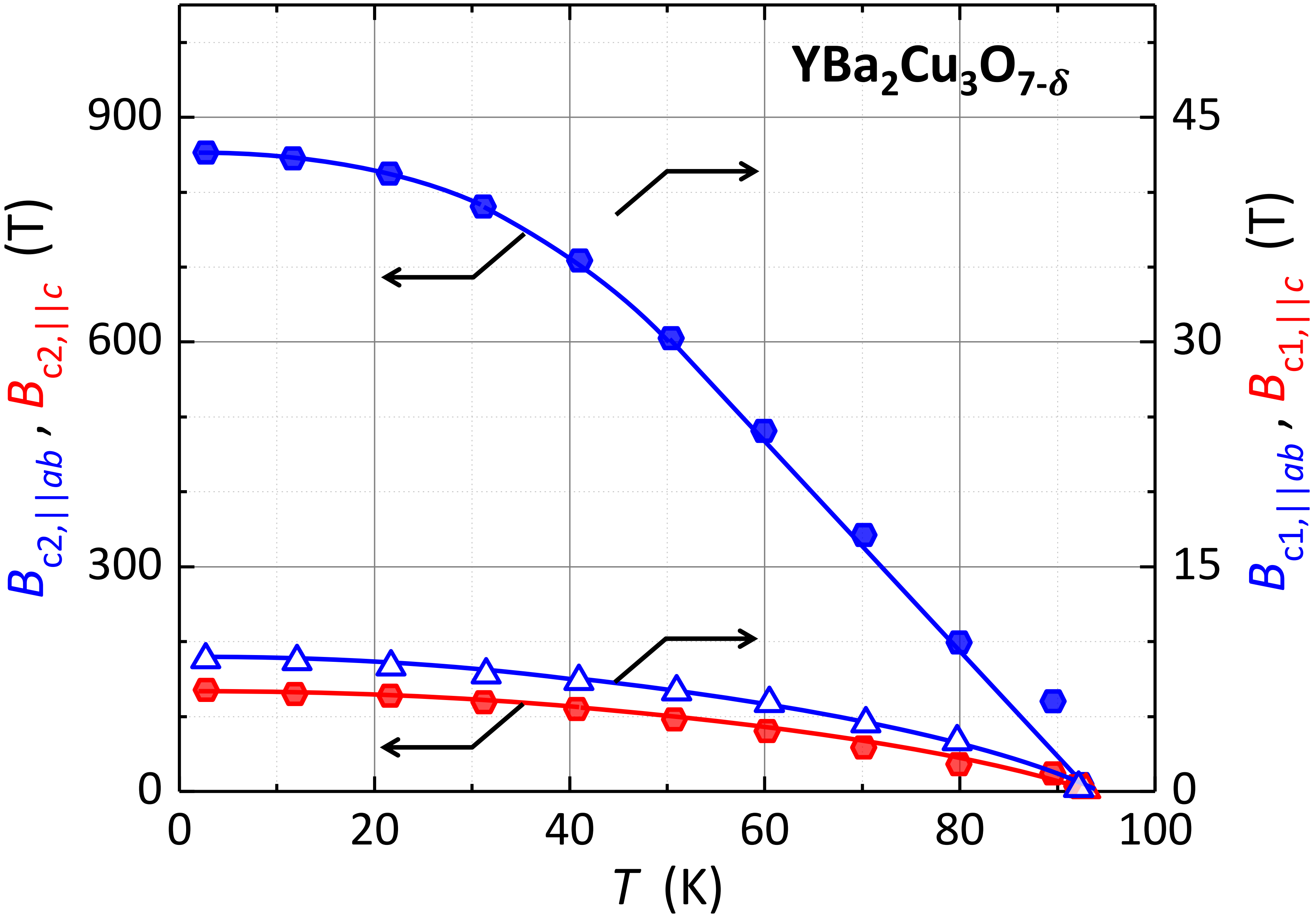

measured quantities:

- penetration depth
- specific heat
  → condensation energy

calculated quantities:

- coherence length
  → upper critical field

7.5.1 Anisotropy

- **dimensionless anisotropy parameter**

$$\gamma \equiv \left(\frac{m_c}{m_{ab}}\right)^{\frac{1}{2}} = \frac{\xi_{ab}}{\xi_c} = \frac{B_{c2,||ab}}{B_{c2,||c}} = \frac{\lambda_c}{\lambda_{ab}} \simeq \frac{B_{c1,||c}}{B_{c1,||ab}}$$

$YBa_2Cu_3O_{7-\delta}$: $\gamma \simeq 6-7$

Bi-2212: $\gamma \simeq 100$

Größe	Einheit	YBCO	Nb_3Sn	Al	Anmerkung
T_c	K	93	18	1.19	
$\Delta(0)$	meV	30	4.3	0.18	
$2\Delta(0)/k_B T_c$		7.4	5.4	3.5	
ξ_{BCS}	nm	1.3	10	170	
B_{cth}	T	1.1	0.9	0.01	
$B_{c1,\|c}$	T	0.05	0.75	–	$\mathbf{B} \parallel c$
$B_{c1,\|ab}$	T	0.009	0.75	–	$\mathbf{B} \parallel ab$
$\lambda_{L,\|c}$	nm	140	80	50	$\mathbf{J}_s \parallel c$
$\lambda_{L,\|ab}$	nm	900	80	50	$\mathbf{J}_s \parallel ab$
$B_{c2,\|c}$	T	160	25	–	$\mathbf{B} \parallel c$
$B_{c2,\|ab}$	T	1000	25	–	$\mathbf{B} \parallel ab$
ξ_{ab}	nm	1.4	4	170	$\mathbf{B} \parallel c$
ξ_c	nm	0.2	4	170	$\mathbf{B} \parallel ab$
κ_c		100	20	0.3	$\mathbf{B} \parallel c$

7.5.1 Anisotropy

- **intrinsic Josephson effect (discovered at WMI by Kleiner & Müller))**

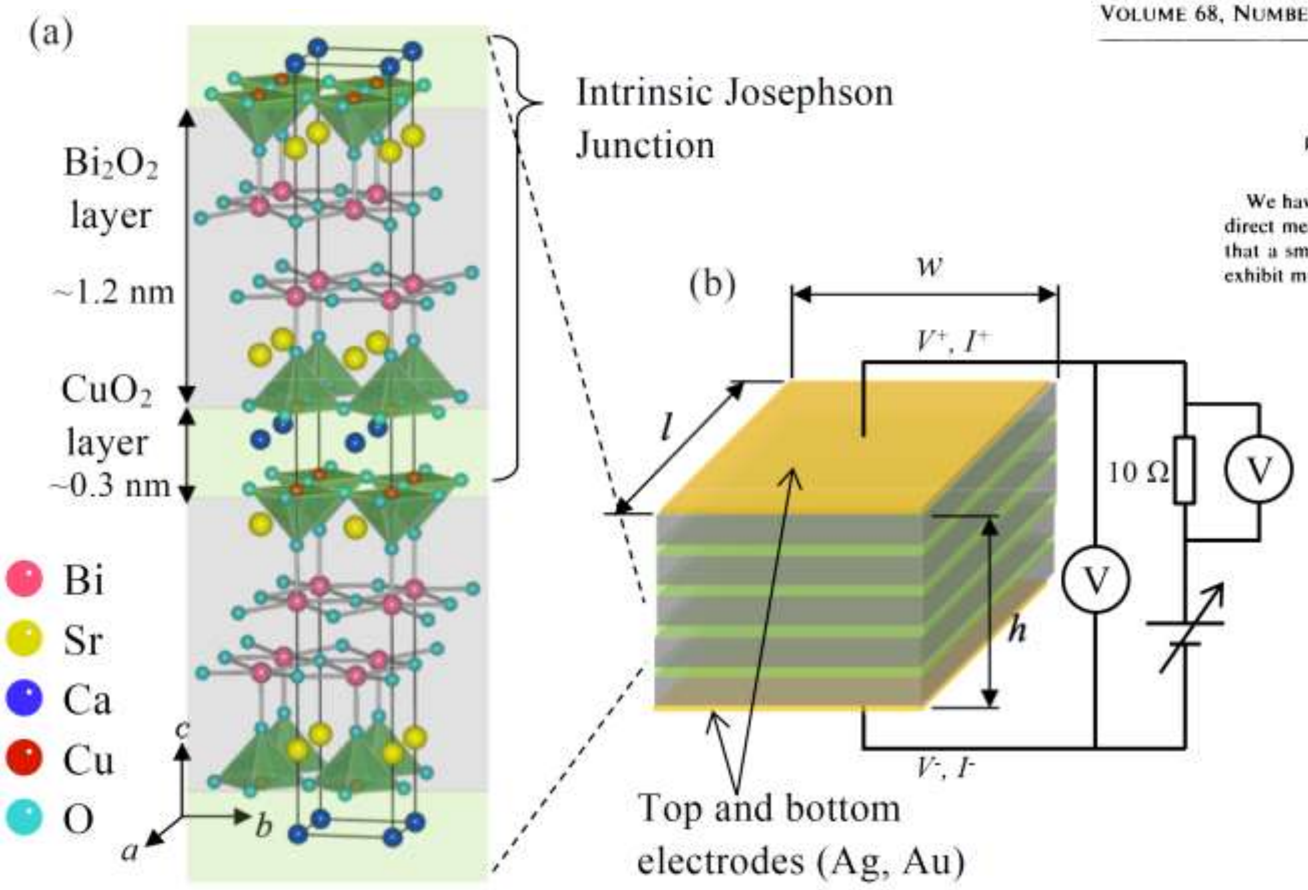

VOLUME 68, NUMBER 15 PHYSICAL REVIEW LETTERS 13 APRIL 1992

Intrinsic Josephson Effects in $Bi_2Sr_2CaCu_2O_8$ Single Crystals

R. Kleiner, F. Steinmeyer, G. Kunkel, and P. Müller
Walther-Meissner-Institut, Walther-Meissner-Strasse 8, W-8046 Garching, Germany
(Received 21 August 1991; revised manuscript received 11 February 1992)

We have observed Josephson coupling between CuO double layers in $Bi_2Sr_2CaCu_2O_8$ single crystals by direct measurements of ac and dc Josephson effects with current flow along the c axis. The results show that a small $Bi_2Sr_2CaCu_2O_8$ single crystal behaves like a series array of Josephson junctions which can exhibit mutual phase locking.

cuprate superconductors
=
stack of Josephson coupled superconducting layers

– R. Kleiner, F. Steinmeyer, G. Kunkel, P. Müller, "Intrinsic Josephson Effects in $Bi_2CaSr_2Cu_2O_8$ Single Crystals, Phys. Rev. Lett. **68**, 2394 (1992)
– R. Kleiner, F. Steinmeyer, G. Kunkel, and P Müller, *Observation of Josephson Coupling between CuO double Layers in $Bi_2CaSr_2Cu_2O_8$ Single Crystals*, Physica C **185**, 2617 (1991).

Summary of Lecture No. 15 (1)

superconducting properties of cuprate superconductors

- $d_{x^2-y^2}$ spin-singlet superconductors
- pairing mechanisms ist still unknown (antiferromagnetic spin fluctuations are likely candidate)
- modelling is difficult: electronic correlations, normal state is not a simple Fermi liquid, competing ordering phenomena (e.g. SDW, CDW)

anisotropy of superconducting properties

- origin is layer structure
- modelling of anisotropic superconducting properties by
  - Lawrence-Doniach model: Josephson coupled stack of 2D superconducting layers
  - anisotropic Ginzburg-Landau model: anisotropy is expressed by effective mass tensor
- strongly anisotropic characteristic parameters: $B_{c1}, B_{c2}, \lambda_\mathrm{L}, \xi_\mathrm{GL}$
- phenomenological description of anisotropy by anisotropy parameter $\gamma \equiv \left(\frac{m_c}{m_{ab}}\right)^{\frac{1}{2}} = \frac{\xi_{ab}}{\xi_c} = \frac{B_{c2,||ab}}{B_{c2,||c}} = \frac{\lambda_c}{\lambda_{ab}}$
- single crystals of cuprate superconductors form stack of intrinsic Josephson junctions
  - application for THz radiation sources